2023

Leaching of Hydrogen Pre-Reduced Mn Ore to Produce MnO_2

NTNU – Department of Materials Science and Engineering

Utsav Shakya and Haldor Andersen Knive
SUPERVISOR: PROF. JAFAR SAFARIAN
COSUPERVISOR: MANISH KUMAR KAR

Preface

This thesis is the final part of our bachelor's in engineering studies – Chemistry at the Norwegian University of Science and Technology(NTNU). The project has been in cooperation with HAlMan project team and Department of Materials Science and Engineering at NTNU. The goal of the thesis was to explore leaching behavior of manganese ore, purification of leachate and precipitation of manganese dioxide and manganese carbonate using different additives. This has resulted in an increase in knowledge about hydrometallurgical processes and sustainability issues as well as possibilities. The project has contained diverse analytical methods and many hours of laboratory work that has resulted in an increase in laboratory experience and expertise. The first experimental work consisted of hydrogen reduction and preparation of the ore. For his help with this we would like to thank Manish Kumar Kar. Further the leaching, purification and precipitation of the solutions were done at Berg, Gløshaugen. For his guidance and help with logistical and practical laboratory issues here, we would like to thank Mengyi Zhu. The solutions were analyzed using ICP-MS at Gløshaugen, for his help with this analytical work we would like to thank Kyyas Seyitmuhammedov. The solid residues and products were analyzed using XRD and XRF. For both these analytical methods we would like to thank Manish Kumar Kar for his help and guidance. Furthermore, we would like to thank our supervisor, Professor Jafar Safarian for his expertise and guidance throughout the entirety of the process.

Abstract

The HAlMan project team aimed to develop a sustainable process for producing manganese dioxide (MnO_2). They also work on production of alloys, with additional objectives of producing Mn-containing commercial steels and aluminum alloys and exploring the extraction of Critical Raw Materials. Among all the goals of HAlman project, this particular study focused on producing manganese dioxide from pre-reduced manganese ore via hydrometallurgical methods. Various purifying and precipitating agents across ten (10) different samples under varying parameters was tested. All 10 samples were leached with sulphuric acid as the leaching agent. Most of the samples were held for 2 hours whereas some were given 30 and 60 minutes of leaching period. The leachate was then purified with purifying agents such as lime (CaO) and calcium carbonate ($CaCO_3$). The purified solutions were then treated with precipitating agents, Potassium permanganate ($KMnO_4$), magnesium oxide (MgO), Magnesium carbonate ($MgCO_3$) and Sodium hydroxide (NaOH) for the recovery of manganese oxides. All the solid residue after filtration from each step were analyzed using XRF, XRD, and SEM while produced solution was analyzed with ICP-MS. The study found that leaching manganese from pre-reduced ore had a yield of around 80%, which was much greater than leaching of raw ore. This yield is still slightly low and improvements in temperature, pH, and S/L ratio could be explored to get a greater yield. Precipitation using potassium permanganate had a yield of 20-27%, while precipitation using magnesium carbonate had a yield of 40% and purity ranging from 47-62%. However, precipitation using magnesium oxide and sodium hydroxide were not successful, with low yields and purity. The study suggests potential adjustments to increase yield and purity for each precipitation method. Overall, the study demonstrates a commitment to sustainable production and finding innovative ways to reduce waste.

Sammendrag

HAlMan project team har som mål å utvikle en bærekraftig metode for produksjon av mangandioksid (MnO_2). De jobber også med produksjon av manganholdige legeringer for stål og aluminium i tillegg til å utforske ekstraksjon av Critical Raw Materials. Blant prosjektteamets mange mål fokuserer denne studien på produksjon av mangandioksid fra hydrogenredusert manganmalm ved bruk av hydrometallurgiske metoder. Ulike tilsetningsstoffers ble brukt på 10 ulike tester for å rengjøre prøven for urenheter og for å oppnå felling av mangandioksid og produkter som kan brukes for produksjon av mangandioksid. Alle 10 prøvene ble løst opp i svovelsyre. De fleste prøvene ble løst opp over 2 timer, mens tester ved 60 og 30 minutter også ble gjennomført. Løsningene ble deretter renset med tilsetningsstoffene kalsiumoksid (CaO) og kalsiumkarbonat ($CaCO_3$). Løsningene etter felling av urenheter ble deretter brukt for utfelling av manganoksider ved tilsetning av natriumpermanganat ($KMnO_4$), magnesiumoksid (MgO), magnesiumkarbonat ($MgCO_3$) og natriumhydroksid (NaOH). Faste stoffer som ikke ble løst opp eller felt ut underveis ble analysert ved bruk at XRF, XRD og SEM, mens løsningene før og etter hvert steg ble analysert ved bruk av ICP-MS. Denne studien oppdaget at 80% av mangan fra redusert manganmalm ble oppløst, som var markant bedre enn resultatene for ikke behandlet malm. Dette utbytte er likevel ikke optimalt og endringer i temperatur, pH og forhold malm/syre kan gjøres for å oppnå høyere utbytte. Felling ved bruk av natriumpermanganat hadde et utbytte på 20-27%, ved bruk

av magnesiumkarbonat var utbytte omtrent 40%, addisjon av natriumhydroksid og magnesiumoksid var mislykket i dette forsøket med lavt utbytte og renhet. Studien har kommet fram til ulike handlinger som kan tas for å oppnå økt utbytte og renhet for produktene hvor størst forbedring kan gjøres ved utfelling av urenheter. Studiet har hatt fokus på at prosessen skal være bærekraftig og utforsket ulike måter å redusere avfallsstoffer.

Table of contents

Chapter 1: Introduction

1.1 History of manganese

Manganese has a rich history dating back to ancient times. The first identification of manganese in minerals like pyrolusite is attributed to the Egyptians, who used it to control the color of glass and remove iron impurities. Romans also utilized it for the same purpose. Manganese was even used by pre-Columbian civilizations in the Americas to create black paint. In the 1400s, all manganese oxide ores were known as Braunstein. However, it wasn't until 1774 a Swedish chemist Carl Scheele recognized manganese as an element. The same year, Johan Gottlieb Gahn isolated it, leading to the industrial production of manganese (LibreTexts, 2023).

The use of manganese gained significant importance in the 1900s, particularly in Britain, where metallic manganese was used as a hardening alloy in the production of High-manganese steel for railways, bridges, dams, and other infrastructure developments. It (MnO2) serves also as a deoxidizer, removing oxygen from molten steel for cleanliness purposes. Today, manganese finds a variety of applications, including as an alloying element in steel, production of fertilizer, ceramics, and batteries. The discovery and development of manganese over the centuries have greatly contributed to our understanding of the natural world and its resources, which are crucial for achieving sustainable development (David B. Wellbeloved, 2000).

1.2 Manganese oxides in batteries

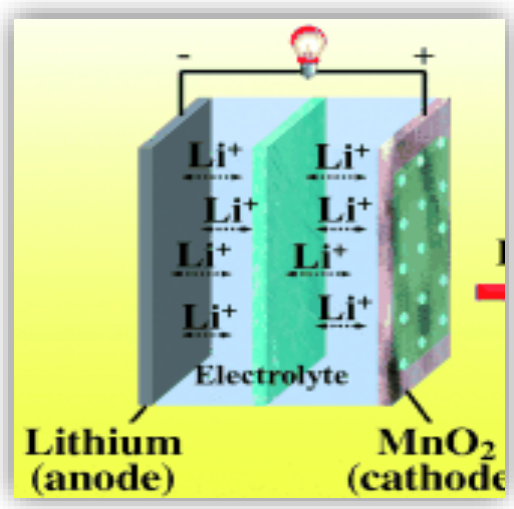

Figure 1.1: Li-ion battery with manganese dioxide (MnO2) as cathode and metallic Lithium (Li) as anode immersed in a favorable organic electrolyte *(Yuxiang Hu, 2015).*

Manganese dioxide (MnO_2) is a crucial component in certain lithium-ion batteries, serving as a cathode material as shown in Figure 1.1 (Liu, 2013). Its high theoretical capacity makes it a preferred alternative to graphite in certain applications, besides being a cost-effective and environmentally friendly material. With a range of lithium-ion batteries available, each with its unique characteristics, including self-discharge, cost, environmental impact, lifespan,

safety, energy density, and output, it's crucial to choose the right type of battery for specific applications (Dragonfly energy, 2022).

Lithium-ion batteries containing manganese oxides are commonly known as LMO batteries (Sino Voltaics, 2019). These batteries are favored for their exceptional safety and stability at high temperatures, making them ideal for use in pacemakers where safety is paramount, and drills where heat can be generated. LMO batteries also strike an efficient balance between specific energy and specific power, enabling their use in electric or hybrid vehicles with high power output and fast charging capabilities. The primary disadvantage of LMO batteries is their shorter lifespan compared to other lithium-ion batteries with comparable power outputs. Additionally, manganese dioxide is utilized in rMB batteries, which are rechargeable magnesium batteries that compete with their lithium-ion counterparts (Ling, 2017). In rMB batteries, manganese dioxide plays a more critical role due to the lack of cathode options, making MnO2 the preferred choice.

1.3 Motivations

The demand for MnO2, a key component in batteries, has been rapidly increasing in recent years, driven in part by the growing production of electric vehicles. The demand for manganese dioxide and other battery components has risen in response to this trend (Carlier, 2022). This is reflected in Figure 1.2, which shows the growth of electric vehicles using batteries which has multiplied almost ten times greater in 2021 than it was five years prior. This trend is expected to continue, as society becomes increasingly focused on environmental sustainability and the replacement of fossil fuels with renewable energy sources.

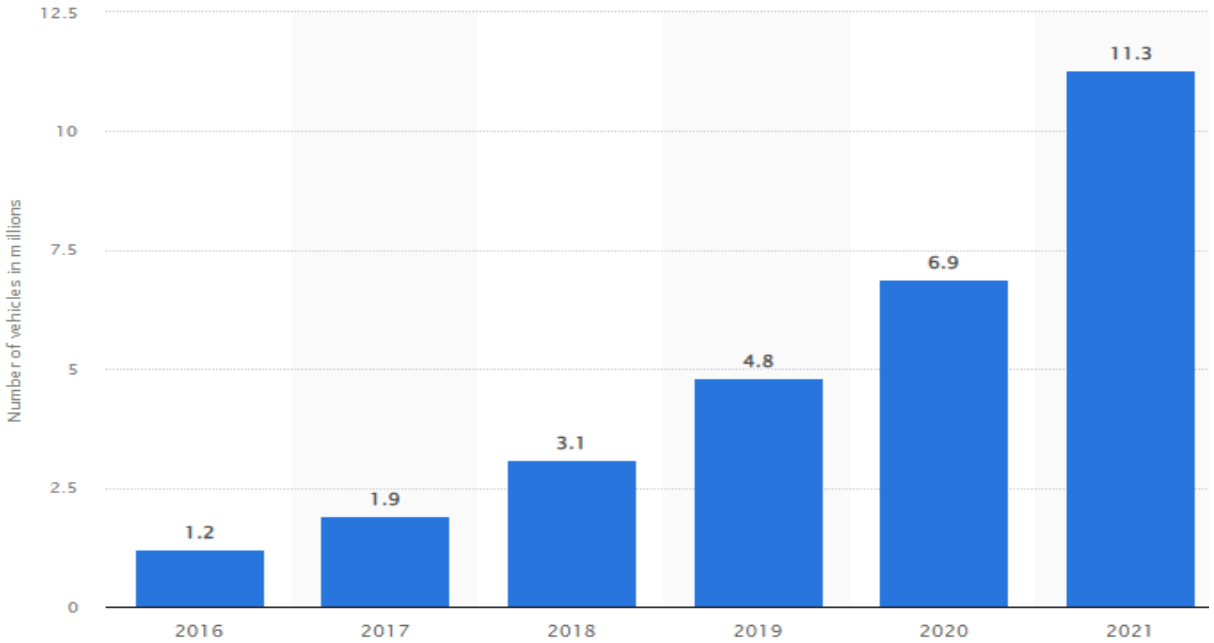

Figure 1.2: This image shows the growth in the market for electrical cars from 2016 to 2021 (Carlier, 2022).

The HAlMan project team's efforts to develop a sustainable process for producing manganese dioxide and alloys are crucial for meeting the increased demand for MnO_2 while ensuring

minimal impact on the environment. With 10 countries, 14 project partners, 3 universities and 4 research centers, the HAlMan project team has a broad and diverse expertise to develop an efficient and environmentally friendly process. The team aims to achieve low carbon footprint and energy consumption, as well as valorization of secondary raw materials, while generating zero solid waste. The team's goals align with the growing societal desire to mitigate climate change and promote efficient use of resources. By developing sustainable production methods, the HAlMan project team can make a significant contribution to the growth of the battery industry while minimizing its environmental impact. (HAlMan project team, 2023)

1.4 Goals of this study

This proposed bachelor thesis aims to investigate the production of manganese dioxide (MnO_2) through an integrated hydrometallurgical process that includes leaching of pre-reduced manganese ore under various process parameters. The primary focus is on achieving the precipitations of manganese dioxide (MnO_2) with minimal energy consumption and zero solid waste. The specific goals of this thesis can be summarized as follows:

- Leachability Comparison: Determining the leachability of pre-reduced Mn-ores (by H_2) as compared to the raw ore. This involves assessing the efficiency and effectiveness of the leaching process with pre-reduced ore and analyzing its impact on manganese extraction.
- Digestion of MnO and Other Components: Evaluating the leaching of pre-reduced Mn ore, specifically focusing on the digestion of MnO and other main components such as iron (Fe), calcium (Ca), magnesium (Mg) as well as other impurities present in the ore. This analysis helps in understanding the efficiency of the process in selectively extracting manganese dioxide while minimizing the extraction of unwanted impurities.
- Purification Agent Application: Exploring the application of purifying agent, namely Lime (CaO) and Calcium carbonate ($CaCO_3$) for the removable of dissolved impurities from leachate. This investigation aims to optimize the purification step and improve the purity of leachate, which is crucial for obtaining high-quality manganese dioxide.
- Evaluation of Various Precipitation Agents: Evaluating the application of different agents such as MgO, $KMnO_4$, $MgCO_3$ and NaOH to facilitate the production of Manganese dioxide(MnO_2) or intermediate Mn- compounds required for MnO_2 synthesis. This experimentation will help identify the most suitable precipitating agents that can achieve the desired precipitation of MnO_2 with the desired purity and yield.
- Characterization Techniques: To ensure a comprehensive understanding of the process and its outcome, the thesis will employ a variety of techniques for the characterization of the materials used in the process. These techniques include chemical analysis (XRF, ICP-MS), spectroscopic analysis, microscopic analysis

(SEM), and elemental analysis (XRD). The characterization aims to assess the properties and purity of produced manganese dioxide.

Chapter 2: Literature survey

2.1 Manganese dioxide production overview

Manganese dioxide (MnO_2) is primarily sourced from natural deposits, typically of sedimentary origin, that contain manganese ores like pyrolusite and manganite. It can also be found in other minerals, including pink rhodochrosite ($MnCO_3$) and Alabandite (MnS). Manganese-nodules or ferro-manganese concretions, which contain approximately 30-36% Mn, are another natural source of manganese and are found on the ocean floors of both the Atlantic and Pacific oceans (Cheng, 2007).

Commercial production of manganese is only possible using blends of ore that contain manganese in the form of an oxide. Among the various oxides of manganese, including Mn_2O_7, MnO_2, Mn_5O_8, Mn_2O_3, Mn_3O_4, and MnO, only MnO_2, Mn_2O_3, Mn_3O_4, and MnO occur naturally in manganese ores. Under normal conditions, MnO2 exists as the stable β-MnO_2 crystal structure, whereas other modifications such as α, γ, δ, and ε are not pure varieties of MnO2. Di-manganese trioxide (Mn_2O_3) exists in the α-modification, while γ-modification is metastable.Under normal conditions, β-MnO_2 crystal structure is the most stable form between the MnO_2 polymorphs (i.e , β- > α-> γ-> δ- and ε-type) (Takuya Hatakeyama a b, 2022).

The relative stability of each of these manganese oxide-states are highly influenced by the oxidation potential (Eh) and the pH level. For an efficient transformation of manganese oxides from Mn-ores into MnO_2 (IV), leaching should be performed in an acidic environment, which is explained through the Figure 2.1 below (Regeane M. Freitas, 2013)**.**

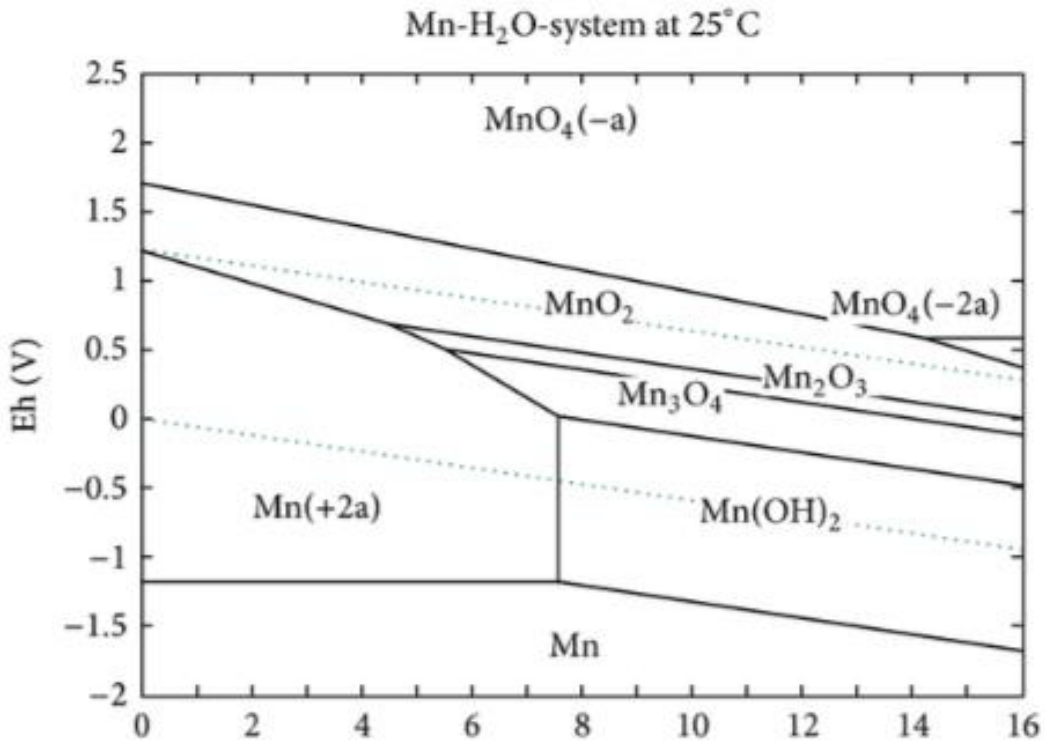

Figure 2.1: Eh-pH diagram showing predominant manganese forms *(Regeane M. Freitas, 2013).*

According to the US Geological Survey (USGS), global production of manganese through ore use was estimated to be 20 million metric tons in 2021 alone (Survey, 2022). Most of which are mined in developing countries like South Africa and Gabon. (JEssica Elzea Kogel, 2009) Whereas a truly small percentage of MnO_2 comes from secondary sources like recycled waste. Waste batteries, spent electrodes, spent catalyst, steel scraps, sludges and slag are few of the examples of secondary Mn-source. Industrial waste could also be an important source of manganese dioxide. Typically, when there is leaching of nickel ores, lots of manganese containing waste effluents gets rejected in subsequent processing steps which can be recovered with low cost (Wensheng Zhang, 2007).

Another major survey done by United Nations Environment Program (UNEP) suggests that about 80% of manganese can be recovered from a used battery. This data may vary depending on different regions, with some continents having advanced recycling technology while others lack infrastructure for efficient recycling. It is also important to note that recycling surely plays a vital role in reducing environmental impact, but this alone may not be a complete solution for the increasing demand of Mn as the process also require both energy and resource consumption. Hence improved product design and efficient (purity) resources must be prioritized (Programme, 2021).

The major reason for the significant interest in producing MnO_2 through natural sources is obviously due to their abundance (12^{th},0.096%) and low mining cost (Cannon, 2014). Production of manganese dioxide from natural sources can be done through different routes, but the most well-known method is surely via hydro-metallurgical route. This route involves leaching of ores by aqueous solutions and then purification takes place with MnO_2- recovery at the end.

2.2 Hydrometallurgical production of MnO_2

Hydrometallurgical method is a well-established process in producing Mn like metals due to their efficiency and flexibility. It has several advantages over the classical pyrometallurgic process, including lower energy consumption, low emission of greenhouse gases and no fossil fuel consumption. On this route, aqueous solution is used for extraction and additives are added for the purification of metals from ores or waste. This method is applied for the production of MnO_2 as well due its effectiveness and for a greener approach. Producing MnO_2 via hydrometallurgy requires three major steps: leaching of Mn-ores followed by purification of leached solution and precipitation of MnO_2.

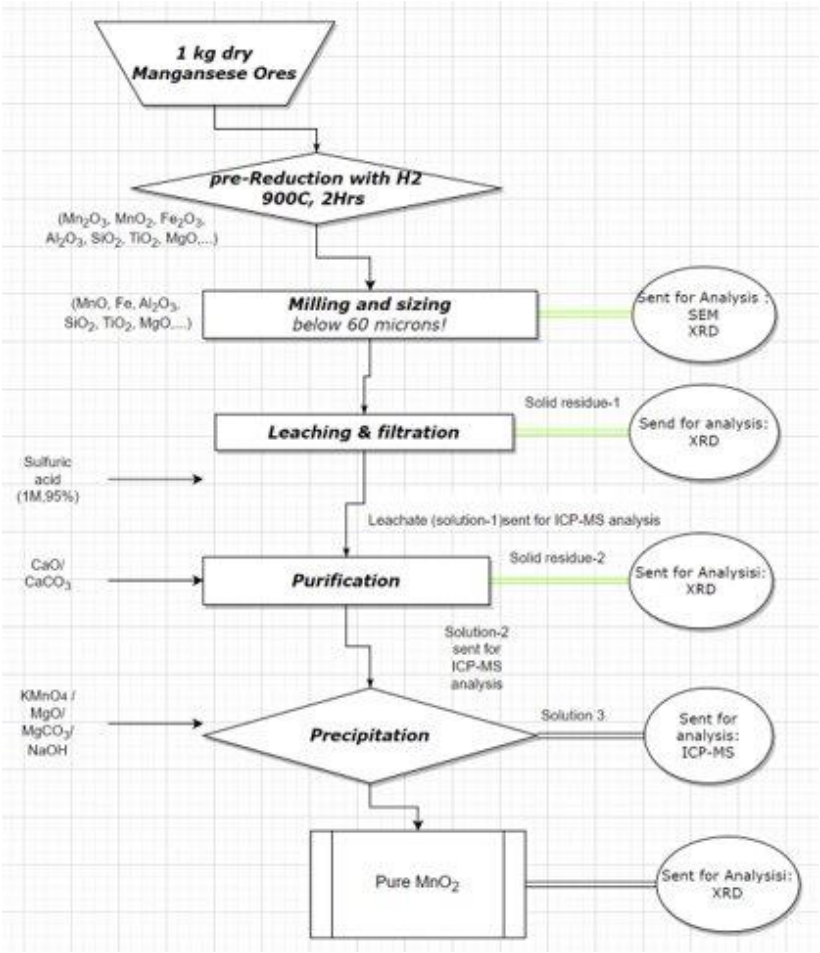

Figure 2.2: Flow diagram for leaching of pre-reduced Mn via integrated hydrometallurgical method for pure MnO_2 production (made by us)

Before hydrometallurgical process, a pre-treatment/pyro-metallurgical process, can be beneficial as it helps in treating low grade Mn-ores and manganese nodules containing Ni, Co etc. as their oxides. These metal oxides occur in lattices of iron and manganese oxide. Thus, breaking up these lattices is essential for proper recovery of valuable metals. Pretreatment of ore is also favorable for improving leaching efficiency. Pretreatments include smelting, reduction/roasting, sulphation and chloridization. However, the most employed method in the manganese industry by far is reduction roasting (700°C-900°C) followed by sulfuric acid leaching (Didier Ngoy, 2020).

2.2.1 Leaching of Mn ores

One of the crucial steps in the hydrometallurgical production of manganese dioxide is leaching. Typically, it involves use of acidic or alkaline solutions such as sulfuric acid, nitric acid, ammonium hydroxide and potassium hydroxide, which helps to dissolve Mn minerals present in the ores. The choice of right leaching agent depends on the grade of the ore and desired purity whereas other factors like particle size and minerology can also influence the process.

Before the leaching process, ores of the sample are usually crushed and milled to favorable size. Leached solution is then separated through filtration or just by settling. The leachate is then subjected to further treatment for recovering valuable metals like Mn. The reaction equation below shows clearly, the formation of manganese sulphate after leaching, meaning separation of Mn from the gangue. Leaching of Mn-ore with sulphuric acid is shown below as a reaction equation(2.1). (Markus Antonius Elinsønn Pedersen, 2022)

$$MnO\ (s) + H_2SO_4(l) \rightarrow MnSO_4\ (aq) + H_2O \qquad (2.1)$$

Leaching can be carried out in both batch and continuous mode, depending on the desired product. For the maximum yield of the product, certain optimization is necessary to be carried out. Factors like acid concentration, temperature and agitation rate are some of the leaching conditions which can be optimized for better results. (Team, 2023)

2.2.1.1 Raw Mn ores

Direct leaching of Mn-ores, without pre-treatment can result in low purity of final product as well as less recovery of valuable metals. This is due to the presence of impurities in the ores like iron and silica which can interfere with the leaching process resulting in low Mn-recovery. It can also raise the leaching duration, making it more energy intensive for metals/metal oxide production. (ONAL, 2021)

To get a successful result, it is recommended to pre-treat the metal ores that helps in converting higher-oxidative state oxides to lower ones, making it readily soluble in leaching agent.

2.2.1.2 Pre-treated Mn ores

Mn-ores collected from natural sources are pre-treated before leaching, to help improve the efficiency of the leaching process and the purity of the final product. These pre-treatment steps are particularly for low-grade ores, where impurities are more than the desired metal.

Roasting involves heating the ore in presence of O_2 or air to convert Mn-ores to more soluble form. In the process, the high temperature causes removal of impurities like sulfur and organic matter, while converting Mn minerals into more reactive oxides or hydroxides. In case of reduction, ores are heated in the presence of a reducing agent such as hydrogen or carbon, making Mn- minerals more soluble. It is used as a pre-treatment step for Mn-ores with high iron content as it reduces the amount of iron present in the ores and makes it more accessible

to the leaching agent. Increased surface area of the ores caused by the reduction takes it further nearer to the leaching agents and improves the leaching efficiency. (Didier Ngoy, 2020)

The reduction reaction by hydrogen can be presented as seen in Formula 2.3-2.5. (Didier Ngoy, 2020)

$$MnO_2(s)+H_2(g)= Mn_2O_3(s)+H_2O(g) \quad (2.3)$$

$$3Mn_2O_3(s)+H_2(g)= 2Mn_3O_4(s)+H_2O(g) \quad (2.4)$$

$$Mn_3O_4(s)+H_2(g)= 3MnO(s)+H_2O(g) \quad (2.5)$$

Reaction equation 2.3-2.5:- Process shows conversion of higher valent manganese oxide to lower ones, making it readily soluble in sulfuric acid.

Sulphation roasting is roasting of Mn-bearing materials in presence of sulfuric acid/ ammonium sulfate. It is more common in recycling zinc-carbon batteries for Mn-production. Maximum Mn-recovery can be achieved in presence of ammonium sulfate where the gaseous SO_2 acts as both reductant and a sulphation agent. The major goal here is to convert metals/oxides into water soluble form so that it can be easily separated from the impure materials (gangue). (Mehta, 2016)

2.2.2 Purification of Mn-containing solutions

After leaching, the solution obtained (after filtration) contains various impurities such as iron, aluminum, calcium, magnesium etc., which need to be removed to obtain pure $MnSO_4$ solution for MnO_2 production. The purity of the product is the major goal of any metal production. The purification technique includes solvent extraction, ion exchange, and precipitation (Zhi-liang ZHU, 2006) (Guillaume Zante a b, 2020). The Choice of method depends on the nature and concentration of unwanted impurities present in the solution, as well as desired purity of the final product.

In Solvent extraction, an extractant such as di(2-ethylhexyl) phosphoric acid (D2EHPA) is used to selectively extract Mn ores to an organic solvent. The organic solution is then separated from the aqueous phase, and then a stripping agent is used to strip Manganese (Guillaume Zante a b, 2020).

When it comes to ion-exchange methods, selective exchanges of ions take place with ions of similar charge on a solid ion exchange resin. Via this method a resin, such as cation exchange resins are used to selectively adsorb impurities in $MnSO_4$ solution and then eluted from the resins carefully to obtain a purified $MnSO_4$ solution. (Zhi-liang ZHU, 2006) . This method is more environmentally friendly and easier to control, but use of resins can draw this method a limitation. This is due to the limited capacity of resins for adsorption of particular metals and

therefore more suitable for removing only trace amount of metal impurities. (Wensheng Zhang, 2007)

One of the most widely used methods for removing impurities from $MnSO_4$ solutions is precipitation technique. In this technique, precipitants like lime, sodium carbonate and caustic soda are used to precipitate impurities from the solution which are later removed via filtration leaving behind a clear and pure $MnSO_4$ solution (Wensheng Zhang, 2007).

2.2.3 Mn dioxide and compounds recovery from solutions

The third and final step in the production of MnO_2 involves recovery of Mn compounds from the purified solution. After all the impurities present in the ores have been removed, the purified leach solution is further treated to recover pure MnO_2. There have been several methods used in recent years depending on the nature of solution, cost, feasibility of the method and purity requirements. Most common methods include precipitation of purified solution with suitable agent(precipitant), electrolytic and thermal decompositions.

2.2.3.1 Precipitation by different agents

The most common method, precipitation, requires an oxidizing agent such as sodium hypochrolite, hydrogen peroxide or potassium permanganate, which is added to the purified solution. The addition of oxidizing agents converts the Mn (II) species to insoluble MnO_2, which is then separated using filtration or letting it settle on its own to obtain pure manganese oxide. The efficiency of precipitation depends on the pH of the purified solution, temperature, and concentration of the precipitating agent.

When using MgO as the oxidizing agent, it promotes oxidation of manganese ions to form MnO_2 due to its strong base nature. The following reaction takes place during precipitation using MgO. (M. Yoshida, 2016)

$$4Mn^{2+} + O_2 + 2H_2O + 4MgO \rightarrow 4MnO_2 + 4Mg(OH)_2 \quad (2.6)$$

Whereas using KMnO4, a strong oxidizing agent, it undergoes reduction to MnO_2 due to the presence of sulfuric acid in the solution. It should also be noted that using KMnO4 results in formation of byproducts like potassium sulfate and manganese sulfate which may degrade the purity of the final product (B.Mishra, 2003). The very reaction is shown below.

$$2KMnO_4 + 3H_2SO_4 + 5MnSO_4 \rightarrow 7MnO_2 + K_2SO_4 + 3H_2O + 3SO_2 \quad (2.7)$$

2.2.3.2 Electrolytic deposition

Electrolytic deposition is known to be highly effective in production of higher grade MnO_2. A study done by J.N. Sahu and his colleagues reported a staggering deposition efficiency rate of

around 95% from a solution containing $MnSO_4$ and H_2SO_4. The deposition was carried out at a constant current density of 2A/dm2, at room temperature for 60 minutes. (Sahu, 2002)

In this method for MnO_2 recovery, Mn-containing solution is electrolyzed using an inert anode and a cathode, usually made of graphite or any stainless steel. Mn(II) ions, under an applied electric potential, get oxidized at the anode and form MnO_2, which is then electrodeposited on the surface of the cathode. It is a promising technique to obtain pure MnO_2, but it is important to note that the quality and purity of the MnO_2 depends purely on the composition and pH of the solution, as well as the current density and temperature.

2.3 Characterization methods

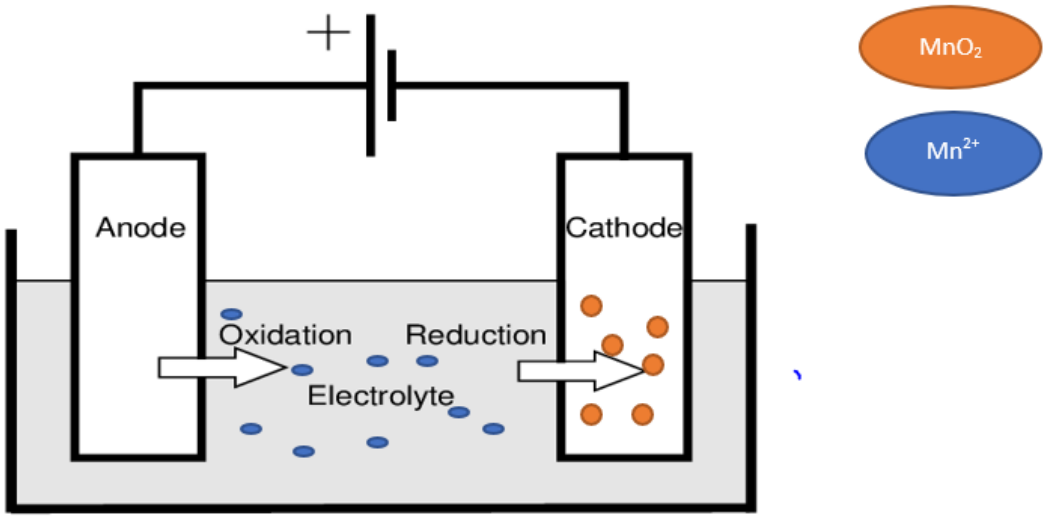

Figure 2.3: A schematic of electrolysis process for MnO2 production *(Katsioulas, 2021)*

There are many different analytical techniques that can be used to characterize properties of materials. It is used to analyze phase and microstructure of materials as well as to determine the composition of the final product. In this thesis, the advanced characterization techniques used are XRD, SEM and ICP-MS, which are presented below.

2.3.1 Phase analysis by XRD

XRD is an analytical technique, commonly used to determine crystallographic structure of materials by enabling chemical composition identification. It is a non-destructive method which provides information on the phase composition of the sample. Under leaching and purification of Mn ores, XRD can be used to determine different phases present in the ore as well as the byproducts obtained after purification. XRD results a patterned graph with several peaks which are identical to the crystalline structure of phases. Additionally, it can be used for estimation of amount of each phase depending on intensity of diffraction peaks. The Following diagram shows a usual XRD machine schematic with a detector device attached to it (Mahadeshwara, 2022).

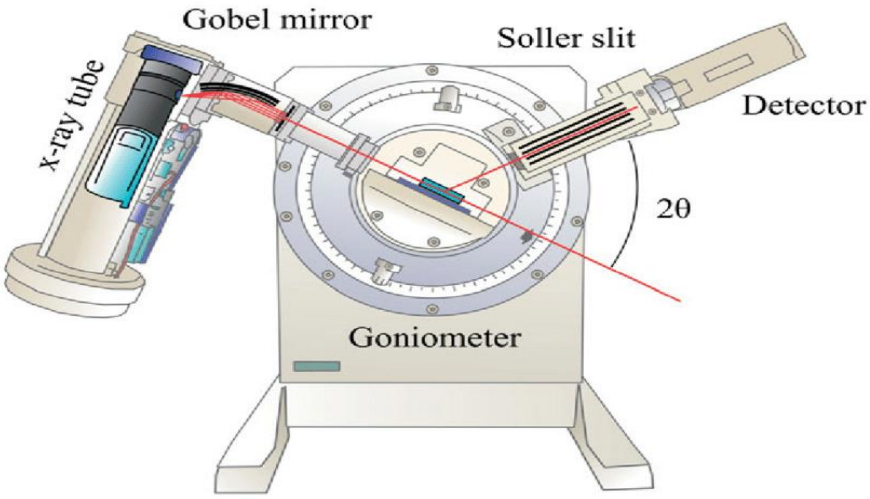

Figure 2.4: Schematic of a XRD machine with detector attached (Mahadeshwara, 2022).

2.3.2 Microstructure analysis by SEM with EDS attached:

SEM is a powerful magnifying technique that allows observation of the morphology, microstructure of material at high magnification. It is used to analyze the morphology of the ore particles, structure and puirty of the product. SEM provides a detailed view of the surface topography and other physical features of any material providing insights into the production processe. This can play a vital role to infer the mechanism of reactions. (board, 2022)

EDS or EDX is a technique used for analysis of micro-scale chemical composition. It is connected with SEM instrument to derive compositional information from X-rays which are emitted when the electron beams scans over the sample. (Technology, u.d.)

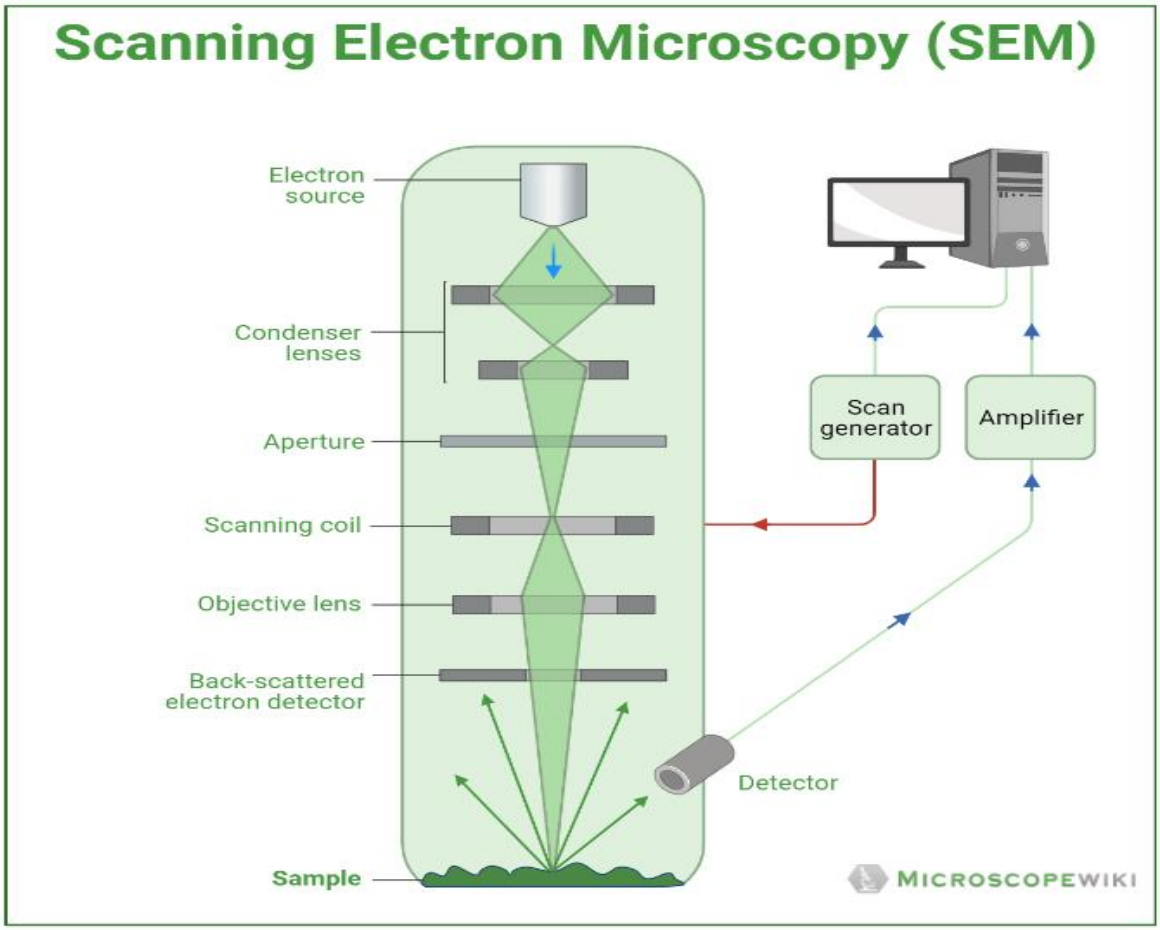

Figure 2.5: A detailed figure of Scanning electron microscopy device which is connected to an output for data display. *(board, 2022)*

2.3.3 Chemical composition study

2.3.3.1 ICP-MS

Abbreviated for "Inductively coupled plasma mass spectrometry", ICP-MS, is an elemental analysis technique used for determining elemental composition of the ore, byproducts resulted after leaching as well as concentration of impurities. It is an extremely sensitive and precise method for quantification of trace elements present in the sample. (Kashani, n.d.)

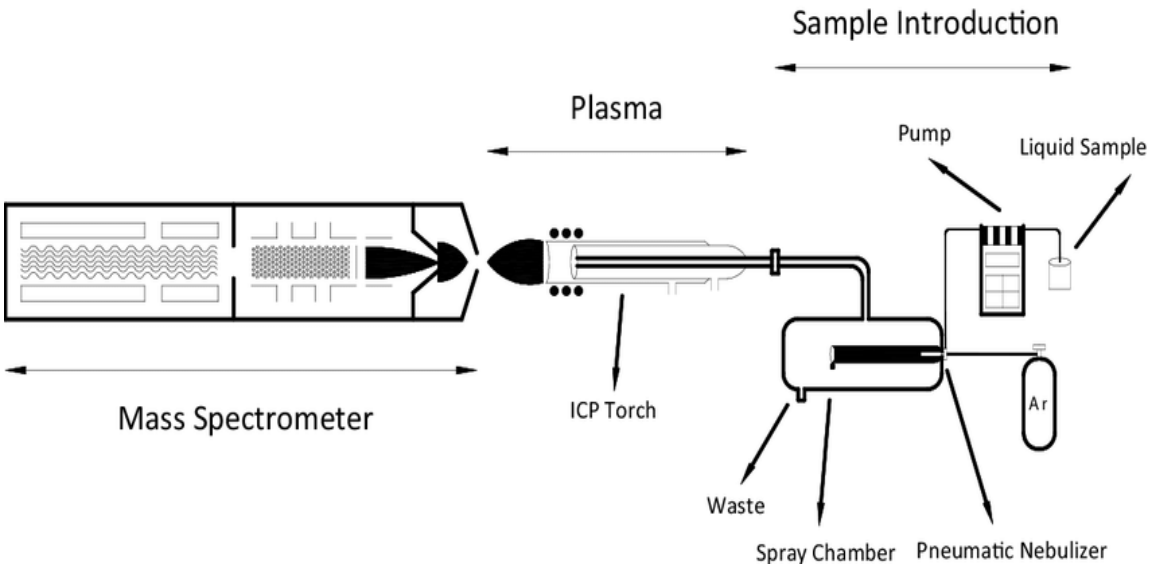

Figure 2.5.: Schematic of ICP-MS major components: sample introduction system, plasma torch, and mass spectrometer *(Kashani, n.d.)*

The mechanism of ICP-MS is such that the sample is introduced into an inductively coupled plasma, a high-temperature ionized gas, that excites the atoms present in the sample, converting it into positively charged ions. These positively charged ions are then directed further into a mass spectrometer for the separation based on their mass to charge ratio. The results are then detected and presented into an output such as a computer.

2.3.3.2 XRF

X-ray fluorescence spectroscopy, a type of spectroscope used to determine the elemental compositions of materials as well as impurities that are present in the product. In producing MnO_2, XRF can be used to determine the concentration of impurities like Fe, Ca, Mg, which can affect the purity of the final product, MnO_2 (Lim, 2013).

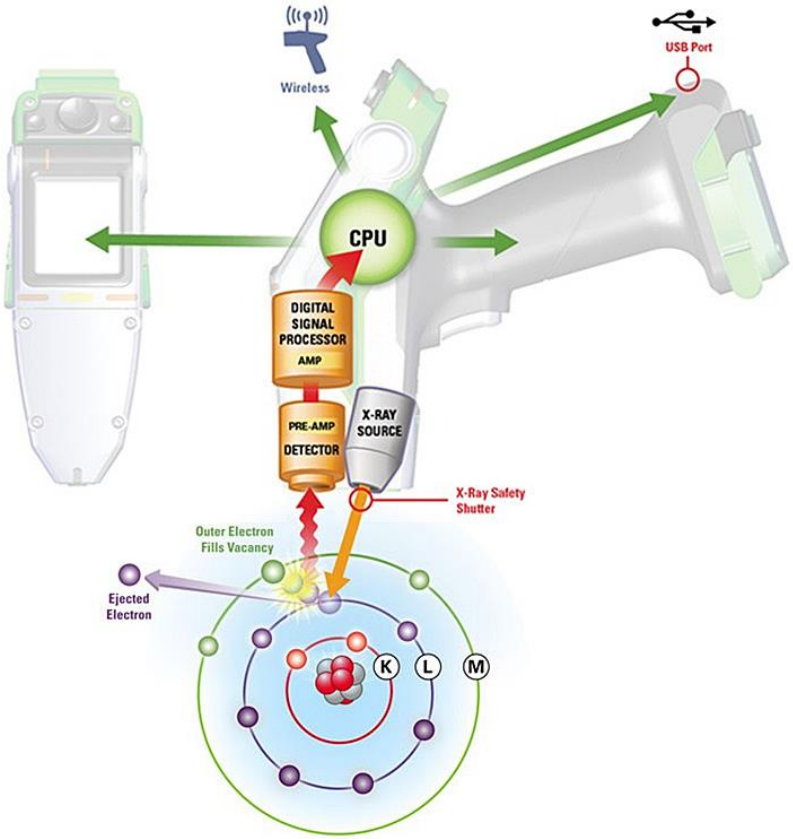

Figure 2.7 : An X-ray fluorescence device where the source (Xray-tube) is used for excitation of the sample electrons and the emitted X-ray-fluorescence radiation is detected by the detector. *(Lim, 2013)*

Chapter 3: Methodology

3.1 Materials and preparations

The materials used in this project was:

- Nchwaning manganese ore received from OFZ in Slovakia shown in Figure 3.1:

Figure 3.1: Nchwaning manganese ore - Non reduced.

- Concentrated sulfuric acid (98%-95%) produced by Sigma-Aldrich
  - CAS-No. 7664-93-9
- Potassium permanganate produced by Sigma-Aldrich, ≥99.0% purity, Cl <0.005%, SO_4 < 0.02% and Hg < 0.05 ppm.
  - CAS-No. 7722-64-7
- Calcium oxide produced by Sigma-Aldrich ≥99.9% purity (Lime, quicklime).
  - CAS-No 1305-78-8
- Calcium carbonate produced by Junsei ≥99.5% purity.
  - CAS-No 471-34-1
- Magnesium oxide produced by VWR chemicals ≥99.6% purity, Cl < 0.05%, Fe < 0.01%, SO_4 <0.1%
  - CAS-No 1309-48-4
- Sodium hydroxide produced by Sigma Aldrich ≥98.0% purity.
  - CAS-No 1310-73-2

3.1.1 Pre-reduction of Mn ore by hydrogen

The manganese ore (1 kg) was reduced by hydrogen in a vertical tube resistance furnace as shown in figure 3.2. The heating of the furnace was done with 1Nl/min of argon gas until the temperature was 200°C. The program then set the gas flow to be 4Nl/min of Hydrogen gas until the furnace was 900°C. The reduction was then done at 900°C with 4Nl/min of pure

hydrogen gas for 120 minutes. After reduction was complete, the cooling program was put on, where the flow consisted of 95% argon and 5% hydrogen for 120 minutes to low temperatures. This process is shown in Figure 3.3. Hydrogen is present in the cooling program to ensure that the gas flow does not contain a significant amount of oxygen seeing that the argon gas is 99% pure, which could mean up to 0.2% of the gas flow could be oxygen. This would result in oxidation of the sample and must be hindered.

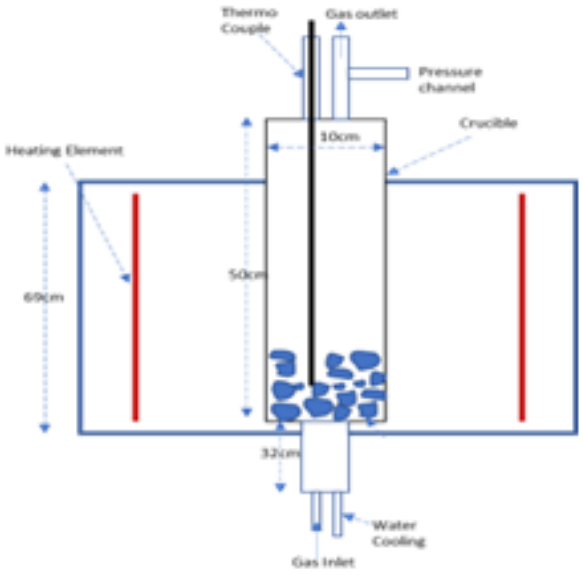

Figure 3.2: Schematic view of vertical tube furnace used to reduce Mn ore.

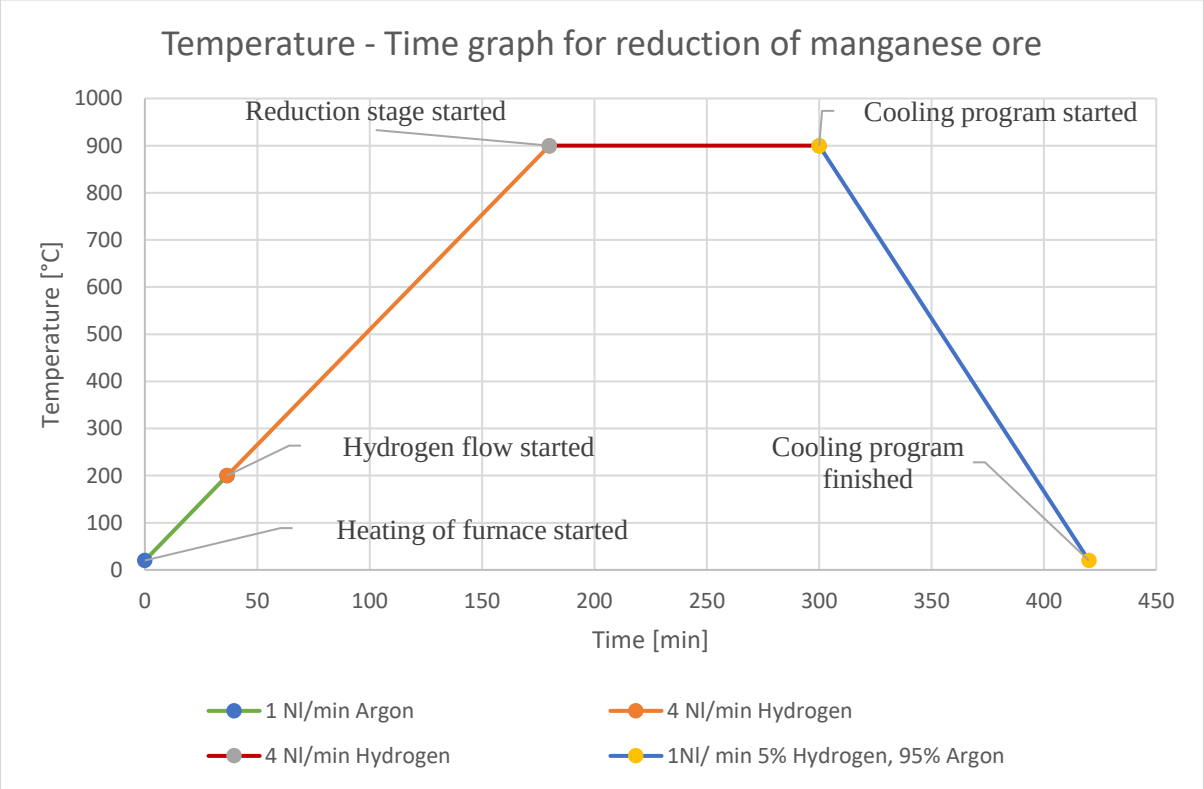

Figure 3.3: Shows the process of manganese ore reduction.

3.1.2 Milling and sizing of pre-reduced ore

The pre-reduced ore was milled by first transferring the sample into a metal container. This metal container was placed inside of the milling machine (ring mill) as shown in Figure 3.4. This machine then rotate/shakes the metal parts and sample until it is crushed into small pieces. After milling the metal container is opened and the sample is transferred into a sieve for sizing. This procedure is done under a local exhaust ventilation and while wearing a mask to prevent breathing in dust. The sieve with the material was then shaken until all particles smaller than 60 microns passed through. The remaining oversized sample was then re-milled, and the sizing process was repeated to have all particles below 60 microns. The powder is shown in Figure 3.5.

Figure 3.4: Shows the milling machine with sample placed inside.

Figure 3.5: Reduced ore after milling to <60 microns.

3.1.3 Preparation of leaching solution

The leaching solution used in this project was 1M sulfuric acid made from concentrated sulfuric acid(98%-96%) through the standard method for acid dilution. Each test would need 500 ml and there would always be 2 tests running at the same time. Therefore, 1 liter of 1M sulfuric acid was made by filling a 1000 ml volumetric flask halfway with distilled water. After this was done, 56 mL of concentrated sulfuric acid was added to the flask inside a fume hood. Finally, the flask was filled with distilled water to a total volume of 1000 ml. This process was repeated each time a new test would be done. In total 5 liters were made for the 10 tests.The calculation of acid necessary to have a concentration of 1M from 96% sulfuric acid is shown below in Formula 3.1-3.4 with density of acid= 1,83 g/cm^3 and molar mass of acid 98,1 g/mol and assuming 100 grams of material.

$$Find\ volume\ of\ 100\ grams: \frac{m}{\rho} = \frac{100g}{1.84\frac{g}{cm^3}} = 54.35\ ml \quad (3.1)$$

$$Find\ mass\ of\ H_2SO_4\ in\ 1000\ ml: 1L * \frac{m_{H2so4}}{V} = 1000ml * \frac{95}{54.35} = 1748\ g \quad (3.2)$$

$$Molarity: \frac{m}{Mm} = \frac{1748}{98.1} = 17.82\ moles \quad (3.3)$$

$$Diluting\ to\ 1M\ C_1 * V_1 = C_2 * V_2 = V_2 = \frac{C_1 v_1}{C_2} = \frac{1\frac{mol}{L} * 1\ L}{17.82\frac{mol}{L}} = 0.056L = 56mL \quad (3.4)$$

3.2 Hydrometallurgical processing

3.2.1 Leaching and classification

The leaching of the raw ore and the pre-reduced ore was done inside a fume hood. Beakers were placed on top of hot plates with magnetic stirring. Thereafter, 500 mL of the acid solution was added to the beakers before weighing 50 grams of reduced ore and adding it to the beakers. For test nr.1, 30 grams of raw ore was added to 300 mL acid. Hence, liquid to solid ratio for all experiments was L/S=10 mL/g. Once the ore was added to the beakers, the top was covered with aluminum foil to minimize any loss under heating. The temperature of the solutions was measured at various stages of the leaching process to ensure that the temperature was stable at roughly 40 °C. The only difference in leaching conditions for the different test was leaching time and data for this is shown in Table 3.1.

Table 3.1: Leaching parameters for each test.

Test number	Material	Leaching time [minutes]
1	**Ore**	**120**
2	**Reduced ore**	**30**
3	**Reduced ore**	**60**
4	**Reduced ore**	**120**
5	**Reduced ore**	**120**
6	**Reduced ore**	**120**
7	**Reduced ore**	**120**
8	**Reduced ore**	**120**
9	**Reduced ore**	**120**
10	**Reduced ore**	**120**

After leaching, the solution was filtrated through a filter with particle retention of 5-13 microns. This was done with a setup shown in Figure 3.6. This was made by placing a Büchner funnel on top of a large glass filtering flask, with a flask support ring made of rubber between them to eliminate air leakage. The flask was connected to an electric pump to create suction. The liquid was collected in the filtering flask and the solid residue retained by the filter paper was moved to a small beaker for drying. The same filtration process was also repeated after purification and precipitation to separate the solid and liquid residues.

Figure 3.6: Filtration setup for separation of solid residues from solutions.

3.2.2 Purification

In this study, the purification was carried out by adding differing amounts of calcium oxide or calcium carbonate as additives to purify the leached reduced ore. The process was started by placing the leachate solution onto a hot plate and heating to 40 degrees before any further actions. Once the solution was adequately warm, different amounts of the additives were added to the solution as shown in Table 3.2. These amounts were based on the results from test number 4 in the table where calcium oxide was added until the color changed from light purple to dark brown. This was also done for test 2 and 3 but had different leaching conditions than the rest of the tests. After the additives were put inside the beakers, aluminum foil was placed on top of the beaker and the solutions were left to mix for 120 minutes. In this process the temperature was also monitored with a thermometer along the way to ensure the stability of the heat.

Table 3.2: Purification parameters for test 2-10.

Test number (leachate number)	Additive	Amount added [g]
2	**CaO until color change**	**0.49**
3	**CaO until color change**	**0.28**
4	**CaO until color change**	**0.57**
5	**0.8*test 4**	**0.46**
6	**0.6*test 4**	**0.34**
7	**0.4*test 4**	**0.23**
8	**0.2*test 4**	**0.114**

9	No additives	No additives
10	$CaCO_3$ 0.6*molar equivalent of test 4	0.61

The amount added in test 5-8 was calculated by multiplying the amounts of grams added with the amounts from 0,8-0,2. The amount of $CaCO_3$ added was calculated as the same amount of moles $CaCO_3$ as CaO in test 6. Shown in Formulas 3.5-3.7 shown underneath.

$$Factor * amount\ added\ for\ color\ change = 0.6 * 0.57 gram = 0.34\ gram \quad (3.5)$$

$$\frac{Weight\ of\ CaO\ additive}{Molar\ mass\ og\ CaO} = moles\ of\ CaO = \frac{0.34 grams}{56.08} = 6.06 * 10^{-3} mole \quad (3.6)$$

$$n\ CaO * Mm\ of\ CaCO_3 = weight\ CaCO_3 = 6.06 * 10^{-3} mole * 100{,}09 \frac{g}{mole} = 0.61 g \quad (3.7)$$

3.3.3 Precipitation of Mn compounds

3.3.3.1 Precipitation using potassium permanganate ($KMnO_4$)

Precipitation of manganese dioxide was carried out by the addition of potassium permanganate. This was done by the addition of a saturated solution containing 5 g/100ml for test 2 and 3. For test 4, potassium permanganate was added as a solid. The addition was done on a hot plate at 40 degrees, while measuring the pH and temperature of the solution until no changes were observed. The reaction that occurs in this precipitation is shown in Formula 3.8.

$$2KMnO_4 + 3Mn^{2+} + 2H_2O \rightarrow 5MnO_2 + 2K^+ + 4H^+ \quad (3.8)$$

108 milliliters of the solution was added to test 2, while 115 ml was added to test 3. To test 4, 5.5 grams were added. Both the solution and the salt were added slowly while tracking the changes in pH between each addition. New additions of agents were made once pH was stable. This was repeated until pH stopped changing with the addition of agent. The data for additives in test 2-4 is shown in Table 3.3.

Table 3.3: This table shows additives in precipitation for test 2-4.

Test number	Additive	Amount	pH after addition
2	$KMnO_4$ (liquid)	108 mL	2.11
3	$KMnO_4$ (liquid)	115 mL	1.93
4	$KMnO_4$ (solid)	5.5 g	-

3.3.3.2 Precipitation using magnesium oxide (MgO)

The precipitation using magnesium oxide was done by transferring 350 mL of filtrated solution from the purification step into a beaker. The beaker was placed on a hotplate at 40°C while stirring. This was done inside of a fume hood. After the solution was pre heated to 40 degrees the magnesium oxide was added to the beaker and aluminum foil was put on top of the beaker.

The color slowly changed from yellow before addition, to grey after addition and finally a cloudy blue-green color after 120 minutes.

This process was repeated for tests 5-7. The details of their additives are given in Table 3.4. The theoretical amount of magnesium oxide added was calculated based on Formula 3.9 and 3.10 with the assumption that a maximum of 20 grams of Mn could be in the sample. Sample 6 and 7 was then calculated by multiplying with the factor of 0.8 and 0.6.

$$Calculation\ of\ moles\ Mn\ in\ 500\ mL: \frac{m}{Mm} = \frac{20g}{54.94\frac{g}{mol}} = 0.36\ mol\ in\ 500\ mL \quad (3.9)$$

$$Calculation\ of\ m\ MgO: \frac{V_1}{V_2} * n_{Mn} * Mm_{MgO} = \frac{350}{500} * 0.36 * 40.30 = 10.16\ g\ MgO \quad (3.10)$$

Table 3.4: shows additives and amount for test 5, 6 and 7.

Test number	Additive	Amount [g]
5	**Theo. MgO**	**10.16**
6	**0.8* Theo. MgO**	**8.12**
7	**0.6* Theo. MgO**	**6.09**

3.3.3.3 Precipitation using magnesium carbonate($MgCO_3$)

The process of precipitating manganese carbonate was done with the addition of magnesium carbonate. This was done in the same way as addition of magnesium oxide explained in Chapter 3.3.3.2. The theoretical amount of $MgCO_3$ added was calculated with the same assumption as in Chapter 3.3.3.2 and is given in Formula 3.9 and 3.11. These amounts are given in Table 3.5.

$$Calculation\ of\ m\ MgCO_3: \frac{V_1}{V_2} * n_{Mn} * Mm_{MgO3} = \frac{350}{500} * 0.36 * 84.32 = 21.25\ g\ MgO \quad (3.11)$$

Table 3.5: Additives and amounts for precipitation of test 8 and 9.

Test number	Additive	Amount [g]
8	**Theo. $MgCO_3$**	**21.25**
9	**0.8* Theo. $MgCO_3$**	**17.0**

3.3.3.4 Precipitation using sodium hydroxide (NaOH)

Precipitation of solids from the solution using sodium hydroxide was only done with test 10. This was done with a beaker filled with 350 mL of solution from purification of test 10. After the beaker was filled, it was placed on a hotplate at 40 °C while stirring. Then sodium hydroxide was slowly added, piece by piece and pH change was observed. This was done until the pH was around 8. Then it slowly dropped to around 7.3-7.5 between each addition. This is because the precipitation only takes place at pH around 8. The process of adding sodium hydroxide until pH 8 was repeated until it stopped dropping. The color of the solution changed from a yellow color to a dark solution with a hint of green. In total 3.6 grams of sodium hydroxide was added.

3.3 Characterization of materials and products

3.3.1 SEM studies

The reduced ore and the raw ore were compared by SEM analysis. For this to be done, the samples were first prepared by molding them. They were then filed by using precision crystal surface grinders and polishers. Water was added and the sample was held flat to the surface while moving it in the opposite direction the grinding-surface was rotating. This was done first at 100 grit and repeated for all available grits up until 4000. After polishing, the sample was washed with water and soap, then ethanol. After washing, the sample was placed inside a shaking device which allowed for all small particles to be removed from the surface. The final stage of sample preparation was then to coat the samples using gold and the area besides the sample is marked with carbon tape to find the sample easily under the microscope. The sample is shown in Figure 3.7.

Figure 3.7: Shows sample 1 prepared for SEM, molded and coated.

Powders of the products, leaching and purification residue as well as powdered reduced ore was also prepared for SEM studies. This was done by first cutting a small aluminum stick into pieces, then grinding the edges of these pieces to hinder sharp edges. Thereafter, small pieces of carbon tape were placed on each aluminum piece. With a spatula, small amounts of powder were placed on top of the carbon tape and pressed down on it. Excess powder was then removed, and the samples were ready for analysis.

The analysis was performed by regulating the height of the sample and then placing it inside the machine. The machine was then locked and vacuum sealed. The images were then obtained at different magnifications while adjustments of the brightness and focus were made for optimal imagery. EDS analysis was also done using the machine by turning on the connected EDS box and choosing the analysis option. Mapping and compositional analysis was performed on all samples, both powdered samples and molded ores.

3.3.2 XRD studies

XRD samples were prepared by first grinding the solid residue by hand with a mortar and pestle until the powder was adequately small. The powder was then transferred to a small sample holder as shown in Figure 3.8. The holders were filled with a surplus of powder to ensure that the surface of the sample will be flat. This is done by scraping the sample with a flat glass piece back and forth before removing the surplus powder. The machine in use is a D8 Discover XRD machine. The machine is operated by first unlocking the doors with the push of the "open door" button which allows for the doors to be opened. Then the sample is placed onto the sample stage fixture. The sample is locked in place by pressing the sample stage up until the sample holder is flush with the sample stage and the overhanging piece of the stage. Thereafter, the doors can be locked, and the scan is done using the computer connected to the machinery. After analysis, the sample is removed by opening the doors with the button and then holding onto the sample holder while lowering the stage until it is loose and can be removed.

Figure 3.8: Shows samples ready for XRD.

3.3.3 ICP-MS sample preparation and analysis

ICP-MS samples were diluted from the process solutions (leachates, purified solutions and after precipitation) to concentrations that can be handled by the machine in use. The limits for the machine used in this project are shown in Table 3.6. The main component in the sample is Mn with a concentration of 67 g/L if 100% is leached. The dilution necessary was calculated based on table and was done in two steps with an overall factor of 8.333 333. To make sure the sample would remain dissolved in the sample, 0,3 grams of HNO_3 was added to 50 ml flasks. Then 20 microliters of liquid sample were added using an automatic pipet. Thereafter, the container was filled to a total volume of 50 mL. The samples were then diluted once more by

adding 0,3 grams of HNO_3 acid to a new 50 mL flask. 15 microliters of diluted sample were then added before the flask was filled to a total volume of 50 mL.

Table 3.6: Shows limitations for ICP-MS sample analysis in this project.

Element	Concentration ranges that can be measured [micrograms/L]
Si	**10 - 5 000**
S	**10 - 5 000**
K	**10 - 5 000**
Na	**20 - 10 000**
Mg	**10 - 5 000**
Al	**2 - 1 000**
Ca	**20 - 10 000**
Ti	**0.2 - 100**
Mn	**2 - 1 000**
Fe	**2 - 1 000**
Zn	**2 - 1 000**
As	**0.1 - 50**
Cd	**0.02 - 10**
Pb	**0.2 - 100**

3.4.4 XRF analysis

XRF analysis was done by preparing powdered residue by grinding it with a mortar and pestle until the powder was adequately small. Then the powder was placed into dedicated sample holders. The XRF-apparatus that was used was a handheld XRF machine. This was then used to analyze the samples three times per sample.

Chapter4: Results

4.1 Mineralogy of raw materials

The raw ore was analyzed with XRF, and the results are given as weight% in Table 4.1. This shows that the main component is Mn_2O_3 with 67.12 wt%, then Fe_2O_3 accounts for 17.339 wt%, CaO accounts for 6.134 wt% and then there are more oxides with smaller contents.

Table 4.1: Shows compositional XRF results from the raw ore (wt%).

Oxide	[wt%]	Oxide	[wt%]
Mn_2O_3	67.120	SrO	0.196
Fe_2O_3	17.339	BaO	0.159
CaO	6.134	SO_3	0.139
SiO_2	4.437	P_2O_5	0.075
MgO	2.517	CeO_2	0.019
Al_2O_3	0.895	Cr_2O_3	0.019
Na_2O	0.671	TiO_3	0.019
K_2O	0.252	Cl	0.009

The reduced ore was analyzed using a handheld XRF device and the results are given in Table 4.2. These show that 54.77 wt% of the reduced ore is elemental manganese. This would mean that in a 50-gram sample as used for leaching, it would contain around 27.39 grams of manganese, 6.87 grams of iron, 2.78 grams of calcium and other elements in smaller amounts. The reason the sum mass percentages in Table 4.2 does not equal 100% is due to the fact that oxygen is not measured.

Table 4.2: The compositional XRF results for reduced ore.

Component	[wt%]	Component	[wt%]
Mn	54.77	Sr	0.31
Fe	13.73	Ba	0.63
Ca	5.55	S	0.30
Si	1.89	P	0.18
Al	1.08	Ce	0.043

4.2 leaching behavior of materials

After leaching all residues were weighed and results are shown in Table 4.3. The solid residue of test 2 weighed 28.32 grams and for test 3 the solid residue weighed 26.67 grams. The values from test 4-10 weighed 30.07 ± 2.97 grams given as mean value ± 2 standard deviations.

Table 4.3: The measured weight of solid residue after leaching.

Test nr.	Solid residue weight [g]	Test parameter	Mass loss (%)
1	24.86	25g Raw ore, 120 min	98.7
2	28.32	50g Reduced ore, 30 min	56.6
3	26.67	50g Reduced ore, 60 min	53.3

4	**27.74**	**50g Reduced ore, 120 min**	**55.5**
5	**29.43**	**50g Reduced ore, 120 min**	**58.9**
6	**30.45**	**50g Reduced ore, 120 min**	**60.9**
7	**29.97**	**50g Reduced ore, 120 min**	**59.9**
8	**28.83**	**50g Reduced ore, 120 min**	**57.7**
9	**33.70**	**50g Reduced ore, 120 min**	**67.4**
10	**30.39**	**50g Reduced ore, 120 min**	**60.8**

The calculated mass losses in Table 4.3 shows that the mass loss due to leaching of raw Mn ore is about 98.7%, while the mass losses in leaching of pre-reduced Mn ore samples are 60.2± 11.8%.

4.2.1 ICP-MS results of leaching solutions

The leaching solutions compositions for manganese, iron, calcium, and magnesium as the main metal components are shown in Table 4.4. Test 4-10 all had identical leaching conditions and the manganese concentration of these test can be given as 46.01 ± 3.66 g/L in the format, mean value ± 2 standard deviations. For test 4-10, the concentration of iron can be given as 5.52 ± 1.68 g/L. The data of calcium concentration from test 4,5,6,9 and 10 can be represented as 23.39 ± 2.52 g/L.

Table 4.4: Shows concentration of manganese, iron, calcium, and magnesium from ICP-MS analysis.

Test nr.	Mn concentration [g/L]	Fe concentration [g/L]	Ca concentration [g/L]	Mg concentration [g/L]	Leaching time [min]
2	**34.27**	**5.78**	**31.99**	**-**	**30**
3	**42.53**	**-**	**25.46**	**0.78**	**60**
4	**45.67**	**6.74**	**24.63**	**0.88**	**120**
5	**43.35**	**7.37**	**25.28**	**0.75**	**120**
6	**49.59**	**4.91**	**21.00**	**0.96**	**120**
7	**46.46**	**5.16**	**33.15**	**1.00**	**120**
8	**44.56**	**4.58**	**-**	**1.10**	**120**
9	**47.51**	**-**	**22.15**	**0.72**	**120**
10	**45.01**	**6.47**	**23.88**	**0.81**	**120**

4.2.2 XRD analysis of leaching residue

The leaching residue was analyzed using XRD and the results are given in Figures 4.1, 4.2, 4.3 and 4.4. These show that the main component for all solid residues after leaching is bassanite or gypsum. The results also show unleached manganese (II) oxide, MnO, that has not been

leached and not converted to another compound during the leaching. The final common factor for these XRDs is that metallic iron is present.

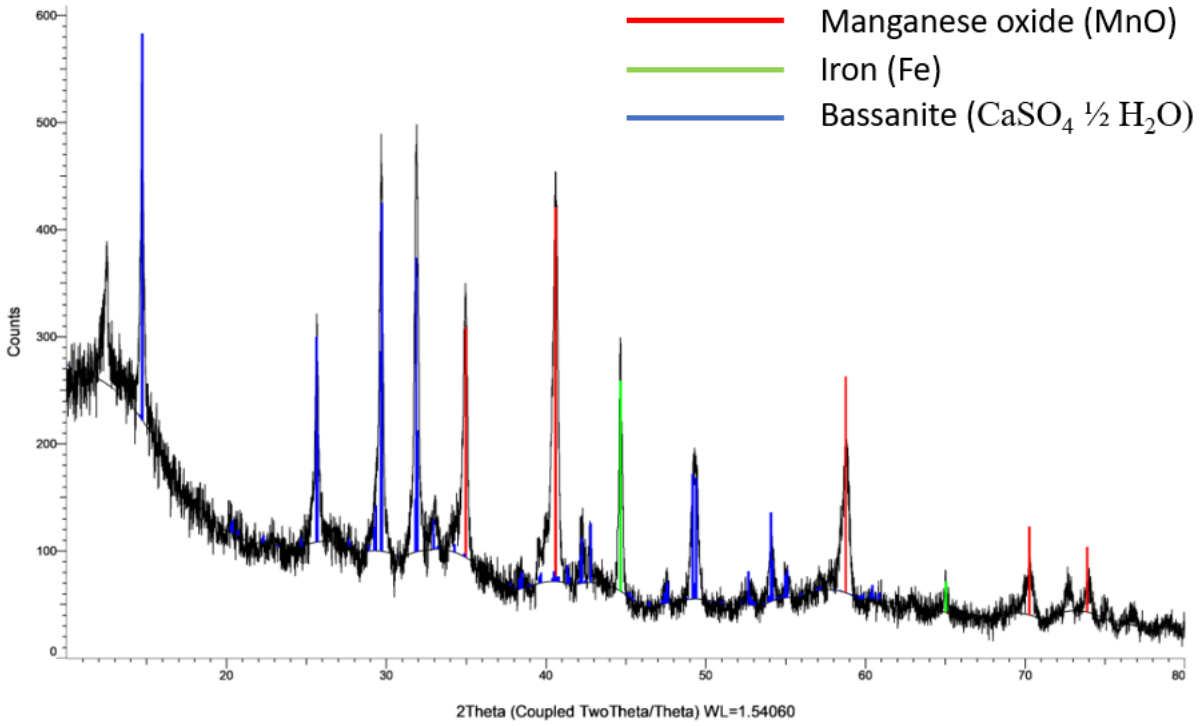

Figure 4.1: The XRD spectrum of solid residue after leaching for test nr. 3 with the identified phases.

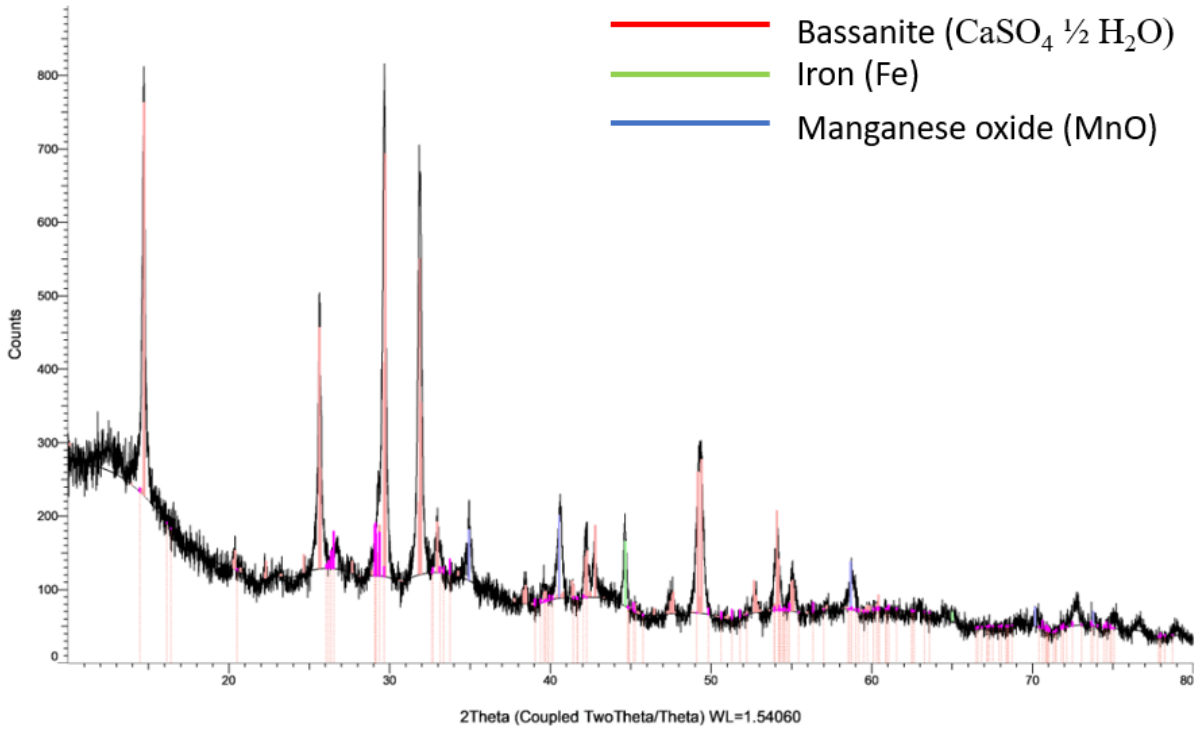

Figure 4.2: The XRD spectrum of solid residue after leaching for test nr. 4 with the identified phases.

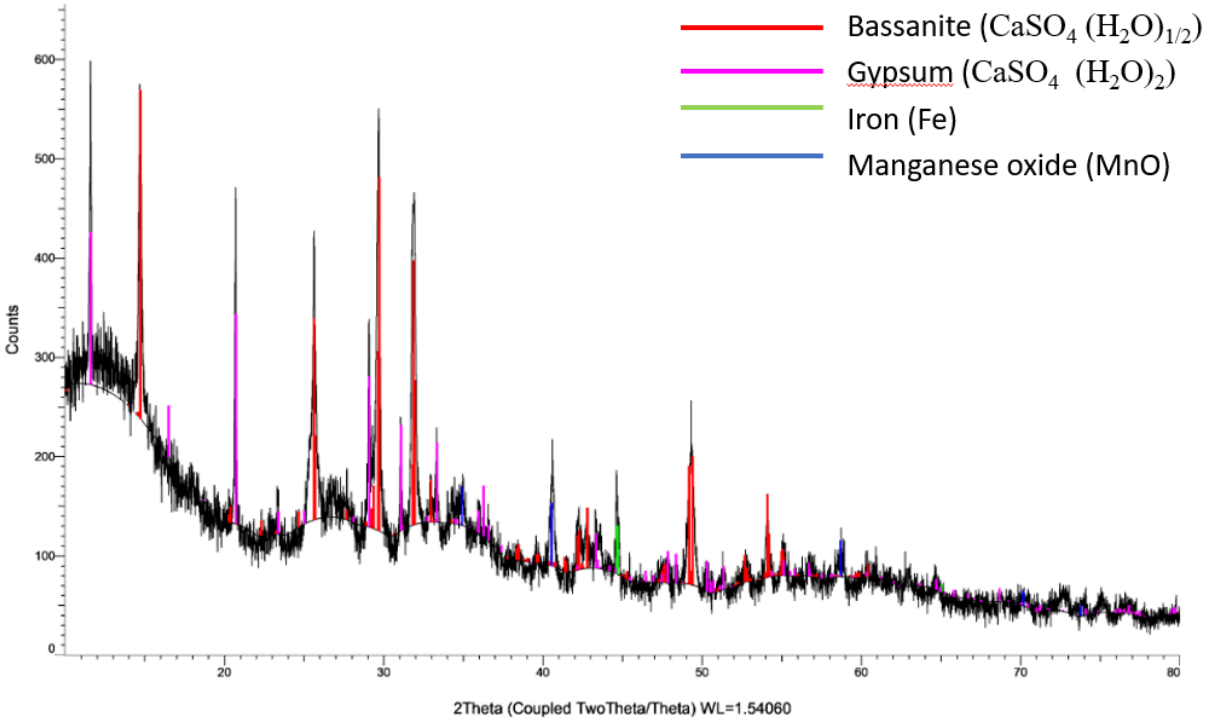

Figure 4.3: The XRD spectrum of solid residue after leaching for test nr. 9 .

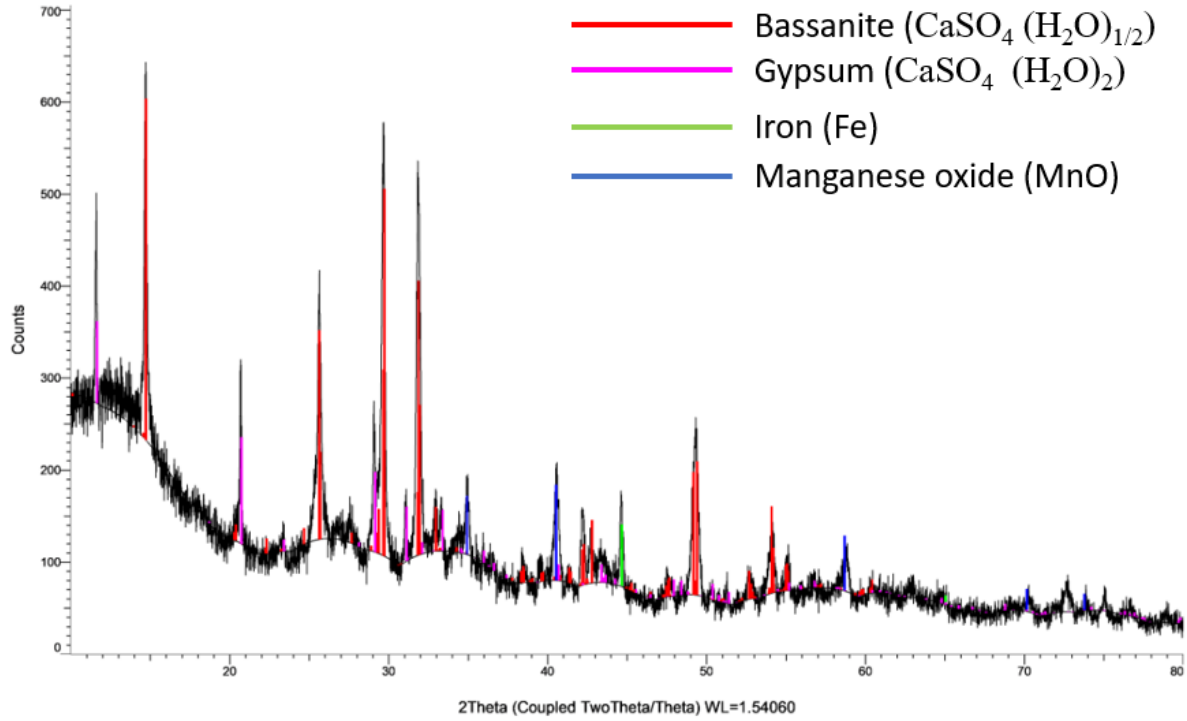

Figure 4.4: The XRD spectrum of solid residue after leaching for test nr. 10 with the identified phases.

For the remaining samples, 2, 5, 6, 7 and 8. The XRD result of the leaching residue was almost identical to that of test nr. 4 and these results are given in appendices 7.2.

4.2.3 XRF analysis of solid residue

The solid residue after leaching was also analyzed using a portable XRF analyzer. The results of solid residue for test 4 are given in Table 4.5. This table shows that 22.68 wt% of the solid residue after leaching is elemental manganese. The average weight of solid residue after leaching was 30.07 for the reduced ore. This average loss of manganese after leaching was 6.82 grams based on these results.

Table 4.5: Shows the XRF results of solid residue after leaching.

Component	[wt%]	Component	[wt%]
Mn	**22.68**	**Sr**	**0.56**
Fe	**14.31**	**Ba**	**0.70**
Ca	**10.92**	**S**	**21.61**
Si	**2.97**	**P**	**0.25**
Al	**0.88**	**Mg**	**-**

4.2.4 Results for leaching of raw ore

As mentioned above, 25 grams of raw ore was leached in 250 mL of 1M sulfuric acid solution, equal to that of the reduced ore leaching. However, the solid residue had a weight of 24,86 grams as shown in Table 4.3. This means only 1.35% of total solids were leached.

4.3 Purification step products analysis

4.3.1 ICP analysis of purified solutions

Table 4.6 shows the concentrations of manganese, iron, calcium, and magnesium for sample 2-10 after purification using CaO or CaCO3. Calcium oxide have been added to most of the tests and the average calcium concentration was 22.17 g/L. The average iron concentration was 5.89 g/L and the manganese concentration was on average 45.67 g/L.

Table 4.6: Shows concentration of manganese, iron, calcium, and magnesium after purification.

Test nr.	Mn concentration [g/L]	Fe concentration [g/L]	Ca concentration [g/L]	Mg concentration [g/L]	Purification additive [g]
2	**45.46**	**6.17**	**-**	**1.27**	**0.49 CaO**
3	**40.91**	**7.64**	**20.57**	**1.18**	**0.28 CaO**
4	**45.23**	**5.74**	**28.79**	**1.07**	**0.57 CaO**
5	**-**	**-**	**20.82**	**1.44**	**0.46 CaO**
6	**-**	**4.69**	**22.23**	**0.91**	**0.34 CaO**
7	**47.29**	**4.24**	**20.84**	**0.92**	**0.23 CaO**
8	**47.63**	**4.59**	**19.74**	**0.75**	**0.114 CaO**
9	**-**	**-**	**-**	**-**	**No addition**
10	**47.50**	**8.18**	**-**	**-**	**0.61 CaCO3**

4.3.2 XRD analysis of solid residue after purification

After purification the most common solid residue was gypsum, bassanite or a combination of the two. Gypsum was the only main component in the XRD of test nr. 2, 3, 6 and 7. For test

nr. 4 and 5 there was a combination of bassanite and gypsum as the main residues. For test number 8, the main component in the solid residue was bassanite. For test number 10 the main component of the solid residue was calcium carbonate. These results are shown in Figures 4.5, 4.6, 4.7 and 4.8. Results that were identical to these are given in appendices 7.3.

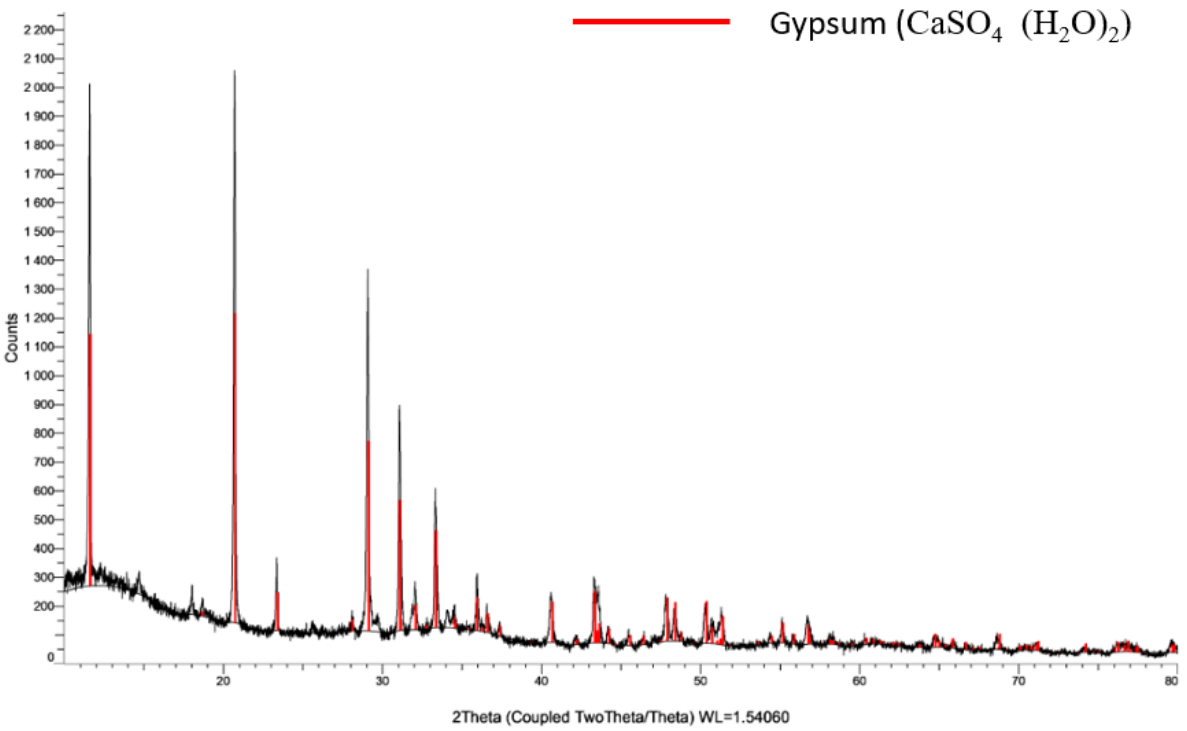

Figure 4.5: The XRD results of purification residue for test nr. 3 after purification.

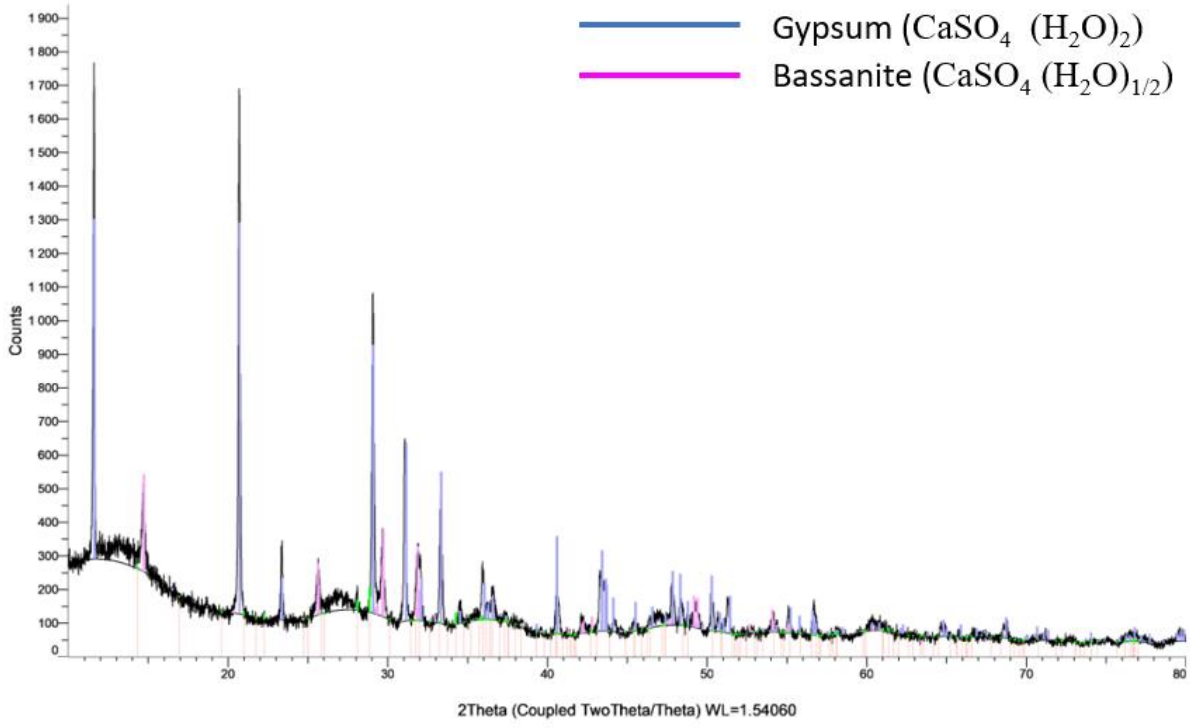

Figure 4.6: The XRD results of purification residue for test nr. 4 after purification.

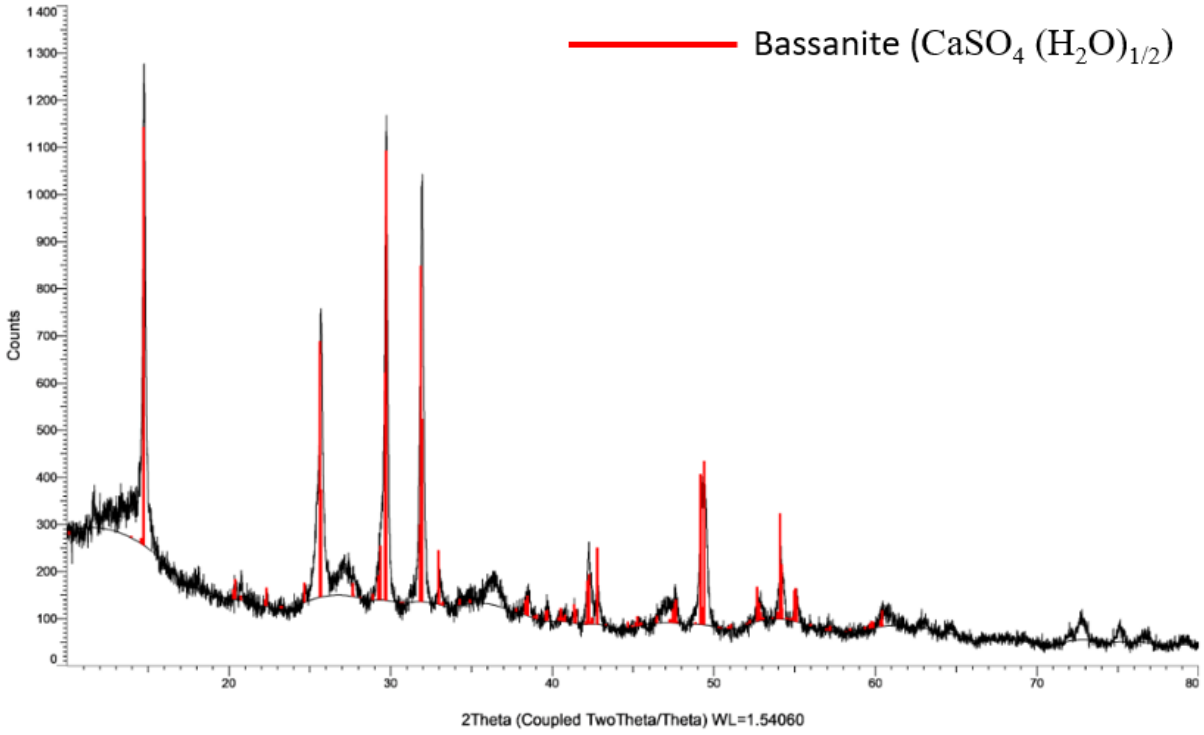

Figure 4.7: The XRD results of purification residue for test nr. 8 after purification.

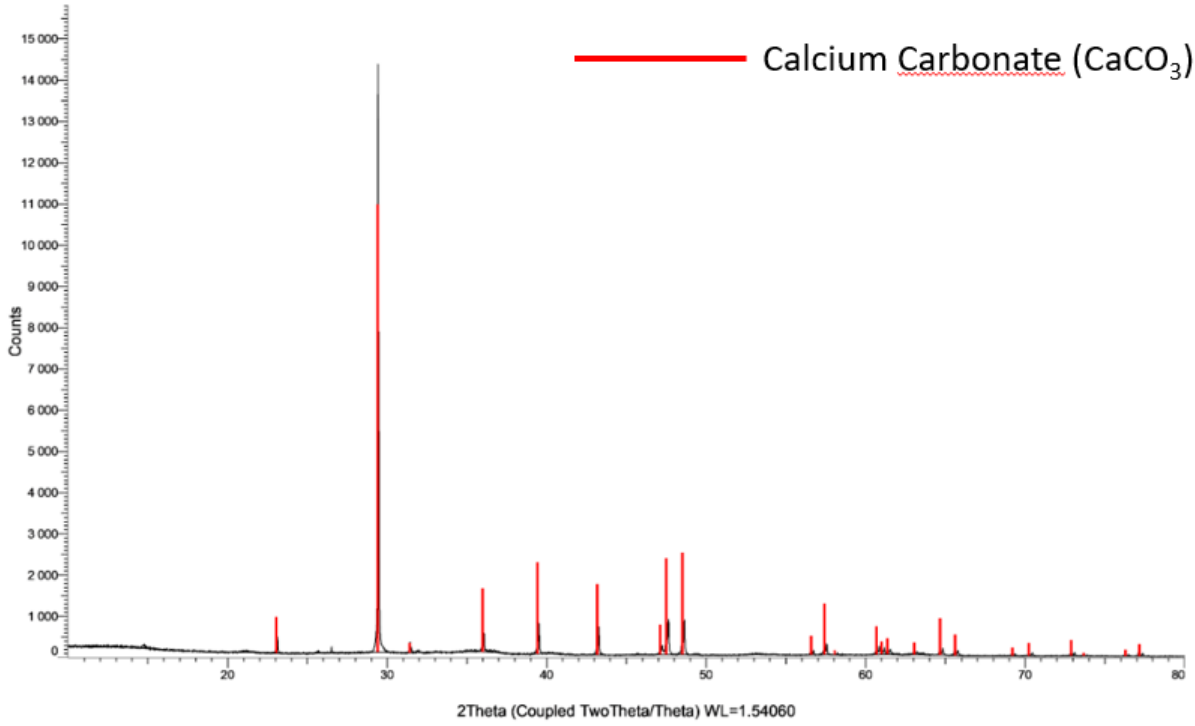

Figure 4.8: Shows the XRD results of purification residue for test nr. 8 after purification.

Table 4.7: Shows the weight of solid residue in the purification trials for test nr. 4-10.

Test nr.	Solid residue weight [g]	Additive [g]
4	3.37	0.57 CaO

5	**2.47**	**0.46 CaO**
6	**1.59**	**0.34 CaO**
7	**1.43**	**0.23 CaO**
8	**1.04**	**0.114 CaO**
9	**-**	**No additives**
10	**1.20**	**0.61 $CaCO_3$**

4.3.3 XRF result of solid residue after purification

From Table 4.8 the results from XRF analysis using a handheld XRF device are shown for test 4. These show that the amount of manganese in the solid residue after purification was 7.32, for calcium it was 10.75, for iron it was 13.58 and for sulfur it was 22.53.

Table 4.8: XRF results of solid residue after purification for test 4.

Component	[wt%]	Component	[wt%]
Mn	**7.32**	**Sr**	**0.023**
Fe	**13.58**	**Al**	**0.30**
Ca	**10.75**	**S**	**22.53**
Si	**0.171**	**P**	**-**

4.4 Precipitation step products analysis

4.4.1 ICP-MS results of solutions

As shown in Table 4.9. The concentrations of manganese, iron, calcium, and magnesium are given. All tests showed a decrease in manganese concentration, indicating a portion of Mn precipitated. All tests also showed a decrease in iron concentrations. Calcium concentrations showed little to no difference and magnesium concentrations increased massively for tests with addition of magnesium.

Table 4.9: Shows the concentrations of manganese, iron, calcium and magnesium remaining in the solutions after precipitation.

Test nr.	Mn concentration [g/L]	Fe concentration [g/L]	Ca concentration [g/L]	Mg concentration [g/L]	Precipitation additive [g]
2	**29.74**	**3.00**	**25.48**	**0.71**	**5.4 $KMnO_4$**
3	**30.20**	**3.55**	**-**	**3.07**	**5.75 $KMnO_4$**
4	**38.89**	**4.42**	**22.86**	**0.80**	**5.5 $KMnO_4$**
5	**3.32**	**0.94**	**32.82**	**20.09**	**10.16 MgO**
6	**11.41**	**0**	**-**	**17.99**	**8.12 MgO**
7	**19.32**	**0**	**24.36**	**12.08**	**6.09 MgO**
8	**31.02**	**-**	**34.75**	**26.32**	**21.25 $MgCO_3$**
9	**30.32**	**0.26**	**27.78**	**14.85**	**17.00 $MgCO_3$**
10	**45.76**	**2.02**	**27.85**	**0.85**	**3.58 NaOH**

4.4.2 XRD results of final precipitated products

4.4.2.1 Precipitations with $KMnO_4$ use

Figures 4.9-4.12 show the XRD spectra of the precipitate from test numbers 2, 3, 4 and 10. These all show 3 peaks, first at around 10-12, second in the range 37-38 and last at

approximately 66-67. This shows that for these four tests, the XRD results are the same or very similar.

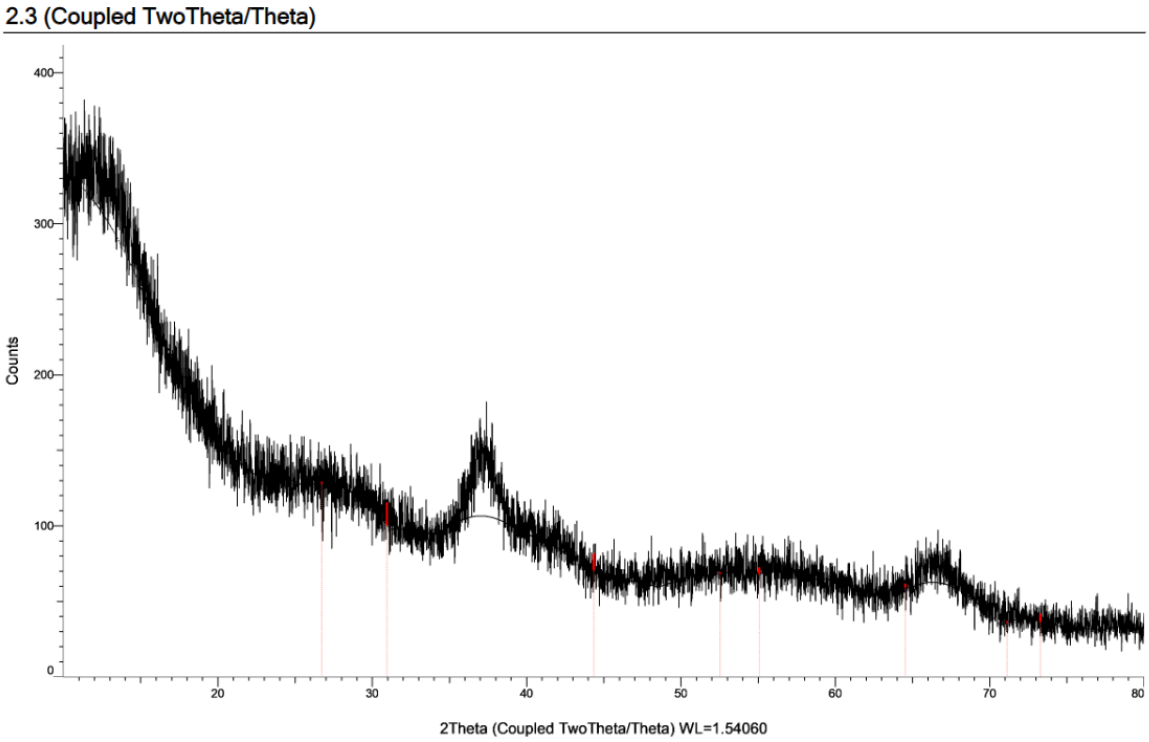

Figure 4.9: XRD spectrum result of precipitate product of test nr. 2.

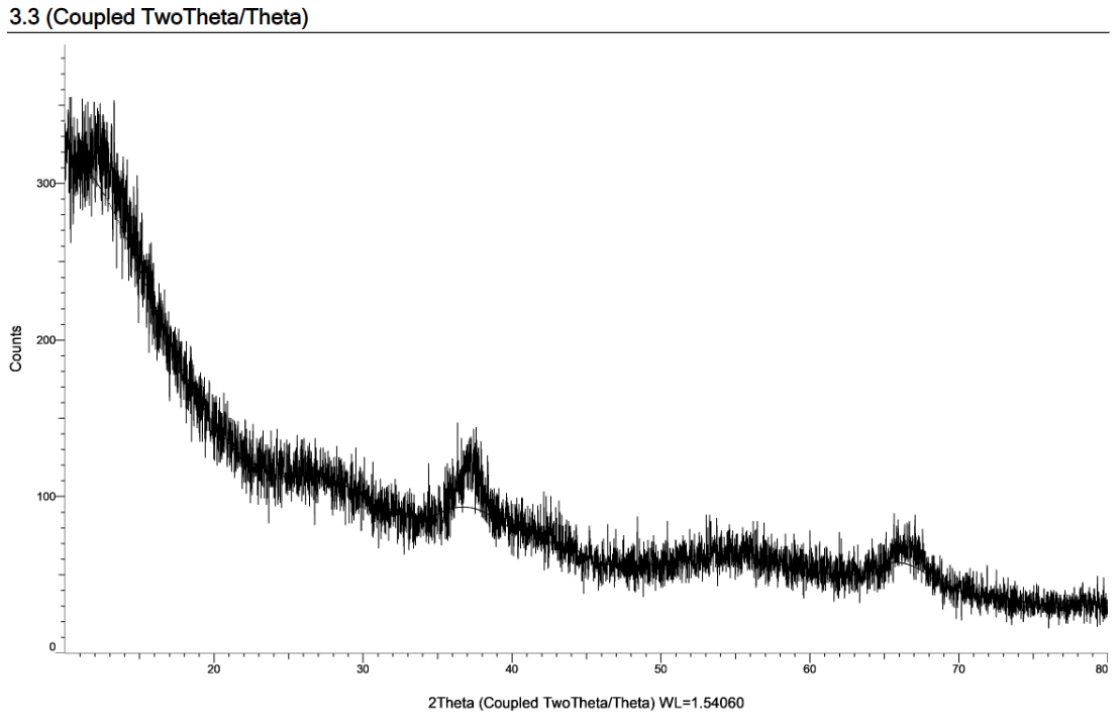

Figure 4.10: XRD spectrum result of the precipitate product in test nr. 3.

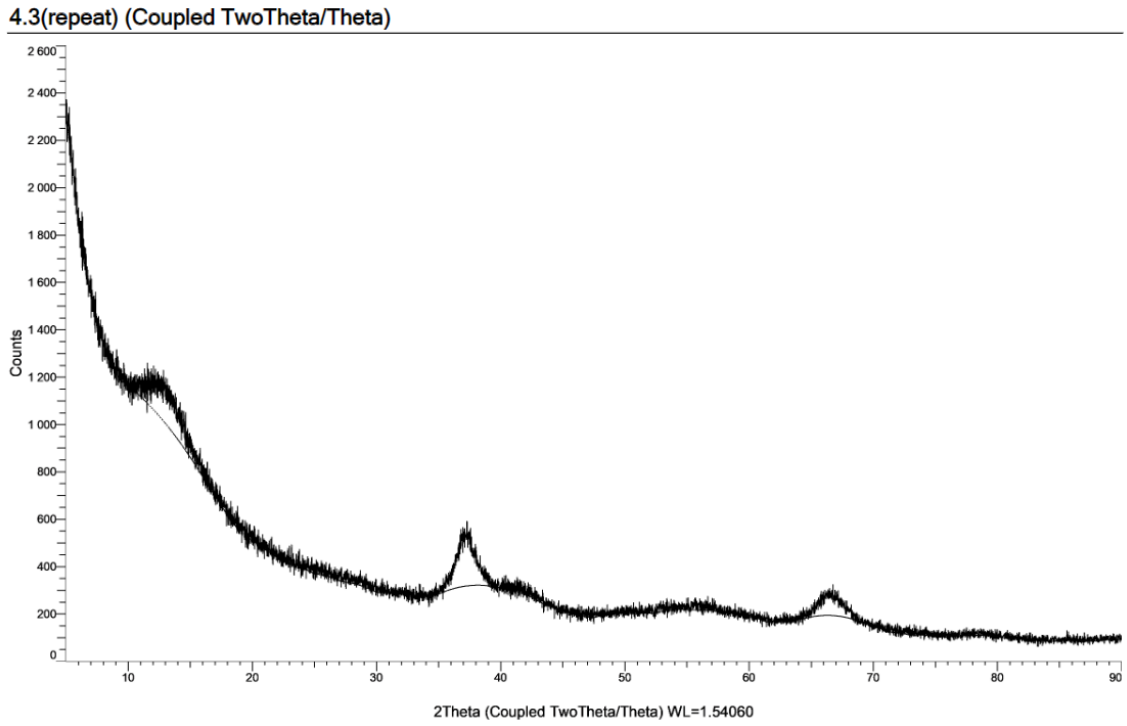

Figure 4.11: XRD result of precipitate product of test nr. 4.

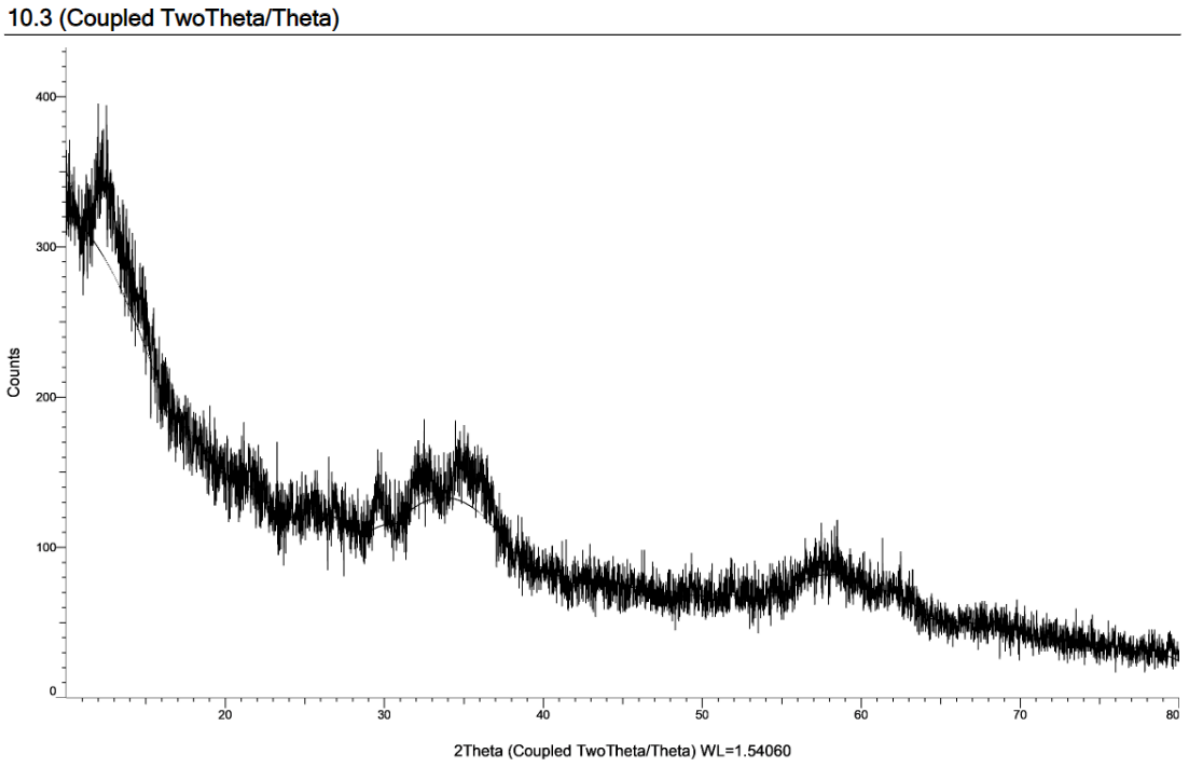

Figure 4.12: XRD spectrum of precipitate product for test nr. 10.

Test numbers 2, 3 and 4 were done by precipitation with potassium permanganate. Test number 10 was done by addition of sodium hydroxide, NaOH. For all these four tests, the solid precipitate that was formed was black brown in color and the total weight of the solid residues

are shown in Table 4.10. The table shows that test 2 and 3 produced a larger quantity of solid residue compared to test nr 4 and 10.

Table 4.10: The masses of solid dark brown precipitates in tests 2, 3, 4, and 10.

Test nr.	Weight of dried precipitate [g]
2	**13.10**
3	**14.09**
4	**8.80**
10	**7.99**

In Figure 4.13 the precipitation process is shown. Far left shows the solution before any addition, in the middle some sodium hydroxide was added and to the right was at the end of addition.

Figure 4.13: Shows precipitation process for test nr.10.

4.5.2.2 Precipitation of $Fe_{0.297}Mn_{2.703}O_4$

Figure 4.14 shows that test nr. 5 using MgO yields a precipitate containing three phases of hausmannite, magnesium oxide and traces of manganese dioxide. The main component of the precipitate is hausmannite containing iron, given as $Fe_{0.297}Mn_{2.703}O_4$, green marks what could be MnO_2.

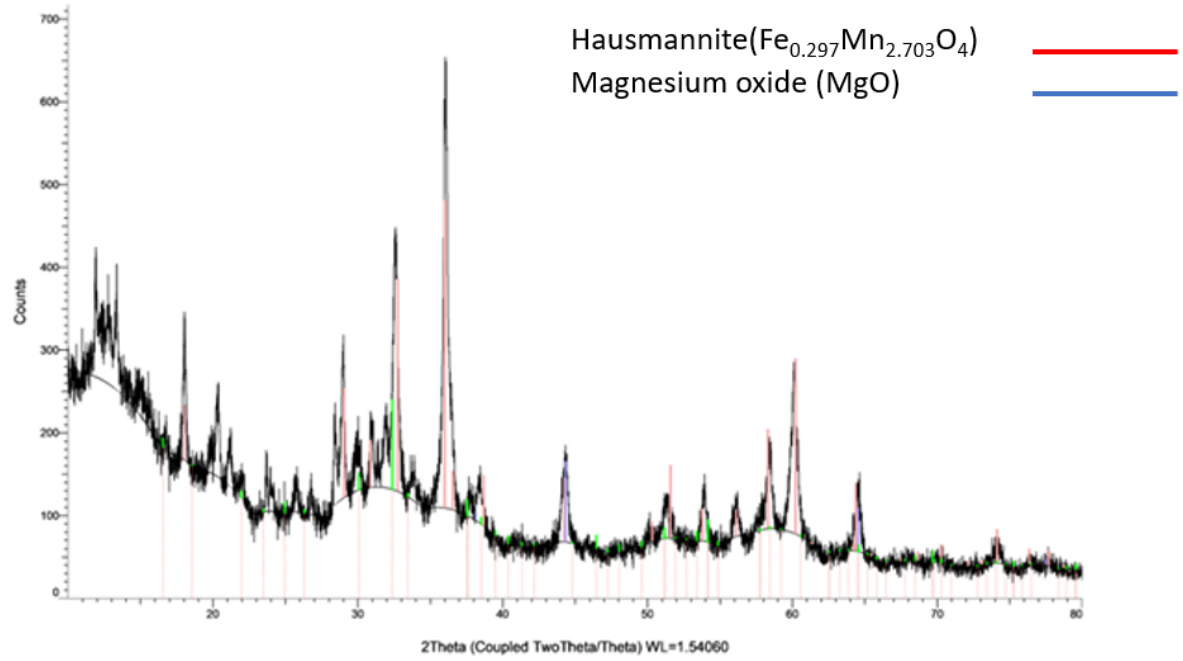

Figure 4.14: XRD result of the precipitate of test nr. 5

The XRD result of the precipitate for test nr. 6 is given in Figure 4.15 and shows again hausmannite containing iron ($Fe_{0.297}Mn_{2.703}O_4$). Again, the blue marked peaks represent MgO which was added to the sample.

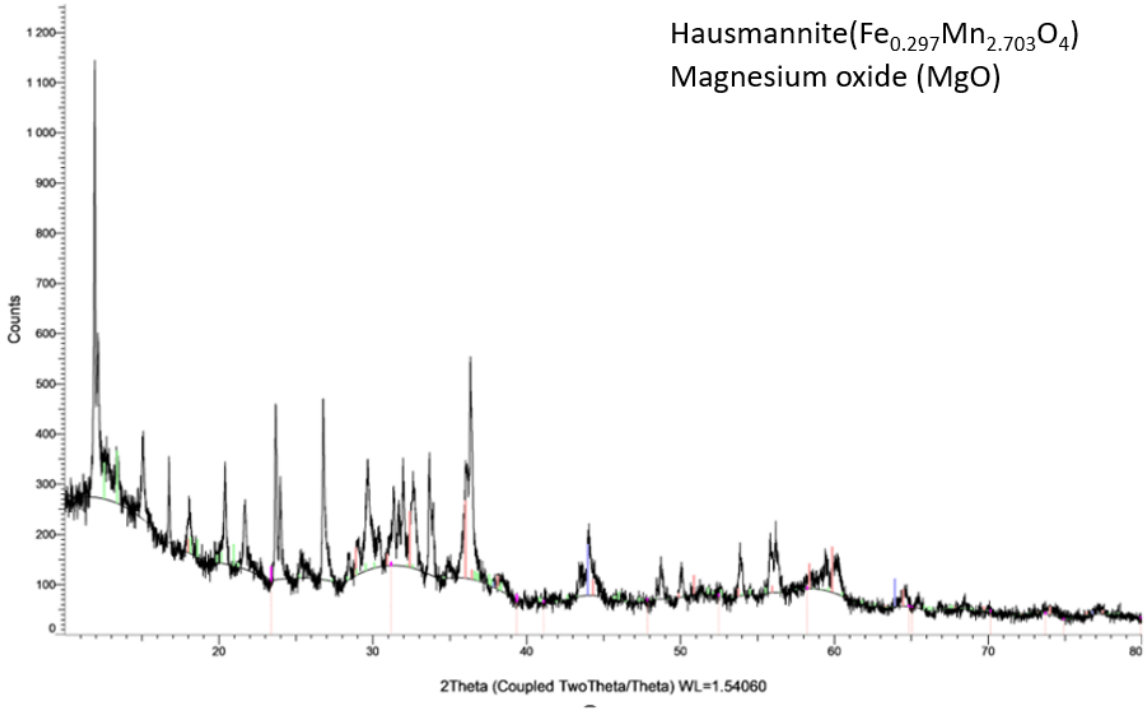

Figure 4.15: XRD result of the precipitate for test nr. 6.

Figure 4.16 shows that the precipitate for test nr. 7 have three phases of hausmannite, magnesium oxide and traces of manganese dioxide. The main component of the precipitate is again hausmannite containing iron, given as $Fe_{0.297}Mn_{2.703}O_4$. Magnesium oxide, added to the solution is marked as blue and finally, the green marks what could be traces of amorphous MnO_2.

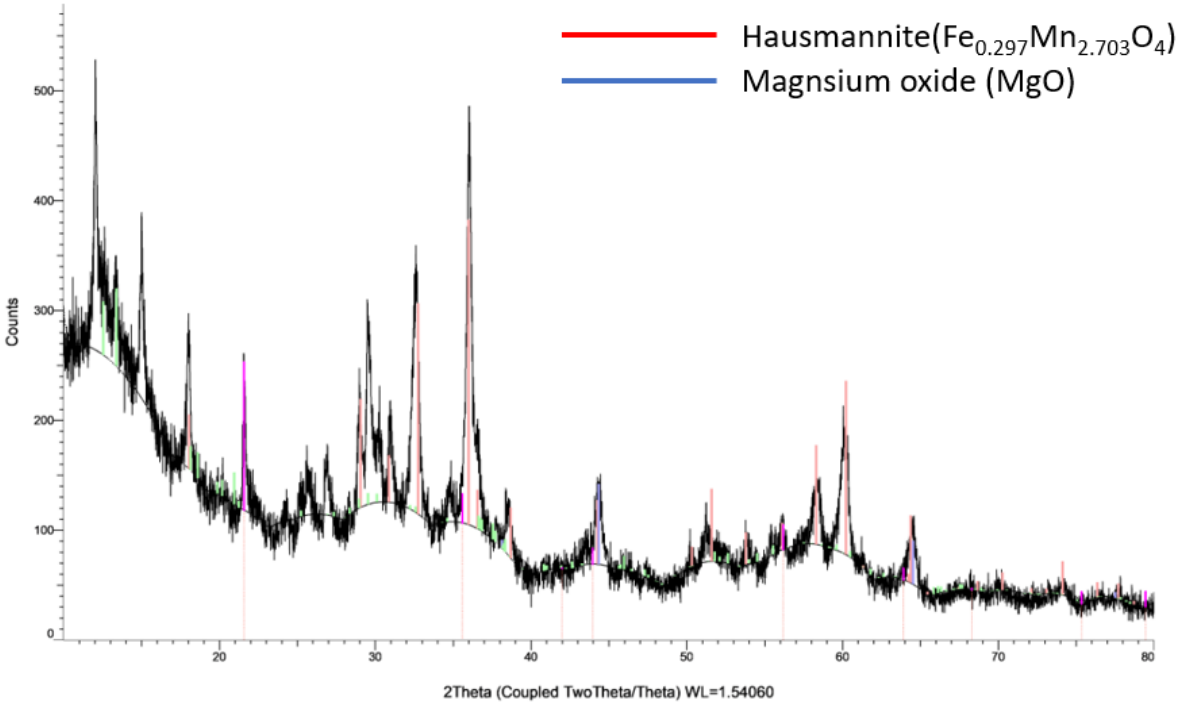

Figure 4.16: XRD result of the precipitate for test nr. 7.

Table 4.11 shows the masses after precipitation with MgO for test 5, 6 and 7. All residues were observed to visually look the same, but as the table shows, there was a large difference in amounts.

Table 4.11: Shows the weight of solid residue after precipitation with test 5, 6 and 7.

Test nr.	Weight after precipitation [g]
5	**40.86**
6	**35.30**
7	**23.82**

4.5.2.3 Precipitations with $MgCO_3$ as the major product

Figure 4.17 shows the XRD results for test nr. 8. This figure shows that all major peaks are represented by $MnCO_3$ marked as orange. There are no other major peaks present in the sample, there are some small shown in blue, however, the blue indicators partly overlap with manganese carbonate for certain peaks and therefore, another potential compound could not be identified with certainty.

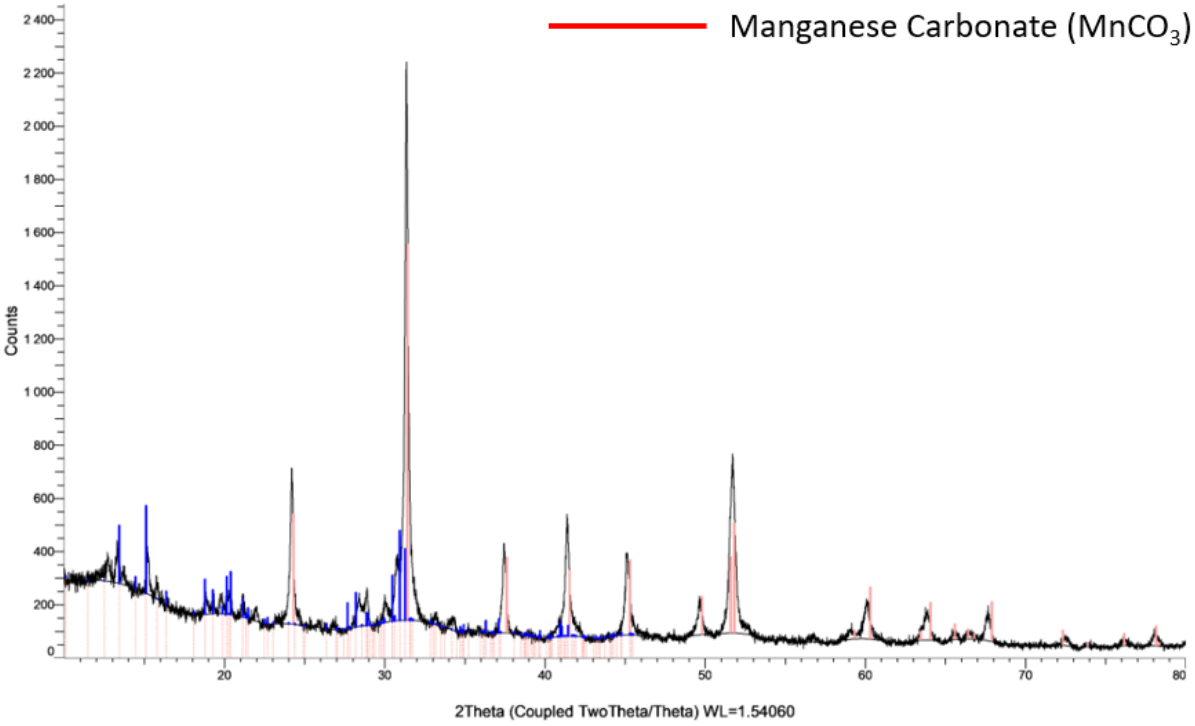

Figure 4.17: Shows the XRD result of the precipitate for test nr. 8.

For test nr. 9 the main component in the solid residue was, likewise with test 8, $MnCO_3$. This is shown in Figure 4.18 where peaks marked as red represent $MnCO_3$. The XRD also shows some unmarked small peaks.

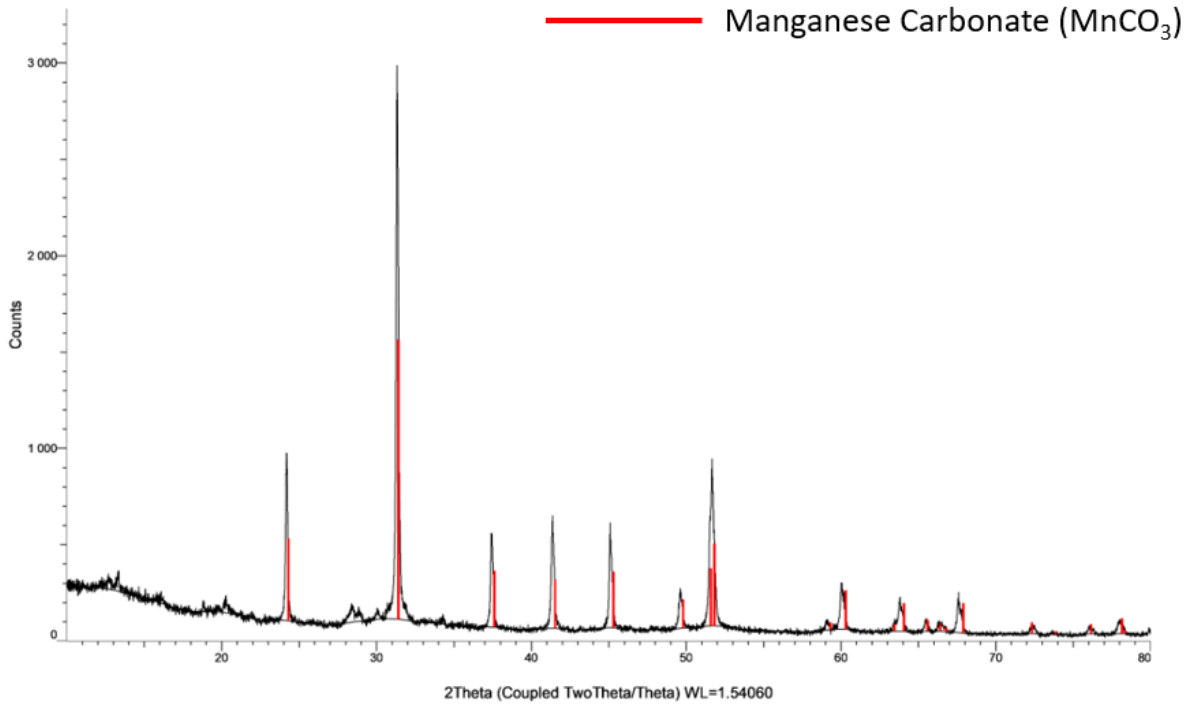

Figure 4.18: XRD result of precipitate of test nr. 9.

The amount of solid residue from test nr. 8 and 9 are shown below in Table 4.12. As there are only two different tests, a graph showing correlation between precipitate and additive is not given.

Table 4.12: Shows amount of solid residue for test nr. 8 and 9.

Test nr.	Weight after precipitation [g]
8	34.73
9	28.25

4.4.3 XRF results of products after precipitation

The concentration of certain elements after precipitation of test nr 2, with a potassium permanganate solution are shown in Table 4.13. They show elemental composition which means that 40.54 wt% manganese only accounts for the manganese and not the oxygen in the MnO_2 product. Fe may be the main impurity in this product.

Table 4.13: XRF result of precipitate for test nr. 2.

Component	[wt%]	Component	[wt%]
Mn	40.54	Sr	0.0023
Fe	7.91	K	1.77
Ca	0.184	S	10.34
Si	0.076	Al	0.59

For test nr. 3 the XRF results after precipitation are given in Table 4.14. They show a big difference from test 2 regarding the concentrations of manganese and iron.

Table 4.14: XRF result of precipitate for test nr. 3.

Component	[wt%]	Component	[wt%]
Mn	28.42	Sr	0.002
Fe	11.54	K	1.16
Ca	0.175	S	10.8
Si	0.082	Al	0.34

Test nr. 4 was precipitated using solid potassium permanganate. The concentration of the solid product is shown in Table 4.15. This shows a decrease in iron and sulfur compared to that of test 2 and 3.

Table 4.15: XRF result of precipitate for test nr. 4.

Component	[wt%]	Component	[wt%]
Mn	45.43	Sr	0.002
Fe	5.05	K	1.73
Ca	0.148	S	7.14
Si	0.085	Al	0.68

Test nr. 5 was precipitated with the addition of magnesium oxide. The XRF results of the solid product are shown in Table 4.16. As the product of this precipitation is different from test 2-4. The concentrations of all components are also different.

Table 4.16: XRF result of precipitate for test nr. 5.

Component	[wt%]	Component	[wt%]
Mn	**35.11**	**Mg**	**2.5**
Fe	**5.50**	**K**	**-**
Ca	**0.37**	**S**	**13.46**
Si	**0.07**	**Al**	**0.50**

Test nr. 6 was precipitated with addition of a smaller amount of magnesium oxide compared to test nr.5. The XRF results for the solid product are shown in Table 4.17 and show slight changes in composition for iron, magnesium, and sulfur.

Table 4.17: XRF result of precipitate for test nr. 6.

Component	[wt%]	Component	[wt%]
Mn	**36.22**	**Mg**	**3.15**
Fe	**3.504**	**K**	**-**
Ca	**0.317**	**S**	**16.8**
Si	**0.089**	**Al**	**0.51**

Test nr 7. was precipitated with addition of a smaller amount of magnesium oxide compared to test nr. 6. The XRF results shown in Table 4.18 show an increase in manganese and iron content and a decrease in magnesium concentration.

Table 4.18: XRF result of precipitate for test nr. 7.

Component	[wt%]	Component	[wt%]
Mn	**39.96**	**Mg**	**2.14**
Fe	**5.60**	**K**	**-**
Ca	**0.23**	**S**	**14.66**
Si	**0.094**	**Al**	**0.60**

Test nr. 8 was precipitated using magnesium carbonate. The XRF results of the precipitate are shown in Table 4.19.

Table 4.19: XRF result of precipitate for test nr. 8.

Component	[wt%]	Component	[wt%]
Mn	**22.60**	**Mg**	**3.61**
Fe	**3.35**	**K**	**-**
Ca	**0.23**	**S**	**8.25**
Si	**0.084**	**Al**	**0.38**

Test nr. 9 was also precipitated using magnesium carbonate, but a lower amount than that of test nr. 8. The XRF results of the solid product are shown in Table 4.20. There is an increase in concentration of manganese and a decrease in concentration of magnesium.

Table 4.20: XRF result of precipitate for test nr. 9.

Component	[wt%]	Component	[wt%]
Mn	**29.44**	**Mg**	**2.40**
Fe	**3.76**	**K**	**-**
Ca	**0.21**	**S**	**8.60**
Si	**0.088**	**Al**	**0.40**

Test nr. 10 was precipitated by addition of sodium hydroxide. The XRF results of the solid product are shown in table 4.21.

Table 4.21: XRF result of precipitate for test nr. 10.

Component	[wt%]	Component	[wt%]
Mn	**15.21**	**Mg**	**-**
Fe	**9.89**	**K**	**-**
Ca	**0.24**	**S**	**10.51**
Si	**0.11**	**Al**	**0.28**

4.5 Microstructure of ore and pre-reduced ore

4.5.3 Sem results of the sample

Both pre-reduced and raw ore were studied for the morphology/microstructure of material at high magnification in Sem, Ultra-55.
Already with 2k magnification, we can observe the porous surface of the reduced ore(fig.4.20) where as the non-reduced ore (fig4.19) has much tighter cell structure. Further increase in magnification on these area shows a much clear pores which are shown below at Figure 4.21 and 4.22. These figures are magnified under Sem Ultra-55 with a magnification of 20k.

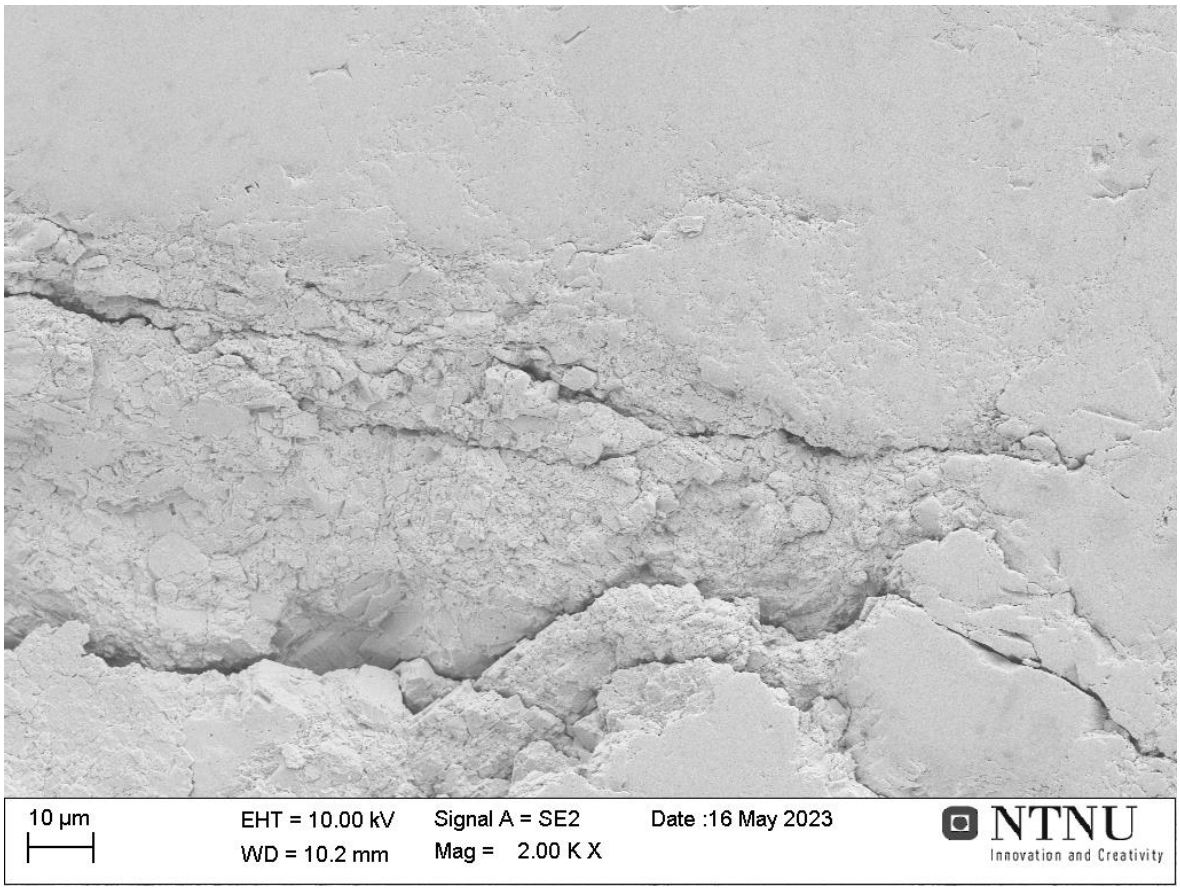

Figure 4.19: Manganese ore sample analyzed under Sem Ultra-55 with 2.00k magnification.

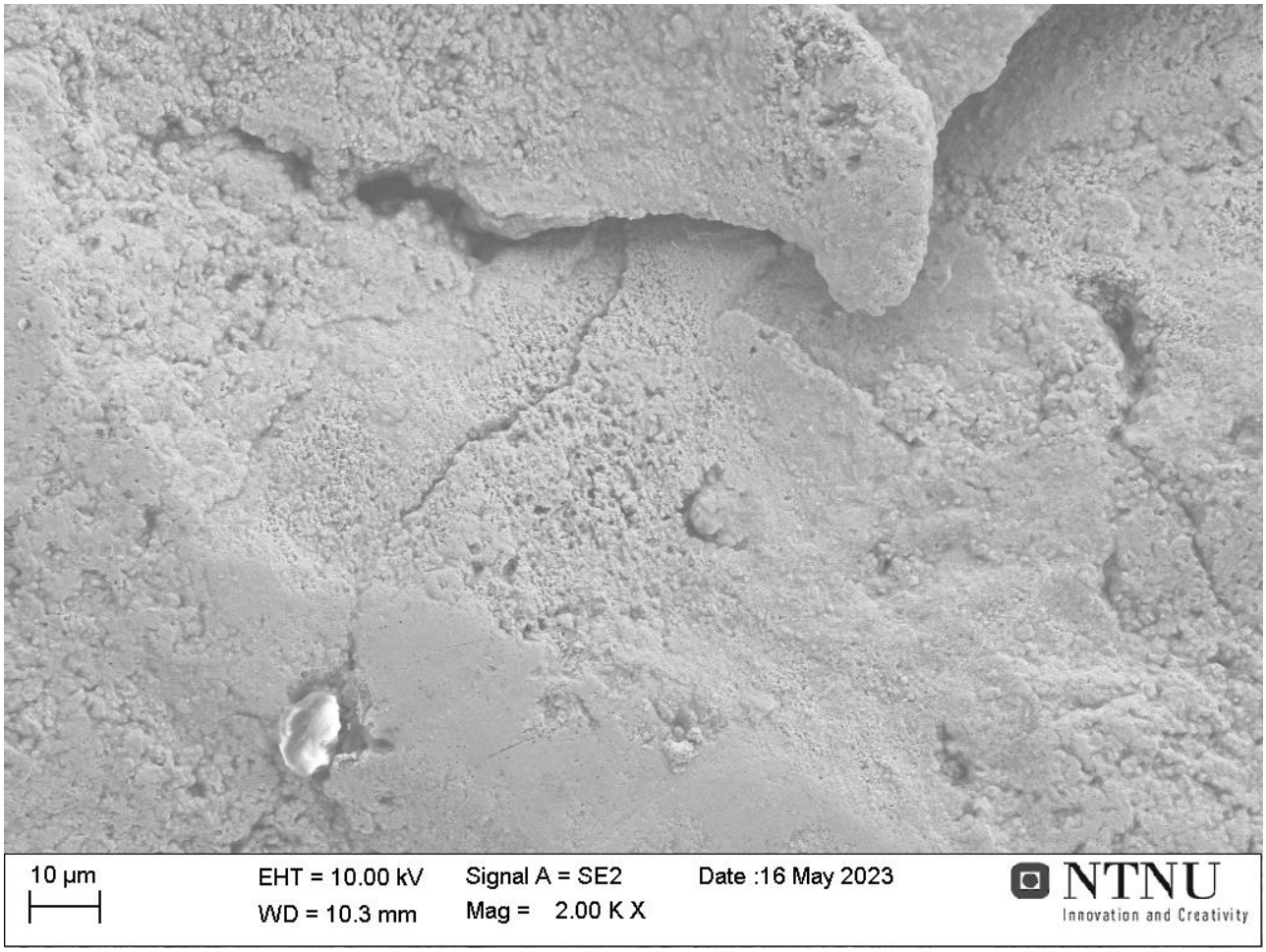

Figure 4.20: Pre-Reduced manganese ore analyzed under Sem Ultra 55 with 2.00k magnification.

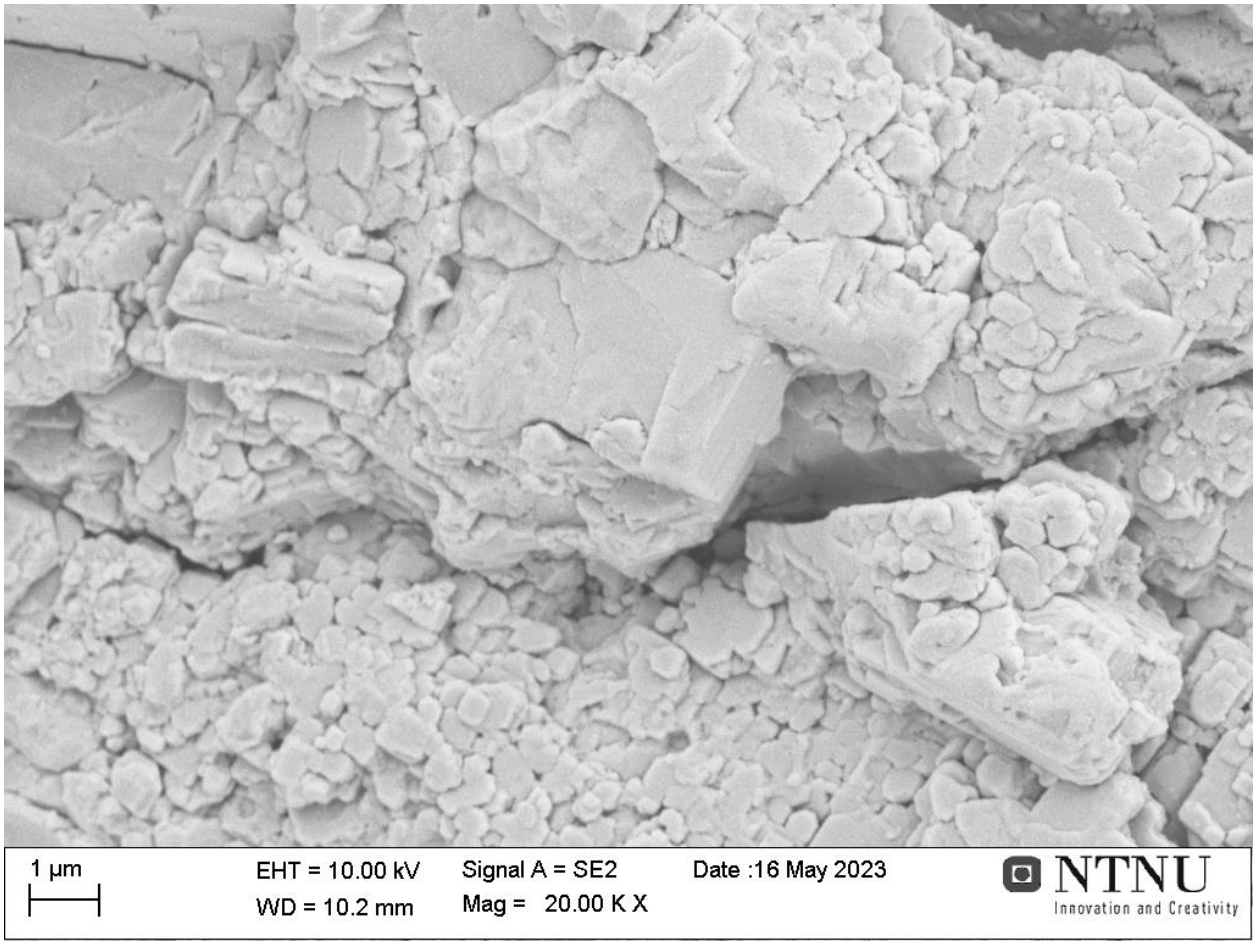

Figure 4.21: Manganese ore analyzed under Sem Ultra 55 with 20.00k magnification.

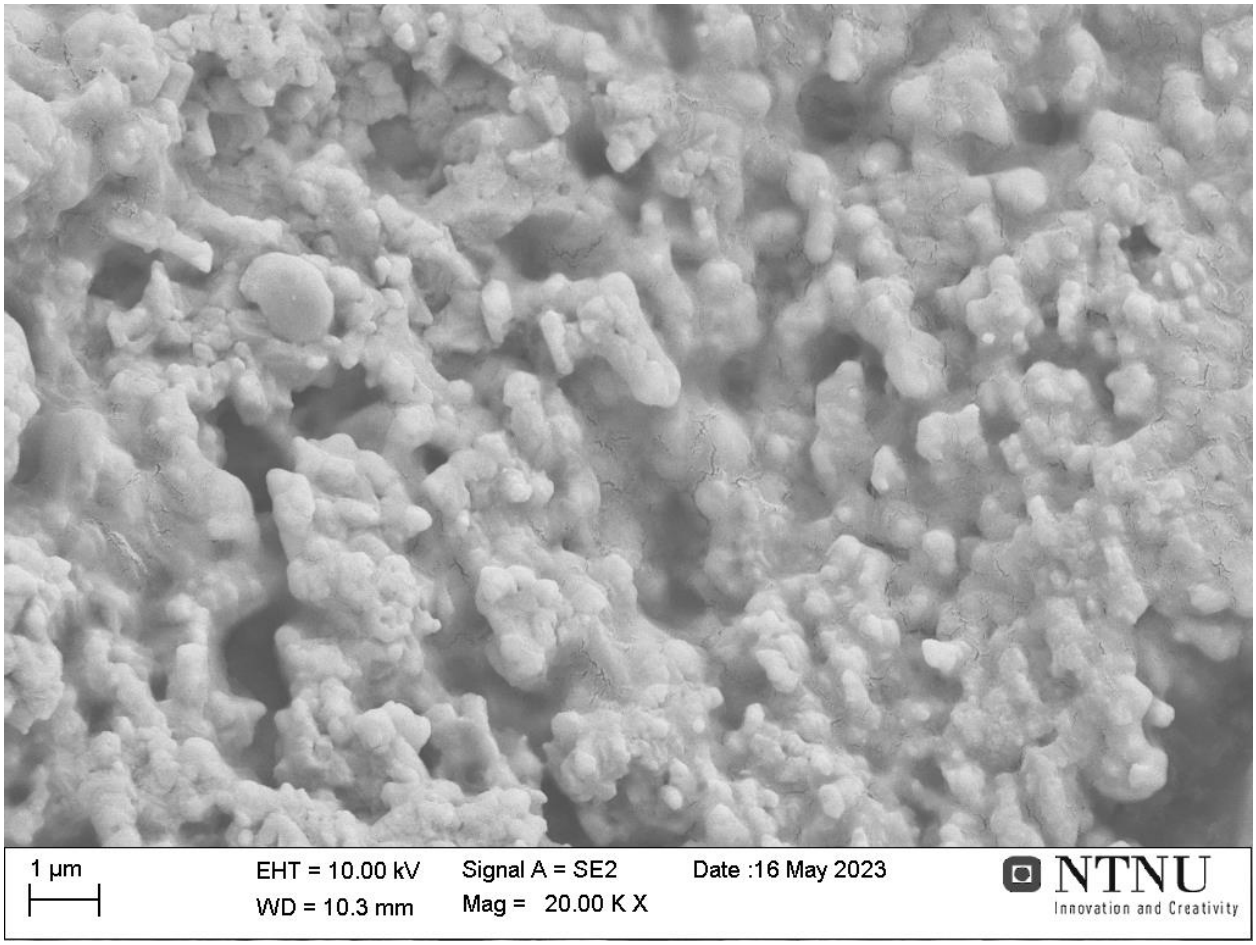

Figure 4.22: Pre-Reduced ore analyzed under Sem Ultra- 55 with 20.00k magnification.

Chapter 5: Discussion

5.1 Leaching behavior of reduced and raw ore

To evaluate if the leaching process has been successful, the yield of manganese leached, as well as impurities leached must be evaluated. The goal is naturally to obtain the highest yield of manganese leached while maintaining a small quantity of impurities in the solution if possible. At the same time, the HAlMan project team's goal of zero solid waste must be considered.

To evaluate whether reduction of ore is beneficial before leaching, the leachability of raw ore and reduced manganese ore by hydrogen can be compared. In the raw ore, it was observed that only 1.35% of the solid weight was leached. This is an exceptionally low amount, even if one were to assume that 100% of this is manganese. On the other hand, for test 4 (reduced ore), 44.52% of the solid weight was leached to the solution, while the main component of this also was manganese. The ICP-MS results showed that test 4 had a manganese concentration of 45.67 g/L. If 100% of the leached solids from the raw ore were manganese, this would only result in a concentration of 0.86 g/L. This means that the leaching of the reduced ore is at least 5310% more effective than leaching of raw ore with respects to manganese at the conditions of 1M sulfuric acid for 120 minutes.

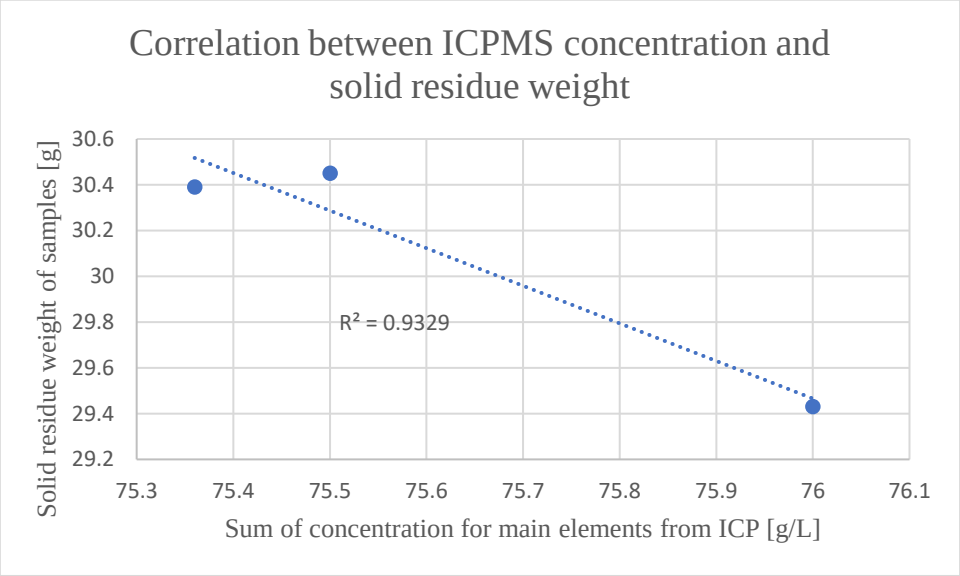

Figure 5.1: Correlation between concentration of main elements (Fe, Mn, Ca) and solid residue weight.

To evaluate the precision of the measurements, the correlation between ICP and solid residue weight can be compared. For the concentrations of main elements to increase in a solution the solid residue weight must decrease. In Figure 5.1 the correlation between these values are shown. This shows that there is a variance in the values that creates a R^2 value of 0.9329. This is after excluding outliers from the data. This value indicates that the variance in the values are greater than expected. One possible reason for this could be incomplete drying, and that some liquid could remain when weighing the solid residues. Another possible reason could be that since the residue was not washed, it could contain different amounts of surface sulfate from the solution which would create different solid residue weights. ICP-MS results are very accurate,

and the variance should not stem from this analysis. However, the volumes that were used for dilution were quite low and some variance will stem from the automatic pipet variance when diluting.

The results from ICP-MS in Table 4.4 show an average concentration of manganese in the solution of 46.01 g/L for test 4-10, which were leached for 120 minutes. The same table also shows that the manganese concentration for test 2 was 34.27 g/L and for test 3 was 42.53 g/L. This indicates that a leaching time of 120 minutes gives a greater yield of manganese leached, compared to leaching times of 30 and 60 minutes. These results also indicate that the leaching is non-linear with 17.14 g leached after the first 30 minutes, then only 5.87 g the following 90 minutes. This is shown in Figure 5.2, with a R^2 value of 0.9259. The fact that this value is slightly lower than 1 could indicate that there was some variance in leaching. This could be due to the fact that there were not enough identical beakers at the Lab. This resulted in use of beakers with slightly different diameters which would affect amount of surface in contact with the hotplate as well as potential differences in temperature from bottom to top of the solution seeing same volume in different diameter beakers gave different solution heights. The experiment was also done over a long period of time, therefore the temperature inside the lab could also have been differing from week to week and again have an impact on the difference in temperature at the top and bottom of the solution. Despite this variance, Figure 5.2 still indicate that the leaching is non-linear and levels out.

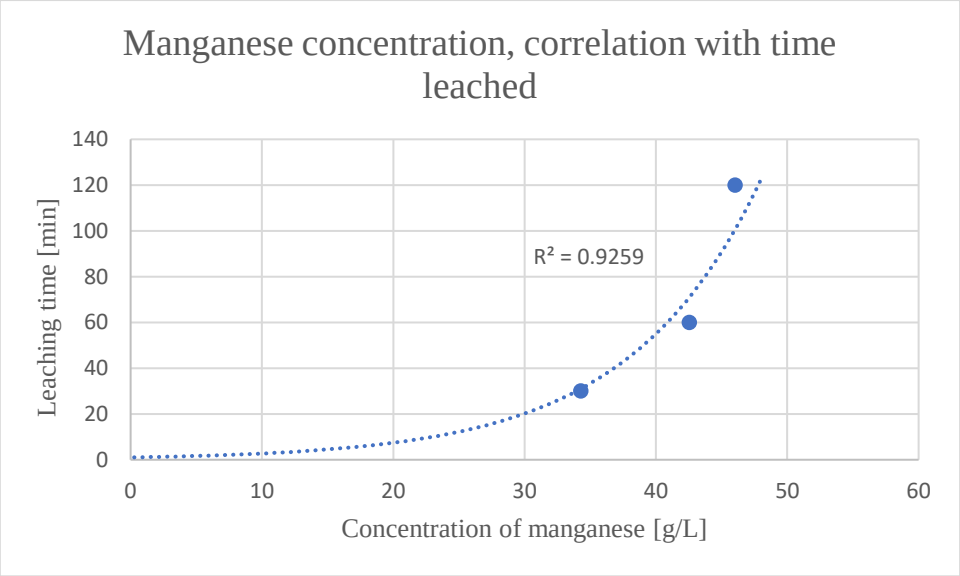

Figure 5.2: Concentration of manganese (X-axis) and time leached (Y-axis).

Another evaluation of the leaching would be to see differences in components leaching time to optimize for purity. The results from ICP-MS indicate that the leaching of iron is faster, but also have a lower yield of leaching. The concentration of iron in the solution after leaching for 30 minutes was 5.78 g/L and the average concentration after leaching for 120 was 5.87 g/L. This difference is insignificant, since the variance in the measurements is larger than the difference between these two values. Therefore, it is not possible to draw a definite conclusion from these results, but they indicate that the leaching process of iron is faster than that of

manganese. This in turn means that the ratio of Mn/Fe in the solution will increase with time leached for 1M sulfuric acid solutions.

The most important part to evaluate for leaching is the yield. To look at the yield of manganese leached, the concentration of 46.01 g/L in a 500 mL solution would result in 23.0 grams leached on average for tests run at 120 minutes. The reduced ore contained 54.77 wt% manganese which means the 50g samples leached contains 27.39g of manganese. Based on these results the yield of manganese leached would be equal to 83.97%. However, the solid residue after leaching was also analyzed with XRF and contained 22.68wt% manganese in a 27.74-gram sample. This would total a loss of 6.29 grams of manganese. These results indicate that the concentration of manganese would be 42.36 g/L. This would result in a leaching yield of 77.33% of all manganese leached. For iron, the reduced ore contained 13.73 wt% and therefore a total of 6.87 g were in the sample before leaching. The average iron concentration of the leachate was 5.52 g/L which would mean 2.76 g of Iron was leached and 4.11 g remained unleached. The XRF results show that the solid residue after leaching contained 14.31 wt% iron and therefore 4.30 g of iron was not precipitated according to the XRF results. This would mean that 59.8% of iron in the ore remained unleached according to ICP results and 62.6% of iron remained unleached according to XRF results.

The results from XRF and ICP-MS do not match completely, which in turn means that the exact yield of manganese leached cannot be determined from these results. For the ICP-MS results the volumes that were measured were low, 15 µL and 20 µL using automatic pipets. A small variation with such low volumes will result in some changes in concentration values. It is therefore difficult to tell whether the yield of this process by one definite number. On the other hand, it is worth to mention that the ICP-MS analysis is in general more accurate than the portable XRF. Despite these, the variation from the two calculations is quite small and shows that the leaching yield will be between 77% and 84% of total manganese in the reduced ore.

One of the goals of this product is to achieve zero solid waste. After leaching the solid residue contains valuable elements, some metallic Fe and some undissolved MnO. To achieve this goal, either the leaching process must be adapted to leach more of the MnO or the solid residue after leaching must be used as low-grade source of consumable materials. The iron in the solid residue would be easy to separate since it is metallic iron and could be done by magnetic separation. The three remaining main components in the residue are then manganese in MnO and calcium and sulfur in gypsum form. The gypsum and MnO can then be separated by dissolving gypsum in water and filtrate the solid MnO that will not dissolve. The solubility of gypsum is 0.2g/100 mL and this process would therefore require copious amounts of water (PubChem, 2023). Therefore, it should be explored if other methods also are viable. Gypsum has many uses, such as in cement, paper, and fertilizer among many others. Therefore, it would be greatly beneficial to separate it from the manganese oxide before attempting to re-leach the manganese oxide to produce manganese dioxide.

An option of optimizing the yield of the process would be to change the leaching process. The results in Table 4.4 indicated that with time the yield of manganese increases, while the maximum amounts of iron and calcium are reached earlier. This in turn would mean that the concentration ratio of manganese over impurities increases with time leached for leaching in

1M sulfuric acid. It can therefore be explored if greater leaching time can give even greater concentrations of manganese in the solution. However, the potential effect of this will most likely not be remarkably high, seeing that the effect of leaching slows down over time. Table 4.4 shows that 42.5 g/L was the concentration of manganese in the solution after leaching for 60 minutes, after another 60 minutes of leaching, the concentration only increased by 3.48 g/L on average. This indicates that leaching for another hour would most likely give a significantly lower increase of concentration than 3.48 g/L. Therefore, other parameters should be explored. In this experiment the solid to liquid ratio remained constant at 50g/500mL. If solubility is an issue lower S/L ratio would be beneficial and increase the yield (Sukhbat Sandag-Ochir, 2021). However, it will most likely create a higher degree of impurity in the solution since calcium and iron reached their solubility faster than that of manganese. Another option is to explore slightly more acidic solutions. Acidity was tested on ore containing 17.31wt% manganese in Mongolia and they found that 4M sulfuric acid was most beneficial for leaching yield of manganese (Sukhbat Sandag-Ochir, 2021). However, ore used in this experiment contains 67wt% MnO_2 and 4M sulfuric acid and would most likely be an unnecessary increase in molarity, yet their results indicate that higher concentrations of sulfuric acid could be beneficial and can therefore be explored in smaller steps, for example 0.5 M increases up to 4M.

Another parameter that remained constant in this experiment was temperature. The leaching was done by having a beaker on a hotplate while stirring. The issue with a hotplate is that the temperature might differ throughout the solution. This would result in small changes however, but different set ups could be attempted. Another change that would likely be more significant would be the temperature itself. According to research on low grade manganese ore, 40 °C was optimal temperature (Sukhbat Sandag-Ochir, 2021). Their experiment was with quite a lot of different conditions and low-grade manganese ore, therefore it remains possible that an increase in temperature would be beneficial for leaching yield. Their research also explored different agitation rates. In this experiment 500 rpm was used while their research found that there was no increase in leaching yield beyond 300 rpm. Therefore, it could be possible to lower the agitation rate and test at 400, 300 and even below 300 seeing that all other parameters are slightly different for this experiment (Sukhbat Sandag-Ochir, 2021).

5.2 Purification of solutions

In this project there are two main purposes of purifying the leachate solutions that were observed to have varying results. The first being that fewer impurities present in the solution hinders precipitation of impurities in the final product. An example of this is that leached iron can be precipitated into iron oxides and create impure solid residue after precipitation. The other being that an impure solution can have a significant effect on the stability of potential products and therefore precipitate the wrong compound. An example of this is the difference in an Mn-H_2O system and an Mn-SO_4-H_2O system as given in Figure 5.3 that will affect what pH and Eh that precipitates certain compounds.

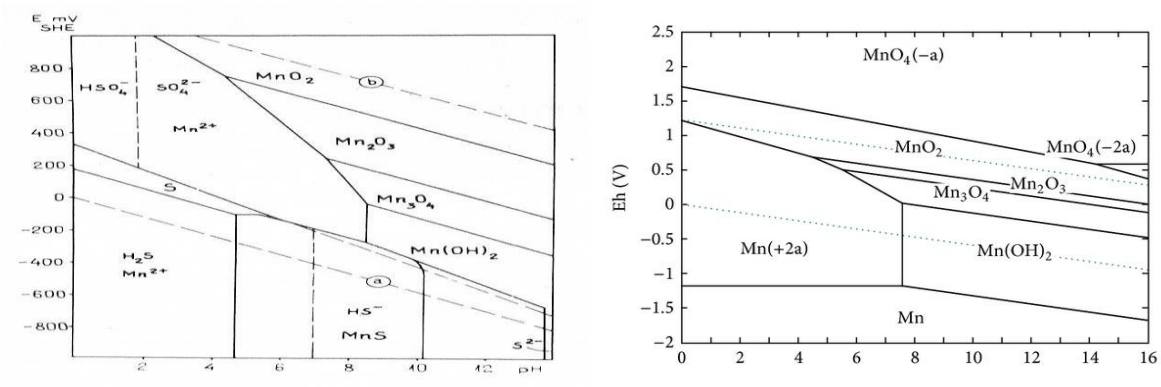

Figure 5.3: Shows the Mn-SO_4-H_2O (left) and Mn-H_2O (right) systems at 25°C *(Николайчук, 2015) (Rose, 2003).*

The samples have two major impurities. These are as given in Table 4.2 and are calcium and iron. In addition to these impurities there was a large amount of sulfur present in the solutions due to the use of sulfuric acid. Different amounts of calcium oxide were added to the different tests and the XRDs shown in Figures 4.5-4.7 show that the main component in the solid residues after purification was bassanite or gypsum for test 2-8. Bassanite and gypsum are the same compound, just with a differing amount of water content. The differing content of water is most likely due to slight variation in drying time and has no real effect on the product. For test nr. 10 calcium carbonate was added instead of calcium oxide. The XRD result shown in Figure 4.8 shows that the main component in the solid residue was calcium carbonate. This means that little to no sulfate is removed from the solution with the addition of calcium carbonate. This is a big issue seeing that the presence of sulfate will influence the precipitation stage.

The amount of calcium added was based on the change in color after addition for test nr. 4. However, it seems that the amounts added are not sufficient to remove the sulfur. This is shown in Table 4.13-4.20. For all products, the sulfur content is between 10-16 wt% of the solid product. Seeing that none of the sought after products contain sulfur themselves (MnO_2 and $MnCO_3$), the content of sulfur is only in impurities. For this issue to be solved, a possible solution would be to increase the amount of calcium oxide added. This should precipitate a larger amount of gypsum and decrease the concentration of sulfur in the solution. The goal is to add enough calcium oxide so there is no sulfur in the final product. At the same time, the amounts of manganese lost with an increased addition of calcium oxide must be monitored. Seeing that the sulfur content is remarkably high, a substantial increase in calcium oxide addition would be needed for a significant reduction of sulfur in the final product.

Tables 4.13-4.20 also show that iron is a significant impurity in all samples even though the XRD results do not show any iron containing compounds or metallic iron for most of the products. The ICP-MS results, however, also indicate precipitation of iron in different quantities seeing that the iron concentration has dropped for all tests after precipitation. Therefore, iron must in some way be removed in a greater effect than in this experiment. For test nr. 4 the purification removed a total of 3.37 grams of solid containing a concentration of iron of 13.58wt% shown in Table 4.7 and 4.8. This means a total of 0.46 grams of elemental iron was removed for test nr. 4. The ICP-MS results show that the concentration of iron before

purification was 7.4 g/L and after purification the concentration was 5.7 g/L. Seeing that the purification was done with 400mL of the leaching solution. This would mean that 0.68 grams of iron were removed based on the ICP-MS results. The total amount of iron in the 400 mL solution purified was 2.96 grams. This would mean that between 16-23% of the iron content in the solution was removed. This amount is far too low. Therefore, greater purification must also be done for the removal of iron. The same action for removing sulfur from the solution can be effective for removal of iron. A greater amount of calcium oxide added could result in a greater percentage of iron content being removed. The same precaution remains, that manganese loss during the purification must be monitored.

According to a study done on removal of iron (II) from manganese sulfate solutions it was found that 100% of iron in the solution was able to be removed while only 2% of manganese content was lost (Kui Wang, 2019). They utilized mechanically activated $CaCO_3$ in a wet stirred ball mill. This method may be efficient to adopt, seeing that they had both great yield of iron removal and very little loss of manganese.

5.3 Precipitation evaluation

5.3.1 Precipitation with potassium permanganate and sodium hydroxide

The precipitation of manganese dioxide using potassium permanganate occurred for all three tests done. For test nr. 2 and 3 the potassium permanganate was added as a liquid and for test nr. 4 it was added as a solid. Both these additions had some complications, and the product was not as desired.

During the experimental part, issues occurred for both the liquid and solid addition. The main issue being that the potassium permanganate seemingly did not dissolve. The pH of the solution was slightly above 3, for all 3 tests. Firstly, with addition of potassium permanganate it was observed that the solid did not dissolve and instead remained solid in the bottom of the beaker. With addition of potassium permanganate solution, it was observed that a black solid formed at the surface of the solution after addition. However, for both additions these solids then dissolved slowly. From addition until complete dissolution, it was observed that the pH slightly increased. However, after the potassium permanganate had completely dissolved the pH decreased and a new black solid precipitated. This is an indication that the first solid formed was not manganese dioxide as the reaction given in Formula 5.1 shows that precipitation of manganese dioxide will acidify the solution. This also indicates that the precipitation after dissolution of potassium permanganate was manganese dioxide.

$$2\mathrm{KMn}O_4 + 3Mn^{2+} + 2H_2\mathrm{O} = 5\mathrm{Mn}O_2 + 2\mathrm{K}^+ + 4\mathrm{H}^+ \quad (5.1)$$

As shown in chapter 4.4.2 the XRD results for test nr. 2, 3, 4 and 10 are all quite different from all other XRD's and could not be identified by the program. This is most likely because the precipitated manganese dioxide is amorphous (Munaiah Yeddala, 2013). This assumption is based on the reference given in Figure 5.4. This shows peaks around 10-12, 37-38 and 66-67. These all match with the results shown in Figures 4.9-4.12. The XRD of test nr. 2, 3 and 10 were only done for 30 minutes which gives slightly unclear graphs, but the peaks are at the same places for all tests. This shows that the product precipitated is amorphous manganese

dioxide. For this product to be usable, it is necessary to form crystalline manganese dioxide which can be done by heating under pressure.

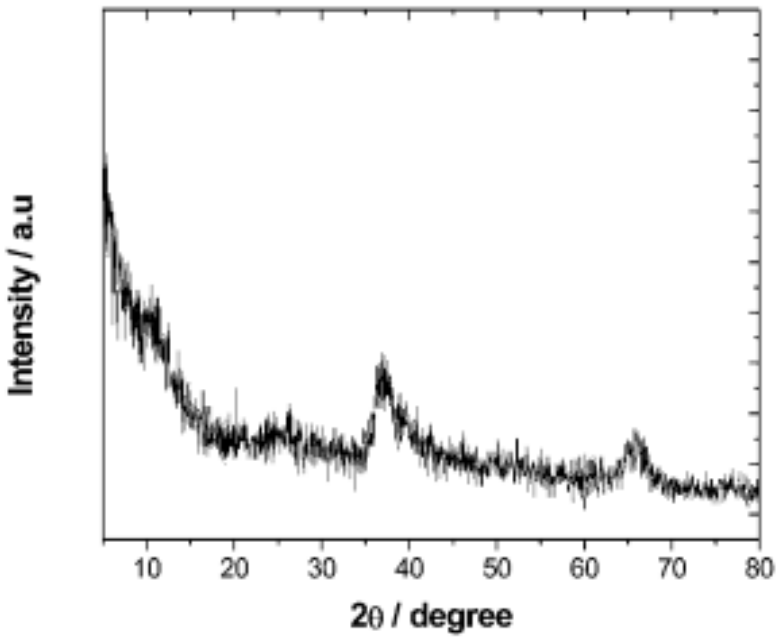

Figure 5.4: XRD spectrum of amorphous MnO_2 (Munaiah Yeddala, 2013).

After the product is crystallized there will remain two large issues. The product has noticeable impurities that need to be removed, and in addition the yield of the process was quite low. The XRDs do not show any impurities due to the amorphous structure of the product. However, the XRF results show that product 2, 3, 4 and 10 all contain between 7 and 10 wt% sulfur in some form. As the XRD has not detected any other compounds than manganese dioxide, it cannot be determined definitely what compound the sulfur has been precipitated as. It would be natural to assume that gypsum once again has been formed, since calcium is present. However, despite calcium presence in the solution, it is not gypsum that has been formed. This is shown in the XRF results in table 4.5.5, 4.5.6, 4.5.7 and 4.5.13 where calcium only accounts for 0.15-0.24 wt% of the solid residue. Iron sulfate on the other hand, is insoluble in sulfuric acid and it could be precipitated when iron is oxidized with addition of potassium permanganate (Vercellotti, 1988). If this is the case, it is not the only form of iron and sulfate precipitation seeing that the ratio of iron and sulfate for test 2-4 does not remain constant. Other compounds are therefore more likely. The majority of the sulfur could be present due to the fact that the solids were not washed before drying and testing. Therefore sulfate in the solution would remain on the surface after the solids were dried. It is not possible from these tests to quantify what portion of sulfur has been precipitated and what is sulfate on the surface. However, both the iron and the sulfur in the product should feasibly be removed before precipitation as explained in 5.2. If this is done, the product should not continue to have the same degree of purity issue.

The yield of manganese dioxide produced varied significantly in the four tests (2,3,4 and 10). The yield of MnO_2 is based on the amount of manganese in reduced ore and the amount of manganese in MnO_2 product. The calculations of the yield are given in appendices 7.4. Table 5.1 shows that for test nr. 3 and 4 the yield of manganese dioxide based on total amount of manganese in the reduced ore is quite similar. At the same time these two tests have vastly different purity in the product seeing that the manganese content of test 4 is almost double that

of test nr. 3. Test nr. 2, which was done the same way as test nr. 2 shows a higher yield than the three other tests, while the purity of the product is only slightly worse than that of test nr. 4. Test nr. 10 shows that both the purity and the yield were worse than any of the other tests. Based on these results, the addition of sodium hydroxide to precipitate manganese dioxide, as done in test nr. 10 is not successful. Both the purity and the yield of the process are too poor. Meanwhile, the results with addition of potassium permanganate shows that the yield is significantly better than test 10, yet quite low at 20-27%. This yield can possibly be increased if the purity of the solution is bettered. Potassium permanganate is not a selective oxidizing agent and other impurities will also be oxidized by its addition. Therefore, it could be possible that both the yield and purity of the product would increase if the purification step removed more iron and sulfate.

Table 5.1: Precipitate weight, manganese content and yield of manganese dioxide production for test 2, 3, 4 and 10.

Test nr.	Solid product weight [g]	Manganese content [wt%]	Yield of MnO_2 [%]	Purity in product [%]
2	**13.10**	**40.54**	**27.70**	**64.15**
3	**14.09**	**28.42**	**20.89**	**44.97**
4	**8.80**	**45.43**	**20.86**	**71.89**
10	**7.99**	**15.21**	**6.34**	**24.07**

The yield can also be improved if the addition process of potassium permanganate is improved. There were solubility issues that could be changed if volume solution were to be changed. This could be done from the start, as explained in 5.1 by changing the S/L ratio for leaching. However, it can also be done by adding water to the solution before precipitation. If this is done, the pH of the solution will also increase, and this must be checked. At the same time, an increase in pH could also increase the yield of manganese dioxide. As shown in Figure 5.5 the increase of pH will lower the electrochemical voltage necessary to precipitate manganese dioxide. The figure also shows that at too high pH levels, the risk of other manganese oxides precipitating can become an issue. Again, impurities will affect whether manganese gets oxidized or other elements in the solution. Therefore, improvements in the solution's purification could result in direct improvements of the precipitation.

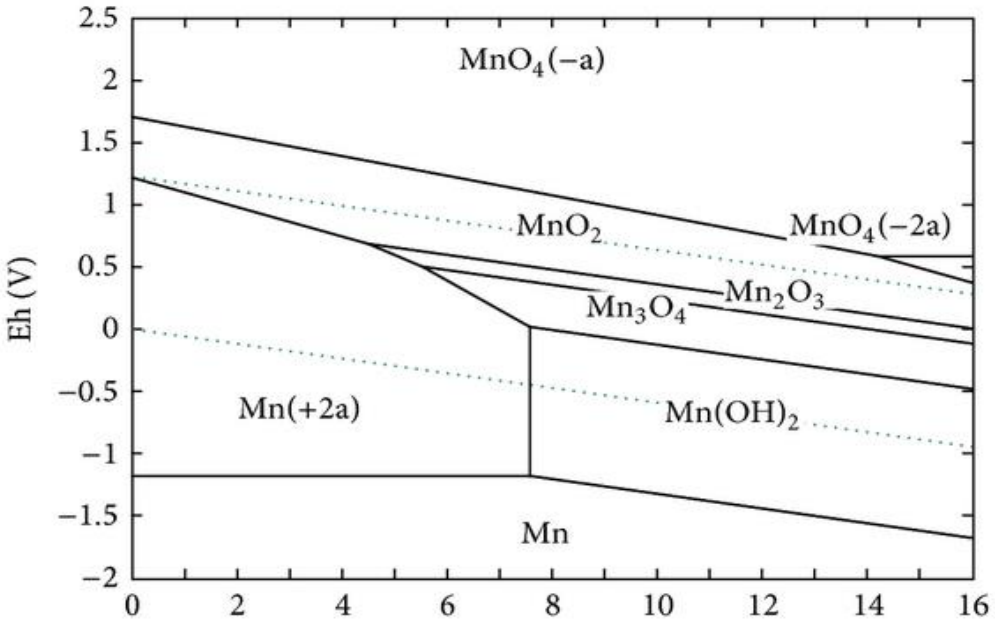

Figure 5.5: Eh-pH diagram for Mn-H_2O system at 25°C (Николайчук, 2015).

For test nr. 10 both yield and purity were poor. Seeing that the yield was only 6.34% it is highly unlikely that increased purification will be enough of a change for sodium hydroxide addition to be viable at the conditions tested. It was observed that the color slightly changed when pH reached 6, furthermore the color became very dark once the pH reached 7. This is before we expect the precipitation of manganese dioxide to occur. This indicated that a different precipitation took place of another compound before precipitation of manganese. The main impurity in the product is, as shown in Table 4.21 compounds containing either iron or sulfur. One possible impurity could be iron hydroxide seeing that the pH increase was rather slow with addition as well as the hint of green in the solution.

The green color was most clearly visible at the top after precipitation. This could be iron sulfate seeing that it is green as a crystal, as well as in solutions. Another possible precipitate is iron (III) oxide seeing the early color change shown in the middle picture. However, this is not green in color and with the significant amount of iron in the solid product, the red oxide should have been visible if enough was precipitated. It could also be possible that different iron oxides were precipitated at different stages of the precipitation, and therefore are not identifiable by the XRD graph. The final product can therefore contain a mixture of iron (II) hydroxide, iron (III) hydroxide, iron sulfate and iron (III) oxide.

If the process of precipitation with sodium hydroxide to precipitate manganese dioxide using pH-levels were to be explored further, changes would need to be made. In this experiment the sodium hydroxide was added to the solution as a solid, it could be beneficial to add it as a solution instead. This would make it easier to add small amounts at a time, however, the volume of the solution would of course change. The maximum pH the solution reached in our experiment was 7.80 and it dropped between 7,4 and 7,5 before new addition of sodium hydroxide. However, from starting pH of around 5 before precipitation the increase to 7.5 was done rather slowly. Small amounts of sodium hydroxide were added at a time in order to not

increase the pH too much. This could have given other compounds time to precipitate at a lower pH, such as iron oxides. The experiment could be done by faster addition of base until the pH is close to 8. This could of course also just produce other iron and sulfate compounds faster. Therefore, the most efficient way to have a pure product would be to have a pure solution before precipitation.

5.3.2 Precipitation with magnesium oxide

Test numbers 5, 6 and 7 were precipitated with the addition of magnesium oxide (MgO). The XRDs of the precipitates for all 3 tests show the precipitation of hausmannite as the main product. In addition to the fact that this is not the product that was wanted from this precipitation, it is also iron containing hausmannite with the formula $Fe_{0.297}Mn_{2.703}O_4$. The XRD also shows that not all MgO was dissolved in the solution as there are remains in the solid product. Manganese hydroxide has not been precipitated as the main product. The desired reaction to form $Mn(OH)_2$ is given in Formula 5.2.

$$MgO + Mn^{2+} + H_2O \rightarrow Mn(OH)_2 + Mg^{2+} \quad (5.2)$$

Since the desired product has not been precipitated, yield and purity are not of interest to evaluate for hausmannite. An evaluation of the impurities in the solid precipitate is however still relevant if the method was to be adjusted for manganese dioxide precipitation. The XRF results shown in table 4.5.8-4.5.10 show that the main impurities yet again are iron and sulfur. In addition, the XRF results confirm the results from XRD, that MgO has not been fully dissolved and therefore there are remains in the solid residue. If the method was adjusted such that the product was manganese dioxide, a smaller amount of magnesium oxide would need to be added so that it does not contaminate the solid product. In test 7, which had the least amount of magnesium oxide addition, 6.09 grams of magnesium oxide was added to the 350 mL solution. The XRF results show that the solid residue from test nr. 7 contained 0.85 grams of magnesium oxide, which in turn means 5.24 grams of magnesium oxide was dissolved in 350 mL solution. The amount of magnesium oxide dissolved in the solutions did not remain constant at that amount. For test nr. 5 there was 1.69 grams of magnesium oxide in the solid product, which means that 8.47 grams of magnesium oxide was dissolved in the 350 mL solution for test nr. 5. These results indicate that the limit of magnesium oxide dissolves is dependent on the amount added and are around 85%. The solid residue amount also is non-linear compared to MgO added as shown in Figure 5.6.

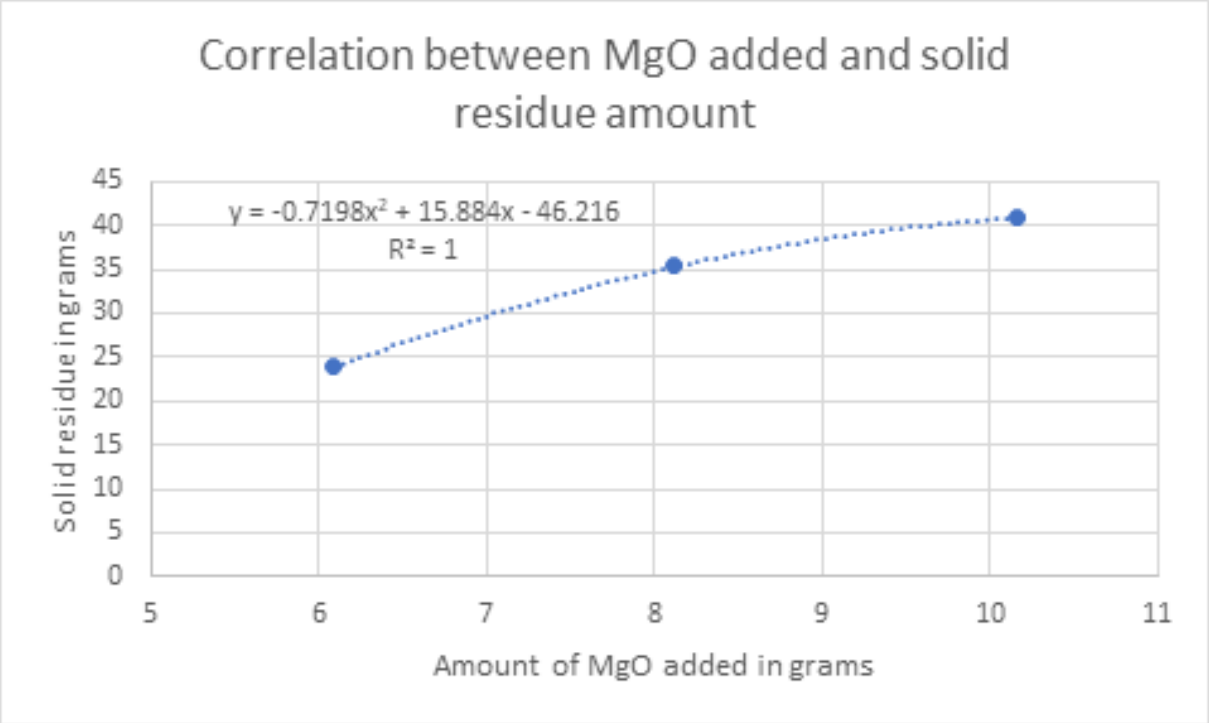

Figure 5.6: Shows correlation between grams of MgO added (X-axis) and solid residue weight (Y-axis).

Above all, it must be explored why hausmannite was precipitated instead of manganese hydroxide as was desired. Firstly, it is of great interest that the hausmannite is iron containing. This indicates that the iron content in hausmannite increases stability seeing that this is formed in favor of ordinary hausmannite (Mn_3O_4). This in turn means that the iron content in the solution will influence what product is precipitated. There is a possibility that the same experiment, but with removal of iron could precipitate other manganese oxides at these conditions. However, since there is not a trace of other oxides shown by the XRD in Figure 4.14, while the iron content in the solution was depleted, as shown in table 4.9, more actions are most likely needed.

One other potential issue, other than the iron content in the solution, is the effect that magnesium oxide has on pH levels. The pH of the solution was not monitored after addition of magnesium oxide and adjustments were therefore not done to lower the pH. At higher pH, as shown in Figure 5.5 Hausmannite is able to form. Therefore, the pH increase from MgO addition would contribute to precipitation of Hausmannite rather than other oxides. This could be monitored by continuously measuring the pH of the solution with the addition of magnesium oxide. Manganese hydroxide also precipitate at high pH levels, therefore different pH levels should be explored by different actions being taken. These actions could be to acidify the solution with addition of sulfuric acid. Another could be to stop addition and assess the product made using small amounts of magnesium oxide. Unfortunately, this would most likely not precipitate a high yield of the product and might not be an effective change for yield but would have a greater impact on purity. Again, the change of S/L ratio would be a possible productive change as the same ratio of magnesium oxide to manganese would have a lower impact on the pH and therefore make it easier to manipulate pH with addition of strong acid or base.

5.3.3 Precipitation results with magnesium carbonate

Test nr. 8 and 9 were done with addition of magnesium carbonate. The main product of the precipitate is shown in Figure 4.17 and 4.18. This is manganese carbonate, a product that can be used for manganese dioxide production by calcination. The calculation of the yield is given in appendices 7.4 and the results are given in table 5.2. This shows that the yield of the process was quite similar for the two tests, with around 40-43% of all manganese in the reduced ore turning into manganese carbonate. On the other hand, the purity of the two tests differs quite a bit. Test nr. 8 shows that the purity of manganese carbonate to be 47.3 wt% while it is 61.6 wt% for test nr. 9. The reaction to precipitate manganese carbonate is given in Formula 5.3.

$$MgCO_3(s) + Mn^{2+}(aq) \rightarrow MnCO_3(s) + Mg^{2+}(aq) \quad (5.3)$$

Table 5.2: Weight of precipitate product, using $MgCO_3$ and yield of process.

Test nr.	Weight after precipitation [g]	Manganese in product [wt%]	Yield of process [%]	Purity of $MnCO_3$ [wt%]
8	**34.73**	**22.60**	**40.95**	**47.29**
9	**28.25**	**29.44**	**43.39**	**61.60**

These results are quite interesting seeing that the XRF results of the two samples are similar. The major differences are the reading of magnesium. For test nr. 8 magnesium accounts for 3.61 wt% of the sample and for test nr. 9 magnesium accounts for 2.40 wt% of the sample. The XRD does not show what compound the magnesium has been precipitated as, however, due to the significant difference in purity and total weight, despite similar weight% of other elements, magnesium is most likely bonded to carbonate. This would mean that not all magnesium carbonate was dissolved. Assuming all magnesium in the solid after precipitation is magnesium carbonate would mean 4.35 grams were not dissolved for test nr. 8 and 2.35 grams were not dissolved for test nr. 9. This means 79.53% was dissolved for test nr. 8 and 86.18% was dissolved for test nr. 9. Seeing that the yield for test nr. 9 and purity of test nr. 9 was superior to that of test nr. 8 shows that a smaller amount of magnesium carbonate might be optimal. In addition, test nr. 8 produced 16.42 grams and test nr.9 produced 17.40 grams of manganese carbonate. This also indicates that an increased amount of carbonate in the solution is not necessarily beneficial, seeing that the concentration is higher for test nr. 8.

Yet again, dissolving the additive completely is an issue. And once more, an alternative that might produce better results in this regard, could be an adjustment of the S/L ratio. With a greater amount of liquid for the same amount of solid as in this experiment, a larger portion of the additive should be able to dissolve. This should create a purer product, seeing that a smaller amount of additive, if any, remains undissolved.

Another issue with this process is that the yield is only around 40%. This is low and means there are a lot of manganese left in the solution, as shown in table 4.9. This should mean that there either is not enough carbonate to react with the manganese, the carbonate is reacting with something else or that the equilibrium of the reaction gives a poor yield with low excess.

According to a paper on manganese carbonate precipitation, it was found that the reaction is slightly endothermic, and the reaction rate increased with temperature for a solution at pH 3 and at 80°C (Ali, 2020). Changes in precipitation parameters can be adjusted to a higher temperature seeing that this should increase the yield of an endothermic reaction. In addition, the pH of the reaction should be monitored, and different pH ranges can be tested. The solution before addition will have a pH slightly above 3 if purification stage is unchanged. The precipitation should be tested at this pH before any possible increase or decrease. If the purification step is changed, the pH will also change, and addition of base or acid must be done to balance the acidity before precipitation.

5.4 SEM results

As we can see in Figure 4.19 and 4.20, the non-reduced ore is far less porous than the pre-reduced ore. Reduction with hydrogen increased the surface area of the sample which has been detected with more pores and holes compared to the non-reduced sample in Figure 4.22 and 4.21, respectively. Increased porosity helps in increasing leachability of the ores. It makes it more accessible to the leaching acid to be extracted which results in minimizing the leaching period/time drastically. The results of leaching behavior also confirmed this to be true.

The sample were analyzed under x-ray mapping with EDS-detector, which made it possible to see whether elements had a correlation in their positioning in the compounds made. For all products made, MnO_2, Mn_3O_4 and $MnCO_3$, a discovery that concurs with the XRD results were made. There were no differences in the positioning of iron and manganese, the only difference was the rate of occurrence, meaning the amounts differed, but not the positions. This is a strong indicator that iron has not been precipitated as an individual product but has replaced manganese in every 4^{th} or 5^{th} manganese position, depending on how impure the products are. This correlation of positioning is shown in Figure 5.7 and 5.8. Red dots represent manganese while blue dots represent iron.

This makes sense due to the similarity of physical properties that manganese and iron possess. Iron and manganese are neighboring elements on the periodic table. This in turn means that both their radius and weight are very similar at 54.94 u and 161 pm for manganese and 55.85u and 156 pm for Iron (Dayah, 2023). These similarities allow for iron to replace a portion of the manganese in a manganese oxide structure. If this is the case, it is of even greater importance to remove iron from the solution, seeing that removal of iron in the crystal structure would not be an option.

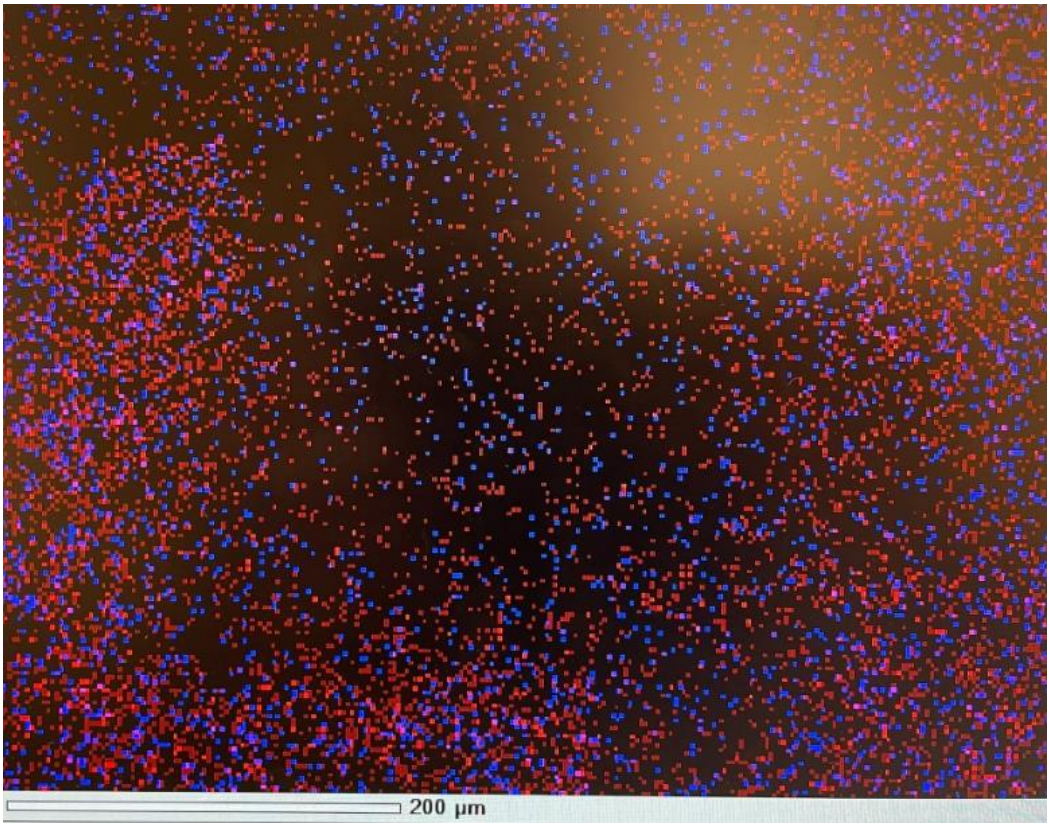

Figure 5.7: Position of Iron and manganese for product 8.

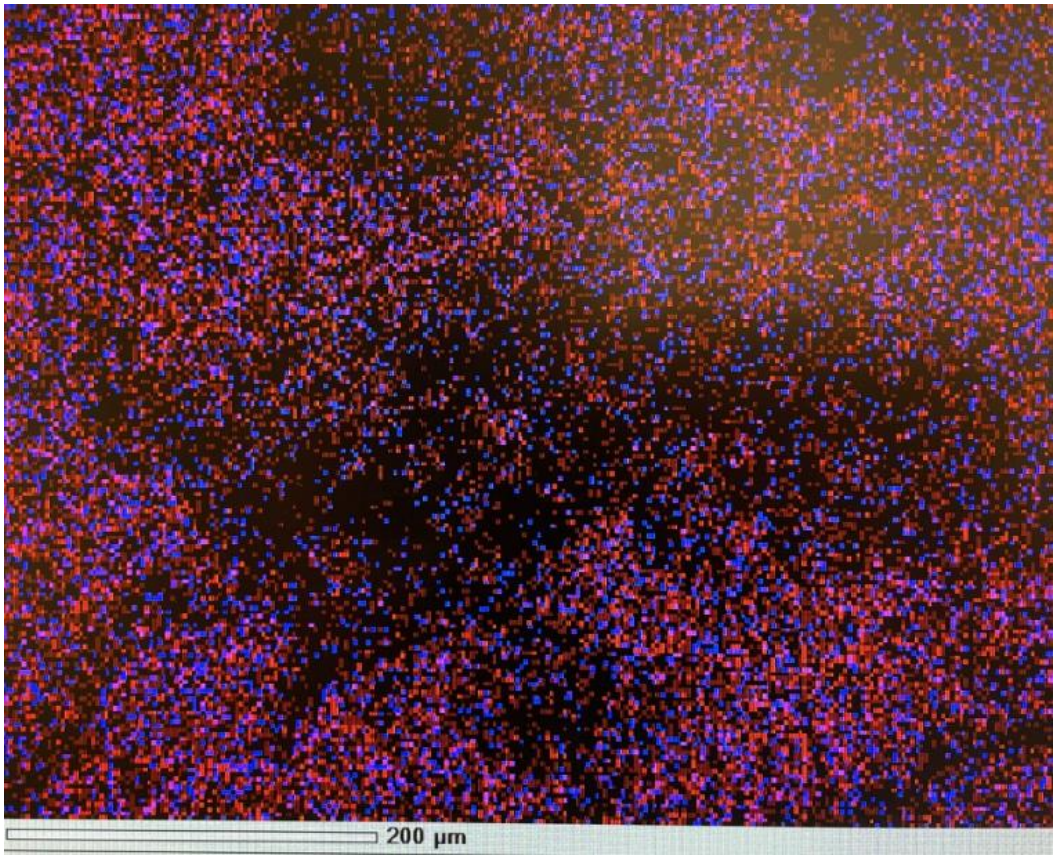

Figure 5.8: Position of Iron and manganese for product 4.

Chapter 6: Conclusions

The main conclusions of this thesis are summarized as follows:

- The hydrogen reduction of manganese ore yields a reduced ore that contains metallic Fe and MnO, while other oxides of the ore are not reduced.
- The yield of leached manganese was measured to be around 80% for the pre-reduced ore under applied conditions, which was much greater than that for the raw ore. Yet there remains room for improvement that should be explored, with temperature increase, acidity increase and S/L ratio being the most likely efficient changes.
- A slight majority of reduced metallic Fe in the reduced ore was stable in leaching (around 60%), while a smaller portion was dissolved in sulfuric acid (40%).
- The produced leachates contained Fe, Ca, Mg and sulfate as the main impurities, and needs purification.
- The purification of the solutions was not satisfying the required purity of solution to achieve a pure product. To increase effectiveness of purification, a greater addition of calcium oxide should be effective, a decrease in S/L ratio might be optimal and greater purification of iron is a necessity.
- Precipitation using potassium permanganate had a yield of around 20-27% of manganese in reduced ore converted to manganese dioxide while the purity of the product ranged from 40-70%. Issues with solubility of potassium permanganate during precipitation could be fixed by an adjustment of the S/L ratio.
- Precipitation using magnesium oxide was not successful. Hausmannite containing iron was precipitated. Monitoring and testing different pH levels could affect which oxide that will precipitate.
- Precipitation using magnesium carbonate successfully precipitated manganese carbonate with a yield around 40% and the purity of the tests were 47% for test nr. 8 and 62 % for test nr. 9. Yield could be increased at elevated temperatures and the purity of the product should be increased with adjustments of the purification step.
- Precipitation using sodium hydroxide produced some manganese dioxide, but both yield and purity was very low. The process of addition could be changed to add the base as a solution, and the purification step should have a great effect on what compounds gets precipitated and therefore increase both yield and purity.

References

[1] Ali, S., 2020. *Synthesis and kinetic modeling of manganese carbonate precipitated from manganese sulfate solution,* Peshawar, Pakistan: Taylor and francis.

[2] Anon., 2022. *MICROSCOPEWIKI.* [Online]
Available at: https://microscopewiki.com/scanning-electron-microscope/
[Accessed 2023].

[3] B.Mishra, M. D., 2003. Oxidation of manganese in a low-grade ore using KMnO4 as a reagent. *International Journal of Mineral Processing,* Volume 70, p. 95.

[4] board, E., 2022. *Microscope wiki.* [Online]
Available at: https://microscopewiki.com/scanning-electron-microscope/

[5] Cannon, W. F., 2014. *USGS.gov.* [Online]
Available at: https://pubs.usgs.gov/fs/2014/3087/
[Accessed 05 2023].

[6] Carlier, M., 2022. *Worldwide number of battery electric vehicles in use from 2016 to 2021.* [Online]
Available at: https://www.statista.com/statistics/270603/worldwide-number-of-hybrid-and-electric-vehicles-since-2009/
[Accessed 10 04 2023].

[7] Cheng, W. &. C. Y., 2007. *science direct.* [Online]
Available at: https://www.sciencedirect.com/science/article/pii/S0304386X0700179X#bib21
[Accessed 12 04 2023].

[8] David B. Wellbeloved, P. M. C. J. W. W., 2000. *Onlinelibrary.* [Online]
Available at: https://onlinelibrary.wiley.com/doi/10.1002/14356007.a16_077
[Accessed 2023].

[9] Dayah, M., 2023. *Ptable.* [Online]
Available at: https://ptable.com/#Properties/Weight
[Accessed 19 05 2023].

[10] Didier Ngoy, D. S. M. T., 2020. Pre-reduction Behaviour of Manganese Ores in H2 and CO Containing Gases. *ISIJ international,* 60(11), pp. 2325-2331.

[11] Dragonfly energy, 2022. *Dragonfly energy.* [Online]
Available at: https://dragonflyenergy.com/types-of-lithium-batteries-guide/
[Accessed 10 04 2023].

[12] Guillaume Zante a b, A. B. a. A. M. a. R. B. a. D. T. a. M. B. a., 2020. Solvent extraction fractionation of manganese, cobalt, nickel and lithium using ionic liquids and deep eutectic solvents. *Minerals engineering.*

[13] [HAlMan project team, 2023. *Halman.* [Online]
Available at: https://halman-project.eu/
[Accessed 23 04 2023].

[14] JEssica Elzea Kogel, N. C. T. ,. J. M. B. S. T. K., 2009. *Manganese.* 7th ed. s.l.:SME.

[15] Kashani, A., n.d. [Online]
Available at:
https://www.researchgate.net/publication/255785750_Aerosol_characterization_of_concentric_pneumatic_nebulizer_used_in_inductively_coupled_plasma-mass_spectrometryICP-MS/figures?lo=1

[16] Katsioulas, I., 2021. *Research Gate.* [Online]
Available at: https://www.researchgate.net/figure/Schematic-diagram-of-a-simple-electrolytic-cell-Arrows-indicate-the-motion-of-ions_fig2_347841630

[17] Kui Wang, Q. Z., 2019. *Efficient removal of iron(II) from manganese sulfate solution by using mechanically activated CaCO3,* Wuhan, China: Science direct.

[18] LibreTexts, 2023. *Libretexts Chemistry.* [Online]
Available at: https://chem.libretexts.org/Courses/Westminster_College/CHE_180_-_Inorganic_Chemistry/10%3A_Chapter_10_-_The_Transition_Metals/10.5%3A_Group_7/Chemistry_of_Manganese
[Accessed 10 04 2022].

[19] Lim, S., 2013. *Semantic scholar.* [Online]
Available at: https://www.semanticscholar.org/paper/X-Ray-Fluorescence-%28XRF%29-Analyzer-Theory%2C-Utility%2C-Lim/303095bc6899c6736ea777a1ad76e33bbaff5097/figure/9

[20] Ling, Z. C. R., 2017. *Manganese dioxide as rechargeable magnesium battery cathode.,* United States: Frontiers.

[21] Liu, C. Z. J. X. C. Y. B., 2013. *A review on the synthesis of manganese oxide nanomaterials and their applications on lithium-ion batteries.,* China: Hindawi.

[22] M. Yoshida, Y. Y. Y. a. H., 2016. Preparation of manganeese dioxide by using MgO as an oxidizing agent. *Hydrometallurgy,* Volume 161, p. 12.

[23]Mahadeshwara, M. R., 2022. *XRD.* [Online]
Available at: https://www.tribonet.org/wiki/xrd-x-ray-diffraction/

[24] Mahadeshwara, M. R., 2022. *XRD.* s.l.:s.n.

[25] Markus Antonius Elinsønn Pedersen, A. S. E., 2022. *Bærekraftig gjenvinning av metaller fra manganslam via syreleaching,* trondheim: ntnu open.

[26] Mehta, S., 2016. *Investigation of capacity fade in dlatplate rechargeable alkaline MnO2/Zn cells.,* s.l.: Universit of British Columbia.

[27] Munaiah Yeddala, G. S. R. B. P. R. a. P. T. K., 2013. *Facile synthesis of hollow sphere amorphous MnO2: The formation mechanism, morphology and effect of a bivalent cation-containing electrolyte on its supercapacitive behavior,* s.l.: Journal of Materials Chemistry A.

[28] ONAL, M. A. R., 2021. *Production of Electrolytic Manganese Dioxide.* [Online]
Available at: https://encyclopedia.pub/entry/11803
[Accessed 2023].

[29] Programme, U. N. E., 2021. *Global Battery Alliance Annual Report 2020-2021.* [Online]
Available at:

https://wedocs.unep.org/bitstream/handle/20.500.11822/35887/GBA%20Annual%20Report%202020-21.pdf?sequence=1&isAllowed=y
[Accessed 12 04 2023].

[30] PubChem, 2023. *Pubchem.* [Online]
Available at: https://pubchem.ncbi.nlm.nih.gov/compound/Calcium-Sulfate-Dihydrate
[Accessed 05 05 2023].

[31] Regeane M. Freitas, T. A. G. P. A. C. Q. L., 2013. *Hindawi.* [Online]
Available at: https://www.hindawi.com/journals/jchem/2013/287257/
[Accessed 2023].

[32] Rose, A. W., 2003. *METHODS FOR PASSIVE REMOVAL OF MANGANESE FROM ACID MINE DRAINAGE,* Pennsylvania State, USA: Pennsylvania State University.

[33] Sahu, J. N., 2002. Electrolytic production of manganese dioxide from manganese sulphate solution. *Transactions of the Indian Institute of Metals,* Volume 55, pp. 39-47,.

[34] Sino Voltaics, 2019. *LMO batteries: properties and usage.* [Online]
Available at: https://sinovoltaics.com/learning-center/storage/lmo-batteries/
[Accessed 10 04 2023].

[35] Sukhbat Sandag-Ochir, Z. T. O. B. J. L. K. D. S.-E. N. B. D. U. B. O. E., 2021. *Beneficiation and Sulfuric Acid Leaching of,* Mongolia: Atlantis Press.

[36] Survey, U. S. G., 2022. *Manganese Statistics and Information.* [Online]
Available at: https://www.usgs.gov/centers/nmic/manganese-statistics-and-information
[Accessed 12 04 2023].

[37] Takuya Hatakeyama a b, N. L. O. a. T. I., 2022. Thermal stability of MnO2 polymorphs. *Journal of solid state chemistry,* 305(122683).

[38] Team, L., 2023. *Linkedin.* [Online]
Available at: https://www.linkedin.com/advice/0/how-do-you-optimize-leaching-conditions-different
[Accessed 2023].

[39] Technology, S. E. w. C., n.d. *thermo fisher.* [Online]
Available at: https://www.thermofisher.com/no/en/home/materials-science/chemisem.html

[40] Vercellotti, J. M., 1988. *Kinetics of Iron Removal Using Potassium Permanganate And Ozone.,* Ohio: Ohio university.

[41] Wensheng Zhang, C. Y. C., 2007. Manganese metallurgy review. Part II: Manganese separation and recovery from solution. *Hydrometallurgy,* 89(3-4), pp. 160-177.

[42] Yuxiang Hu, T. Z. m., 2015. *Wiley online library.* [Online]
Available at: https://onlinelibrary.wiley.com/doi/10.1002/anie.201411626

[43] Zhi-liang ZHU, H.-m. M. R.-h. Z. Y.-x. G. J.-f. Z., 2006. Removal of cadmium using MnO2 loaded D301 resin. *Journal of Environmental Sciences,* Volume 19.

[44] Николайчук, П. А., 2015. *The potential - pH diagram for Mn - H2O system,* Chelyabinsk, Russia: Chelyabinsk State University.

Chapter 7: Appendices

Appendices 7.1: Raw data given from ICP-MS lab and diluting calculation.

Appendices 7.2: XRD results of residue after leaching.

Appendices 7.3: XRD results of residue after purification.

Appendices 7.4: Calculation of product yield.

Appendices 7.5: Risk assessment

Appendices 7.1: Raw data given from ICP-MS lab and diluting calculation

Shows raw data given from ordered ICP-MS lab.

Table 7.1: Shows raw data recieved from ICP-MS lab.

Sample			24 -> 24 Mg [O2]		27 -> 27 Al [NH3]		28 -> 44 Si [O2]		44 -> 44 Ca [NH3]		47 -> 63 Ti [O2]		55 -> 55 Mn [O2]		56 -> 56 Fe [NH3]	
Acq. Date-Time	Sample Name	Comment	Conc. [ug/l]	Conc. RSD	Conc. [ug/l]	Conc. RSD	Conc. [ug/l]	Conc. RSD	Conc. [ug/l]	Conc. RSD	Conc. [ug/l]	Conc. RSD	Conc. [ug/l]	Conc. RSD	Conc. [ug/l]	Conc. RSD
4/25/2023 13:20	1	0	0.22	11.9	0.29	2.5	31.70	1.8	3.84	3.5	0.023	14.7	4.11	0.4	0.69	1.2
4/25/2023 13:22	2	2.2	0.15	8.7	0.49	2.6	43.28	2.1	3.99	0.5	0.018	15.2	5.46	0.7	0.74	0.2
4/25/2023 13:25	3	2.3	0.085	4.4	0.29	0.9	39.55	2.7	3.06	4.3	0.024	18.0	3.57	0.4	0.36	2.4
4/25/2023 13:27	4	3.1	0.094	7.6	0.29	0.6	32.92	1.8	3.05	3.0	0.025	4.1	5.10	0.3	2.33	0.5
4/25/2023 13:30	5	3.2	0.14	9.4	0.33	0.3	32.05	2.7	2.47	7.7	0.022	16.0	4.90	0.5	0.92	1.5
4/25/2023 13:32	6	3.3	0.37	6.3	0.33	0.8	28.29	2.0	5.68	2.0	0.021	22.4	3.62	0.3	0.43	1.5
4/25/2023 13:35	7	4.1	0.11	7.0	0.26	1.3	32.51	1.6	2.96	3.8	0.024	9.6	5.48	0.9	0.81	0.4
4/25/2023 13:37	8	4.2	0.13	6.0	0.28	2.3	36.25	1.6	3.45	3.1	0.027	7.5	5.43	0.5	0.69	0.4
4/25/2023 13:40	9	4.3	0.096	4.3	0.31	1.8	33.18	0.2	2.74	2.9	0.024	12.2	4.67	0.1	0.53	0.8
4/25/2023 13:42	10	5.1	0.091	7.0	0.26	1.4	32.83	1.1	3.03	1.7	0.022	26.1	5.20	1.1	0.88	0.5
4/25/2023 13:45	11	5.2	0.17	7.5	0.30	1.5	32.57	1.1	2.50	1.3	0.030	25.9	6.24	0.2	0.97	1.6
4/25/2023 13:47	12	5.3	2.41	2.0	0.32	0.8	32.79	2.4	3.94	4.1	0.027	14.3	0.40	0.2	0.11	2.1
4/25/2023 13:50	13	6.1	0.12	8.6	0.24	1.3	22.56	1.0	2.52	7.1	0.024	16.1	5.95	0.5	0.59	1.7
4/25/2023 13:52	14	6.2	0.11	8.1	0.34	1.3	33.87	3.1	2.67	3.0	0.027	3.7	6.74	0.9	0.56	0.6
4/25/2023 14:07	15	6.3	2.16	2.4	0.30	2.4	33.07	2.7	11.11	2.5	0.024	11.4	1.37	0.8	0.00	N/A
4/25/2023 14:10	16 rep1	7.1	0.13	4.2	0.30	0.7	42.29	1.2	4.01	1.8	0.024	10.7	5.56	0.8	0.62	1.5
4/25/2023 14:12	16 rep2	7.1	0.11	1.9	0.29	2.3	40.96	2.1	3.95	1.9	0.027	16.8	5.59	0.4	0.61	0.3
4/25/2023 14:15	17	7.2	0.11	3.0	0.29	1.2	34.17	1.5	2.50	5.6	0.027	3.4	5.67	0.6	0.51	0.4
4/25/2023 14:17	18	7.3	1.45	1.7	0.28	1.4	34.65	2.1	2.92	4.5	0.027	13.3	2.32	0.3	0.00	N/A
4/25/2023 14:20	19	8.1	0.13	0.8	0.79	1.6	33.01	2.3	6.34	0.8	0.026	9.9	5.35	0.1	0.55	1.7
4/25/2023 14:22	20	8.2	0.090	5.2	0.31	2.1	33.65	1.1	2.37	5.5	0.025	25.1	5.72	0.6	0.55	2.3
4/25/2023 14:25	21	8.3	3.16	2.3	1.70	1.1	32.12	2.0	4.17	2.0	0.020	48.8	3.72	0.8	2.67	1.8
4/25/2023 14:27	22	9.1	0.086	10.3	0.27	1.5	36.73	0.2	2.66	4.5	0.024	21.5	5.70	0.2	0.41	2.2
4/25/2023 14:30	23	9.3	1.78	1.9	0.26	4.2	32.49	1.8	3.33	1.3	0.023	5.6	3.64	0.2	0.031	10.3
4/25/2023 14:32	24	10.1	0.097	6.2	0.28	0.7	34.32	1.4	2.87	4.9	0.022	16.5	5.40	0.3	0.78	1.0
4/25/2023 14:35	25	10.2	2.23	1.3	1.89	1.0	31.28	2.0	12.08	3.4	0.021	24.5	5.70	0.4	0.98	0.7
4/25/2023 14:37	26	10.3	0.10	8.4	0.32	1.1	34.94	0.9	3.34	1.2	0.026	5.5	5.49	0.5	0.24	0.4

The dilution factor is given as 50000/20*50000/15 which is equal to 8.333.333,33 which gives the following table for concentration of the samples. ICP-MS data given are all from this table. Given concentration are in g/L.

Table 7.2: Shows concentration of solutions based of ICP-MS data given and calculation with dilution factor.

Sample		24 -> 24 Mg [O2]		27 -> 27 Al [NH3]		28 -> 44 Si [O2]		44 -> 44 Ca [NH3]		47 -> 63 Ti [O2]		55 -> 55 Mn [O2]		56 -> 56 Fe [NH3]	
Sample Name	Comment	Conc. [ug/l]	Conc. RSD	Conc. [ug/l]	Conc. RSD	Conc. [ug/l]	Conc. RSD	Conc. [ug/l]	Conc. RSD	Conc. [ug/l]	Conc. RSD	Conc. [ug/l]	Conc. RSD	Conc. [ug/l]	Conc. RSD
1	2.1	1.80	11.91	2.44	2.47	264.18	1.78	31.99	3.49	0.20	14.69	34.27	0.39	5.78	1.21
2	2.2	1.27	8.74	4.05	2.61	360.64	2.12	33.27	0.51	0.15	15.18	45.46	0.71	6.17	0.15
3	2.3	0.71	4.44	2.44	0.91	329.58	2.67	25.48	4.32	0.20	17.97	29.74	0.41	3.00	2.38
4	3.1	0.78	7.64	2.42	0.58	274.33	1.80	25.46	2.97	0.20	4.10	42.53	0.29	19.39	0.52
5	3.2	1.18	9.41	2.79	0.31	267.12	2.68	20.57	7.71	0.19	16.01	40.81	0.54	7.64	1.53
6	3.3	3.07	6.29	2.76	0.84	235.73	2.01	47.33	2.04	0.18	22.38	30.20	0.28	3.55	1.49
7	4.1	0.88	6.96	2.20	1.32	270.88	1.59	24.63	3.77	0.20	9.55	45.67	0.95	6.74	0.42
8	4.2	1.07	6.02	2.32	2.32	302.05	1.63	28.79	3.15	0.22	7.51	45.23	0.53	5.74	0.40
9	4.3	0.80	4.27	2.57	1.76	276.47	0.23	22.86	2.94	0.20	12.25	38.89	0.14	4.42	0.85
10	5.1	0.75	6.96	2.15	1.36	273.59	1.09	25.28	1.74	0.19	26.07	43.35	1.12	7.37	0.46
11	5.2	1.44	7.53	2.47	1.51	271.41	1.14	20.82	1.31	0.25	25.91	51.97	0.18	8.11	1.62
12	5.3	20.09	2.01	2.68	0.81	273.27	2.39	32.82	4.07	0.23	14.32	3.32	0.20	0.94	2.07
13	6.1	0.96	8.55	2.02	1.33	188.01	0.96	21.00	7.10	0.20	16.13	49.59	0.48	4.91	1.69
14	6.2	0.91	8.12	2.82	1.27	282.24	3.14	22.23	2.95	0.22	3.73	56.21	0.86	4.69	0.56
15	6.3	17.99	2.41	2.53	2.40	275.54	2.68	92.57	2.47	0.20	11.37	11.41	0.75	0.00	N/A
16	7.1	1.06	4.17	2.47	0.73	352.41	1.19	33.38	1.78	0.20	10.68	46.31	0.84	5.19	1.46
16	7.1	0.94	1.92	2.40	2.28	341.31	2.14	32.92	1.85	0.22	16.83	46.61	0.44	5.12	0.28
17	7.2	0.92	3.03	2.44	1.24	284.76	1.49	20.84	5.60	0.22	3.44	47.29	0.59	4.24	0.38
18	7.3	12.08	1.73	2.31	1.39	288.72	2.13	24.36	4.46	0.22	13.26	19.32	0.34	0.00	N/A
19	8.1	1.10	0.84	6.60	1.60	275.11	2.30	52.80	0.76	0.22	9.90	44.56	0.12	4.58	1.69
20	8.2	0.75	5.19	2.62	2.14	280.44	1.15	19.74	5.50	0.21	25.12	47.63	0.60	4.59	2.34
21	8.3	26.32	2.27	14.14	1.12	267.65	2.02	34.75	1.98	0.17	48.79	31.02	0.83	22.23	1.80
22	9.1	0.72	10.32	2.28	1.46	306.11	0.20	22.15	4.47	0.20	21.52	47.51	0.25	3.39	2.24
23	9.3	14.85	1.90	2.16	4.16	270.79	1.76	27.78	1.28	0.19	5.65	30.32	0.18	0.26	10.25
24	10.1	0.81	6.23	2.37	0.68	285.99	1.37	23.88	4.92	0.18	16.47	45.01	0.30	6.47	0.99
25	10.2	18.62	1.29	15.71	1.00	260.65	1.98	100.64	3.36	0.18	24.53	47.50	0.40	8.18	0.72
26	10.3	0.85	8.42	2.68	1.12	291.15	0.92	27.85	1.20	0.21	5.55	45.76	0.51	2.02	0.40

Appendices 7.2 XRD results of residue after leaching

All XRD's shown here are the same, or similar to that of the XRD for test nr. 4 given in chapter 4.3.3.

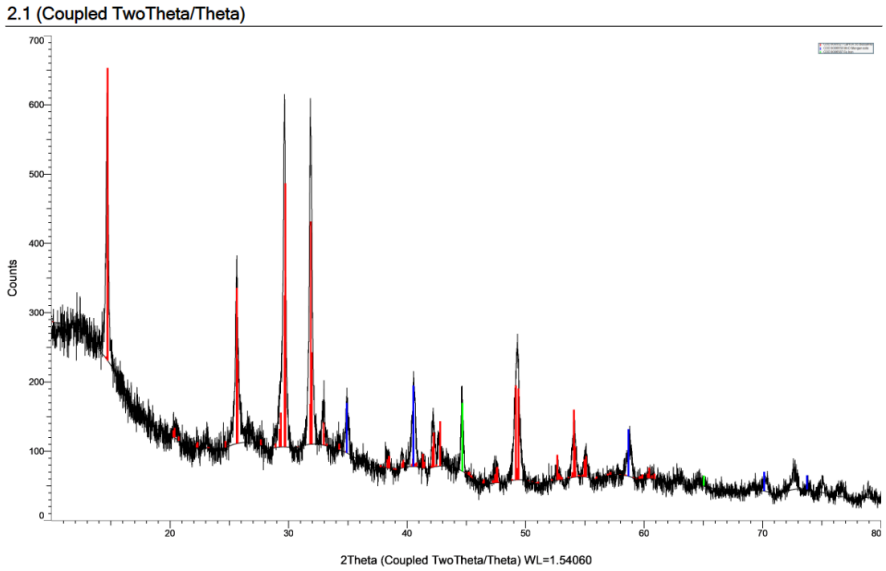

Figure 7.1: Shows XRD of solid residue from test nr. 2 after leaching (RED – Gypsum/bassanite, BLUE – MnO, GREEN – Iron).

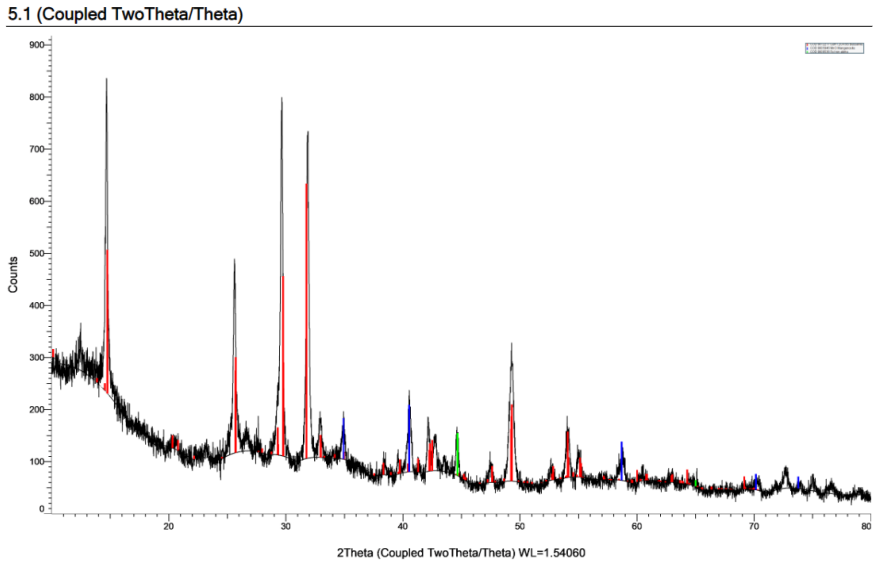

Figure 7.2: Shows XRD of solid residue from test nr. 5 after leaching (RED – Gypsum/bassanite, BLUE – MnO, GREEN – Iron).

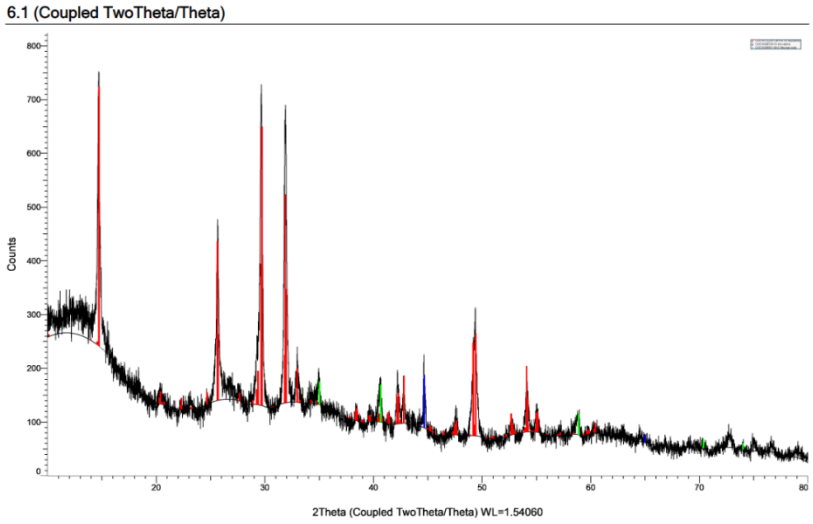

Figure 7.3: Shows XRD of solid residue from test nr. 6 after leaching (RED – Gypsum/bassanite, GREEN – MnO, BLUE – Iron).

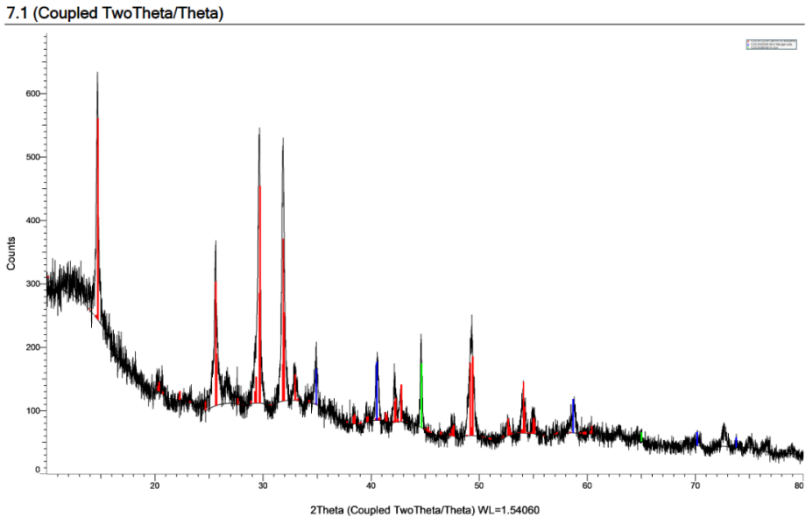

Figure 7.4: Shows XRD of solid residue from test nr. 7 after leaching (RED – Gypsum/bassanite, BLUE – MnO, GREEN – Iron).

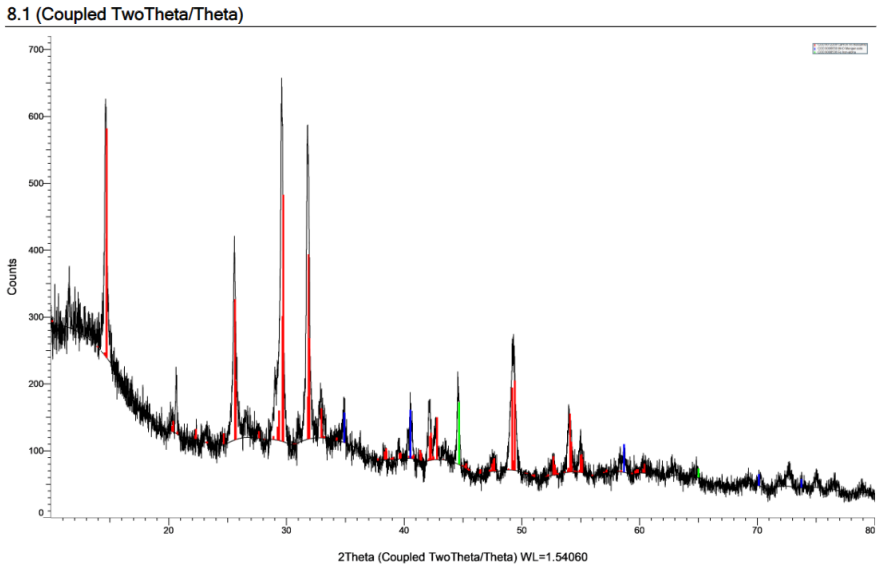

Figure 7.5: Shows XRD of solid residue from test nr. 7 after leaching (RED – Gypsum/bassanite, BLUE – MnO, GREEN – Iron).

Appendices 7.3 XRD results of residue after purification.

Underneath XRD results of test nr. 2, 5 and 6 are given. These are similar to those given in 4.3.4.

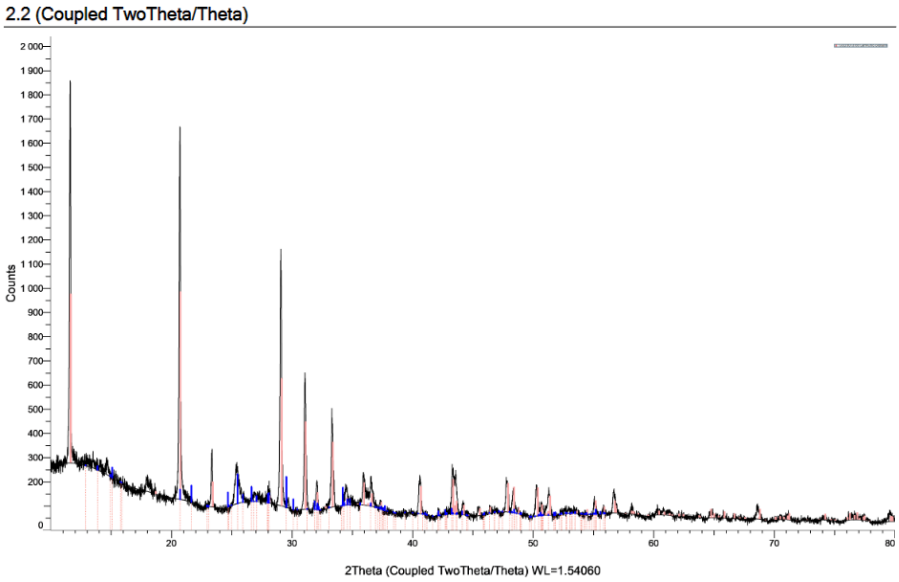

Figure 7.6: Shows the XRD results of test nr. 2 after purification. Red – Gypsum

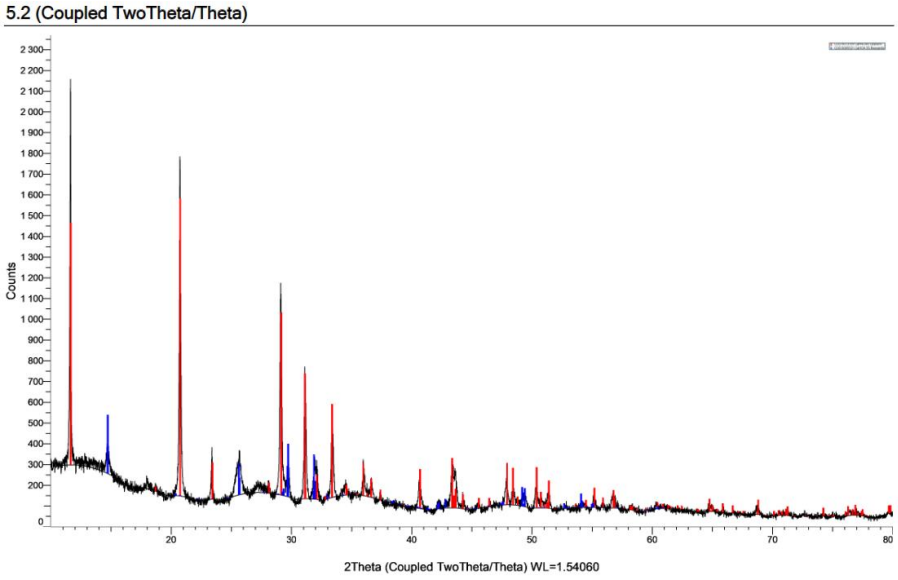

Figure 7.7: Shows the XRD results of test nr. 5 after purification. Red – Gypsum, Blue – Bassanite.

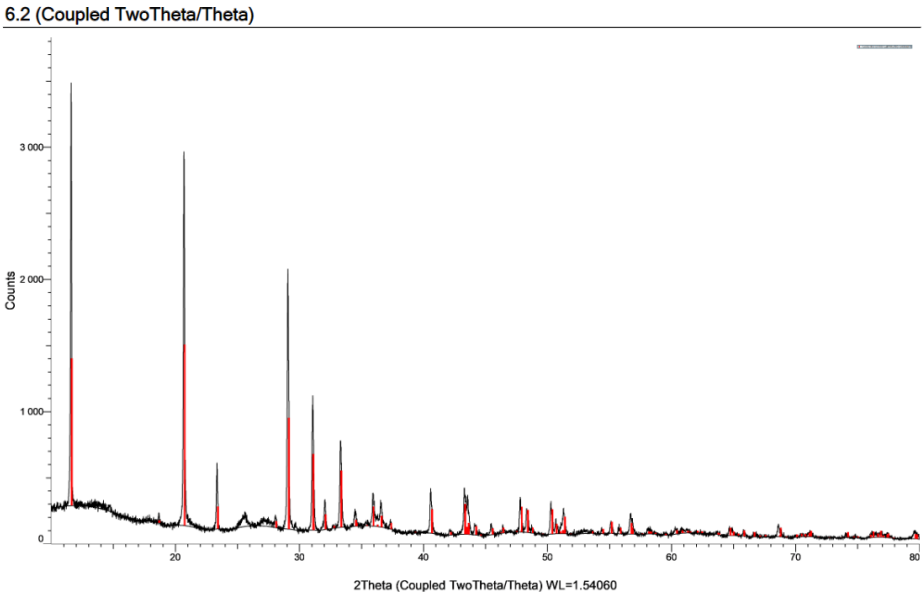

Figure 7.8: Shows the XRD results of test nr. 6 after purification. Red – Gypsum

Appendices 7.4 Calculation of product yield.

The calculation of manganese yield is given in formula 7.1. The content of manganese in reduced ore is given as 54.77 wt% of 50 grams. The content of manganese in product is given as solid residue weight*wt% based on XRF results. The product is made from 350 mL of the original 500 mL solution and therefore the calculation for total yield must include the ratio of 500/350

$$\frac{Mn\ in\ product}{Mn\ in\ reduced\ ore} * \frac{500mL}{350mL} * 100\% \quad (7.1)$$

$$\frac{13.10g*40.54w\%}{50g*54.77w\%} * \frac{500mL}{350mL} * 100\% = 27{,}70\% \quad (7.2)$$

$$\frac{14.09g*28.42w\%}{50g*54.77w\%} * \frac{500mL}{350mL} * 100\% = 20{,}89\% \quad (7.3)$$

$$\frac{8.80g*45.43w\%}{50g*54.77w\%} * \frac{500mL}{350mL} * 100\% = 20{,}86\% \quad (7.4)$$

$$\frac{7.99g*15.21w\%}{50g*54.77w\%} * \frac{500mL}{350mL} * 100\% = 6{,}34\% \quad (7.5)$$

$$\frac{34.73g*22.60w\%}{50g*54.77w\%} * \frac{500mL}{350mL} * 100\% = 40{,}95\% \quad (7.6)$$

$$\frac{28.25g*29.44w\%}{50g*54.77w\%} * \frac{500mL}{350mL} * 100\% = 43{,}39\% \quad (7.7)$$

Appendices 7.5: Risk assessment

Activity / process	Unwanted incident	Existing risk reducing measures	Probability (P)	Consequence (C) Evaluate the categories individually. *Health should always be evaluated.*				Risk value (P x C)	Risk reducing measures - suggestions Measures reducing the probability of the unwanted incident happening should be prioritized.	Residual risk after measures being implemented
			(1-5)	Health (1-5)	Material values (1-5)	Environment	Reputation (1-5)			
Manganese ore	Harmful when inhaled Can irritate the skin and eyes	-Particulate mask with R/N/P95 filter are available -Wear direct vent goggles -Recommended glove materials for Mn are Nitrile and Neoprene If eyecontact is made, rinse cautiously for 10 minutes. Medical attention must be seeked if symptoms persist. If skincontact is made, irritation may occur and thorough washing with water must be done. Medical attention must be seeked if symptoms persist. The ore will be stored in a plastic zip bag that is air tight to not release any dust.	*1*	*2*	*1*	*1*	*1*	*2*		*2*
Drying ore sample and residues (below 100 C)	Skin burn	Using gloves to put/take samples in Oven. The potential burns will only be mild, and cooling the burns with tempered water is sufficient. After drying, the ore can again be stored in a plastic zip bag that is air tight to not release any dust.	1	2				2	Follow the regular lab instructions for working with raw materials, ores, and use of mask, glasses, gloves. Follow the lab rules	2

Oven being at 900 degrees celsius	Fires could start if flammable objects are near an oven or heated objects taken out of the oven	Minimize amount of flammable objects in the lab, such as paper. Handeling objects taken out of the oven with correct tools such to minimize the chance of dropping or spilling heated object. This ensures that the heated object does not get in contact with or near unwanted flammable objects. If a fire takes place an attempt to extinguish the fire can be made, only if deamed safe. The firefighters ariving to the scene must be informed of what is burning, and potential gases (H2 in this case).	1	2	1	1	1	2	The work will be performed with a skilled perso	2
	Sulfuric acid can be corrosive to metals. Will cause seriuos irritation and can cause damage in contact with eyes. Can cause chemical burns in contact with your skin.	To minimize the probability of your skin being in contact with acid it is mandatory to allways use a lab coat, pants, and gloves suited to the concentration of the acid in use. Gloves that can be used are PVC gloves are best, and neoprene gloves are okay for shorter periods. If the acid comes in contact with skin and clothes, remove all clothes contaminaited and rinse affected area with water. If the spill on the body is over a large area and cant be washed by using the spring, the safety shower can be used. If the acid comes in contact with the eyes, they must be rinsed carefully for several minutes. Clothes that may be contaminated must be washed before reuse or thrown away if there is too much spillage. The acid will be diluted into a beaker	2	3	1	1	1	6	Making an instruction to do safe work with acids, and the work will be started under the supervision of a lab engineer. For the cleaning, the supervisor will advise, however the general rule for sulfuric acid is to clean the equipment with copious amounts of tap water, but slowly and check if heat will be generated. After cleaning with tapwater rinsing 3-4 times with deionized water. The cleaning process will also be done under a fume hood.	4

Handeling of H2SO4 acid, and making d		before use, and wil be stored in a glass flask with a lid and put in a plastic box with other materials for the project. After precipication the remaining acid will be handled as acidic waste and therefore be thrown away in designated acid waste-container before being handled. This is to minimize environmental impact and damages. To prevent risks from fumes the dilution of the acid will be done under a fume hood.								
Milling in ring mill and sizing by sieves	Inhaling dust during milling/sizing of Mn-ore	Use of proper protectiive equipment can reduse this risk drastically. Lab-Goggles, N95 mask or dust mask and face-glass can be used for instance. If irritation in the airways happen, this must be taken seriuosly and the issue must be checked by a medical profesional if the problem remains.	2	3	1	1	1	6	For opening the ring mill, it will be done under v	3
	Hydrogengas can explode in contact with oxygen	To ensure that there are no gas leaks there must allways be 2 gas sensors near that is able to detect hydrogen gas. If any of these 2 alarms go off, the leak must be found and all possible hydrogen tanks and sources must be shut off. The people that are responsible for the lab must be informed. If hydrogen gas "burns" it will not be visible on its own and only massive amounts of heat will be generated. Therefore potential firefighters must be informed of the gas.	2	2	1	1	1	4	A skilled person will be present to start the work. The work will only be done once and therefore it will be supervised under the entire process.	3

Hydrogen gas used in ovens										
Use of XRD analysis	Injuries due to exposure to a primary beam or leakage or scattered radiation.	Shielding-Ensure that the instument is complety covered/closed before starting since the X-ray gets generated only after power supply. If there is any suspicion of radiation leakage medical assesment must be made for all that may have been affected.	1	3	1	1	1	3	Follow the XRD lab rules, and under the supervision of the lab responsible	2
Precipitation with dry NaOH	If NaOH comes in contact with your skin it will cause severe burns	The pieces of NaOH added to the solution will be moved to its beaker using a spoon. In addition the spoon must never hover above any part of the body in the case it is dropped.	2	2	1	1	1	4	Following the labrules and handeling the sodium hydroxyde carefully	4